SEDIMENTOLOGY AND PROVENANCE STUDIES OF LOWER PART OF THE BAGALKOT GROUP OF KALADGI BASIN: IMPLICATIONS OF TECTONIC AND SEDIMENTATION HISTORY

A THESIS SUBMITTED TO
GOA UNIVERSITY

FOR THE AWARD OF THE DEGREE OF
DOCTOR OF PHILOSOPHY
IN
GEOLOGY

by

MEGHANA SHIVANAND DEVLI, M.Sc

DEPARTMENT OF EARTH SCIENCE
GOA UNIVERSITY

2018

This thesis is dedicated to

My Mentors

Shri Harish S S Nadkarni

Dr. H M Ramachandra

and

My Parents

CERTIFICATE

This is to certify that the thesis titled, "**SEDIMENTOLOGY AND PROVENANCE STUDIES OF LOWER PART OF THE BAGALKOT GROUP OF KALADGI BASIN: IMPLICATIONS OF TECTONIC AND SEDIMENTATION HISTORY**" submitted by Meghana Shivanand Devli for the award of degree of Doctor of Philosophy in Geology is a record of research work done by her during the period of study and is based on the results of experiments carried out by her independently. The thesis or a part thereof has not previously formed the basis for the award to the research scholar for any other degree, diploma, associate ship, fellowship or other similar titles.

RESEARCH GUIDE

Dr. MAHENDER KOTHA,
Professor,
Department of Earth Science,
Goa University,
Taleigao Plateau, Goa

STATEMENT

I hereby state that this thesis titled, "**SEDIMENTOLOGY AND PROVENANCE STUDIES OF LOWER PART OF THE BAGALKOT GROUP OF KALADGI BASIN: IMPLICATIONS OF TECTONIC AND SEDIMENTATION HISTORY**" for the award of Ph.D. degree is my original contribution and that the thesis or any part thereof has not previously formed the basis for the award of any other degree, diploma or other similar titles of any university or institute. To the best of my knowledge, the present study is the first comprehensive study of its kind from the study area. The literature pertaining to the investigated problem has been duly acknowledged. Facilities availed from other sources have also been duly acknowledged.

RESEARCH SCHOLAR

MEGHANA SHIVANAND DEVLI,
Department of Earth Science,
Goa University,
Taleigao Plateau, Goa.

ACKNOWLEDGEMENTS

I would like to thank my Guide, Dr. Mahender Kotha, Professor and Head, Department of Earth Science, Goa University for his valuable guidance and allowing me to work under him. He has always been supportive during the entire time of my pursuance of the degree..

Extraordinary support came from my Mentor Shri Harish S S Nadkarni, Vice-Principal and Head, Department of Geology, Parvatibai Chowgule College for his untiring encouragement, critical discussions, doing the proof readings with lots of patience. During the entire process, he remained a pillar and backbone of this research.

This work would have been impossible without the support, guidance and expert advice of my Mentor Dr H M Ramachandra, Retired Director, Geological Survey of India and I express my gratitude to him for his invaluable guidance and contribution in the progress and process of gaining knowledge. His willingness to share time so generously will always be cherished.

I would like to thank my Vice-Chancellor's nominee, Dr Rahul Mohan, Scientist, National Centre Antarctica and Ocean Research (NCAOR) for being always supportive and allowing me to work on Scanning Electron Microscope-Electron Dispersive Spectroscopy (SEM-EDS). You supported me greatly and were always willing to help.

Gratitude is due to Miss Sahina Gazi, Technician, NCAOR Vasco- Goa for teaching me to use SEM-EDS.

Immense gratitude to my friend Dr Thamban Meloth, Scientist, NCAOR for his support and kindness in allowing me to work on Inductively Coupled Plasma- Mass Spectroscopy (ICP-MS) and being a constant support. It was a pleasure working on ICP-MS with Dr Latika Padmanabhan, Scientist, NCAOR who guided me to use the instrument.

I wish to acknowledge the help provided to me at the right time by Dr Abhay Mudholkar, Scientist, National Institute of Oceanography (NIO), Dona Paula Goa and allowing working on the X-Ray Fluorescence (XRF) and also to my student Mr Brahmanad Sawant, Research Scholar, NIO, Goa for helping me in getting the XRF analysis done.

I am particularly grateful to the assistance provided to me by my student Akshay Kelkar, Assistant Professor, Parvatibai Chowgule College, Margao-Goa who patiently digitised the maps and prepared the illustrations for me.

Gratitude to Dr. Makarand Kale and Dr RA Duraiswami, Associate Professor's, Department of Geology, Savitribai Pule Pune University for always supporting me in my work.

I extend thanks to my department colleague Magnolia Miranda, Assistant Professor, Parvatibai Chowgule College for generously sharing books.

I would like to express my appreciation to all my students who accompanied me during field visits.

Thanks are due to Miss Anisha Noronha, Miss Anushka Dessai, Mrs Suveena Naik, and Mr Cedric Barretto; Administrative staff, Parvatibai Chowgule College of Arts and Science for helping me gracefully every time I requested.

I wish to thank the Goa University admistrative staff, Mrs Sneha Naik, Shri Premakant Gawas (retired), Mrs Sangeeta, Dr Gopakumar V, Librarian, Goa University and all those who remained associated with me during the process of completion of this thesis.

Finally I thank my parents and my other family members for their patience, encouragement and support and The Almighty for giving me the strength to complete my thesis.

C O N T E N T S

LIST OF FIGURES

LIST OF TABLES

ABSTRACT

The lithounit **c**onglomerate of the thickness about 6m - 30m is seen exposed at Ramthal and Salgundi belonging to the Salgundi Conglomerate Member of the Ramdurg Formation in the Bagalkot Group of the Kaladgi-Badami sequence of rocks. The lithounit is exposed at Bilgi and Jamkhandi within the Kaladgi basin. Even though the Kaladgi basin is studied extensively by many workers on a larger scale, the minute intricacies have remained untouched. This includes studies on individual lithounit with respect to its lithological characters, textural features, provenance, deformation history, paleocurrent directions and mapping on a larger scale of the area. Therefore, this lowermost rock unit provides an opportunity to understand the paleocurrents, provenance and deformation history of the Mesoproterozoic Bagalkot Group. To understand this, field studies were combined with analytical studies to come to a conclusive result. To understand the deformation history of the area, field studies were combined with micro section observations. At Bilgi and Jamkhandi the Mesoproterozoic rock unit is classified as an arkosic sandstone constituting clasts of quartz and K-feldspars whereas at Salgundi and Ramthal it is an oligomictic conglomerate.

Presence of current bedding and ripple marks in the immediately overlying quartzites is indicative of a shallow depositional basin. The study areas at Salgundi and Ramthal are located on the two limbs of a fold. Based on the imbrications of the pebbles observed in the field and reconstruction to a prefolding position of the limbs of the fold based on the dip directions recorded at two places show Ramthal (dipping North) and Salgundi (dipping South) suggesting the upstream side of the basin to be towards the eastern side of the basin. The rock at Salgundi and Ramthal which is mineralogically matured has abundance of silica varieties and lack in feldspars. While percentage of Fe_2O_3 increases along with SiO_2 at both

places that of Al_2O_3, K_2O, CaO and Na_2O is much less. The Al_2O_3+Na_2O+K_2O versus SiO_2 plot indicates Compositional Maturity Index is relatively higher at both the study areas suggesting removal or lack of mobile elements like Na_2O and MgO. The lower concentrations of U and Th in the samples with lower ΣREE probably reflects a control by grain size fractionation during transport suggesting a contribution from a mafic source with lesser concentration of such elements. Bivariant log/log plot of the ratio of Qp/F + R values represent the region to have been a moderate to low lying plain experiencing hot, tropical, oxidizing, humid climatic conditions. Further, the Eu/Eu* versus Gd/Yb determined for the conglomerate denote a post-Archean age which is in accordance with the Mesoproterozoic age determined by earlier workers.

At Bilgi, penetrative features in the arkosic sandstone suggest effects of mild, low temperature deformation. The east-west striking beds have a gentle 15° southward dip, marked with a primary S_0 foliation that is superposed by secondary S_1 and S_2 foliations. Field observations are substantiated by microsection studies. Low temperature deformational mechanisms exhibited in the form of grain boundary migration, overgrowths in crystallographic continuity, recrystallisation of quartz, neocrystallisation of micas, indicate the deformation involved a (<300°C) temperature regime.

In this work, for the first time, a chrome bearing variety of tourmaline "Chromdravite" is reported as a detrital mineral within the host rock, arkosic sandstone at Bilgi. Their provenances studies are left untouched since the immediate basement rock, Closepet Granite has not been reported to show presence of chromdravite. A two source provenance thus, cannot be ruled out for the host rock at Bilgi.

Trace elements and REE percentages determined from geochemical analysis point to a felsic source for the host rock at Bilgi and Jamkhandi; in contrast a mafic source is revealed for the host rock from Ramthal and Salgundi. While SiO_2 dominates, K_2O percentage is higher than Na_2O in the arkosic sandstone as well as the conglomerate both of which are poor in Al_2O_3.

CHAPTER 1

INTRODUCTION

1.1 Foreword

Towards the end of the Archaean Era after a hiatus, changes started occurring during the Middle Proterozoic (1600-900Ma) on the Dharwar craton. These changes involved creation of large basins, especially at the borders and interiors of the craton. The erosion of the Archean rocks subsequently resulted in a new cycle of deposition of sedimentary rocks. As such, in the Dharwar craton no sedimentary deposit of an age prior to the Mesoproterozoic (1600-900Ma) is found. The deposition during the Mesoproterozoic began over the older eroded and denuded rocks of the Archean age that include schist, gneisses as well as granites. One such basin which formed towards the Northern part of the Dharwar craton is the Kaladgi-Badami basin (at places referred to as Kaladgi basin in this work). The contractional forces enhanced by intraplate extensional tectonics resulted in the formation of this intracratonic Kaladgi basin.

The Kaladgi basin is popularly known as Purana Basin and the hiatus period represents an erosional unconformity in the Indian geological literature. The sediments from the Kaladgi basin deposited over the Archean basement rocks constitute detritus of gneisses, metasediments, and granites and covered under the extensive Deccan flood basalts of the late Cretaceous age towards its northern margin. Based on the sedimentation history, the sedimentary sequence of rocks has been classified into the older Bagalkot Group which is deformed by the compressive forces and the younger Badami Group which remained

undisturbed. The separation between the two Groups is marked by a prominent and geologically significant angular unconformity.

1.2 Introduction

The Kaladgi-Badami basin occupying the northern part of the state of Karnataka, even though is studied by many workers previously, a lot remains unsaid of the individual lithounits, their mapping on a larger scale, and a detailed study of the mineral constituents. Also, the deformation history and the resulting structures are not well defined. The tectonic and geologic history of a region controls in some way the source area characteristics and the depositional environment in which sediments accumulate (Boggs, 2009). This has prompted to take up a part of the Kaladgi-Badami basin for a study involving the depositional history and provenance of sediments deposited in the region, besides, the relation of structural features observed both on megascopic and microscopic scale in understanding the deformational history of the sequence.

After a look through the previous literature, followed by reconnaissance studies, the lower Ramdurg Formation of the Lokapur Subgroup of the Bagalkot Group was marked for study. This part of the Formation composed of clastic sedimentary rocks and intruded by a few mafic sills, is well exposed at Bilgi, Jamkhandi, Salgundi and Ramthal. Being accessible it was easier to carry out field investigations and collect samples. While the study areas of Bilgi and Jamkhandi lie towards the Northern part of the basin, Salgundi and Ramthal are towards the south of the basin.

The thesis titled – "Sedimentology and Provenance studies of lower part of the Bagalkot Group of Kaladgi basin: Implications of tectonic and sedimentation history" comprises of an assessment of the study involving the mineralogy, sedimentology, provenance and deformation structures that have developed in the rocks during this mild tectonic disturbances they were subjected. The primary data was collected through reference of previous work, and later by carrying out extensive field work in the localities of Bilgi, Jamkhandi, Salgundi and Ramthal. Samples were collected during field traverses and named as: Jamkhandi (numbered as JAM-1, JAM-2, JAM-3, JAM-4, JAM-5), Salgundi (numbered as SAL-9, SAL-9A, SAL-9B, SAL-9C, SAL-9D) and Ramthal (numbered as RAM-2, RAM-2A, RAM-2B, RAM-2C, RAM-2D) respectively. As a variation in the character of the rock unit was observed at Bilgi the samples from lower levels are numbered as BIL-13, BIL-13A, BIL-13B, BIL-13C, BIL-13D whereas from the upper levels they are numbered as BIL-15, BIL-15A, BIL-15C, BIL-15D respectively.

.

The mineralogical and sedimentological studies are based on microsections of the fresh rock samples collected during field work. Identification of the mineral constituents in the matrix is substantiated and supported by studying the sections using Scanning Electron Microscope. Geochemical analysis is done to determine major oxide compositions using X-Ray Fluorescence (XRF), Inductively Coupled Plasma-Mass Spectrometer (ICP-MS) for trace elements and Rare Earth Element to help in understanding the provenance, deformation and tectonism. Calculation of mineral formula was done using SEM-EDS. SEM-EDS analysis is done to derive the mineral formula of the variety of tourmaline reported in the work. All the data is analysed in detail and supported by field evidences.

The thesis in all comprises of eleven chapters excluding bibliography. Chapter 1 provides an overview of the topic; chapter 2 deals with previous work; chapter 3 involves geology and stratigraphy of the regions, chapter 4 gives the details of field observations and samples collected at Bilgi, Jamkhandi, Salgundi and Ramthal and covers the analytical methods employed. A discussion of the mineralogy and petrology is provided in chapter 5, geochemical analysis is presented in chapter 6, chapter 7 involves provenance studies, chapter 8 deals with depositional environment and paleocurrents, chapter 9 covers deformational history, chapter 10 is dedicated to tourmaline in the rock unit at Bilgi and in Chapter 11 summary is presented and conclusions are drawn based on the interpretations from the work carried out with a concluding remark on further scope of work.

1.3 Aim and Objectives

- **Aim**

  To study the provenance and sedimentation history of the lower part of the Bagalkot Group of Kaladgi basin and its implications on the tectonic and sedimentation history.

- **Objectives**

  The main objectives of the proposed study on the lowermost Member of the Bagalkot Group of Kaladgi basin are:

1. Detailed field investigation of the clastic sequence (mapping, sample, sediment/structural data collection);
2. Determination of the textural, compositional (mineralogical and chemical) parameters;

3. Understand the depositional and diagenetic history of the sequence and finally

4. To evaluate the provenance, depositional mechanisms/environments of the study area in order to understand the implication of tectonic and sedimentation history.

CHAPTER 2

PREVIOUS WORK

Foote (1876) systematically mapped and studied the Kaladgi basin occupying the northern part of the state of Karnataka on a regional scale. A substantial study has since been carried out in the basin by many workers which include investigations on sedimentation history (Kale and Phansalkar, 1991), variation of facies (Bose *et al.*, 2008), paleoweathering, geochemistry (Dey *et al.*, 2009) and deformation history (Mukerjee *et al.*, 2016); yet an in-depth study remains with respect to individual lithounits, their large scale mapping, mineralogy, provenance and also its deformational history in interpreting the evolution of the basin.

The Kaladgi sedimentary cover is considered to have been deposited within an intracratonic basin by some workers (*for e.g.* Radhakrishna and Vaidyanathan, 1994) whereas some workers assumed the basin to be marine in origin (Viswanathaiah, 1969; Jayaprakash *et al.*, 1987; Peshwa *et al.*, 1989; Kale *et al.*, 1996). On the premise of the availability of an insufficient data (Miall *et al.*, 2015); Dey (2015) in his report reiterates the need to carry out intensive investigations on the age of sedimentary detritus, the nature of evolution of the basin as well as its geological and tectonic history. He opines, this will provide immense knowledge to understand the evolution of this intracratonic basin, to reconstruct Proterozoic supercontinents and to study the atmospheric changes and primitive life forms.

While the presence of framework clasts of quartz, K-feldspar, tourmaline, sphene, zircon, biotite point towards a granitic source for the sediments towards the northern margins of the basin, an occurrence of Banded Hematite Jasper, Banded Heamatite Quartzite, chert etc. suggest that the metasediments from the Hungund Schist Belt to be the subordinate source rock towards the central eastern part. An upliftment of the granitic rocks constituting the basement towards the northern margin of the basin could have created a rugged topography. This led to the rapid erosion and burial of the feldspars forming a typical 'granite wash' towards the northern margin of the basin. Long periods of erosion on upliftment of this granitic body acted to create a productive source of sediments for the deposition of the sequence involving the formation of arkose. The feldspars represent different stages of alteration in forming a tectonic arkose (Krynine, 1935). The presence of both fresh and altered feldspar of same species (here microcline), in fact, is very common in arkosic rocks (Williams *et al.*, 1954; Folk, 1974; Pettijohn, 1972). The arkose at Bilgi is determined to have K-rich feldspars along with some Na-plagioclase. Studies have also suggested an existence of highly K-rich source to the north of the Kaladgi basin. Vishwanathaiah and Murthy (1977) have reported that at Bilgi an influx of material derived from quartzofeldspathic veins have contributed to the enrichment of feldspars in the rocks.

Petrographic and geochemical data of the sandstones from the Kaladgi basin was adopted in understanding the paleoweathering pattern, composition and tectonics of their provenance by Dey *et al.,* 2009. They suggest the deposition within the basin to comprise a cyclic arenite-pelite-carbonate association resting unconformably over the Archean basement.

Dey (2015), in his report presents that the sandstone all along the northern margin of the Kaladgi basin show typical arkosic texture and composition. In his observation quartz and feldspar generally show systematic relation in grain size, while, in conglomerate beds, quartz and feldspar are present as pebbles as well as sand sized grains in the matrix. He has opined that considerable down cutting through rapid erosion was responsible for the mixture of altered feldspar from the weathered zone with fresh ones from the bed rocks. Some of the fresh feldspar grains show subrounded to subangular nature with or without secondary overgrowth. Though fresh, these feldspar grains are suggested to be definitely detrital.

Dey *et al.*, 2009, have proposed that during the initial phase of deposition, the basin received detritus from a restricted, uplifted and less weathered source dominated by potash rich granites occurring towards the north. This is interpreted by the presence of immature arkosic sandstone of the Saundatti Quartzite Member of the older Bagalkot Group which contains fresh and angular feldspars along the northern borders of the basin. On the contrary they quote that the same Member displays a mature, quartz-rich nature with lesser amount and intensely weathered feldspars, and higher SiO_2 and CIA values but lower Al_2O_3, TiO_2, Rb, Sr, Ba, K_2O and K_2O/Na_2O, Zr/Ni and Zr/Cr ratios along the southern margin of the basin. This is interpreted in terms of a tectonically stable, considerably weathered mixed provenance (including gneisses, granites and greenstones) along the southern margin of the basin. Higher up the succession within the basin they have reported the quartz-arenite belonging to Muchkundi Quartzite Member also belonging to the Bagalkot Group to be highly matured and displaying minor but highly weathered feldspars, and higher SiO_2, Na_2O, CIA, Cr and Ni with lower K_2O, Al_2O_3, TiO_2 and K_2O/Na_2O. It proves that with the passage of time the source evolved to a uniform,

extensively altered, tectonically stable peneplained provenance which constituted less evolved TTG gneisses and greenstones. This was followed by the closure, deformation, and upliftment of the Bagalkot Group of rocks and subsequently followed by deposition of the younger Badami Group. The Cave-Temple Arenite and Belikhindi Arenite Members of the Badami Group range in mineralogy from arenites to arkose and the geochemical analysis of the same point to a provenance that was less evolved consisting of denuded TTG gneisses and greenstones as well as detritus from the older Bagalkot Group. Their study interprets the variable weathering patterns of feldspars and severe depletion of Ca, Na and Sr in the associated shales to indicate a humid tropical (tropical and subtropical) climate facilitating chemical weathering.

The basal Salgundi Conglomerates are recently studied as products of terrestrial scree formed along the margins of the basin and fan deposits that graded downslope to form braided sediments (Bose *et al.,* 2008). The authors conclude that the tectonic influence on the gradient of the marginal slope of the basin controlled the nature of the sedimentary package and a subsequent build-up of the sequence.

In their study Mukerjee *et al.,* 2016, state that towards the northern margin (Bilgi-Jamkhandi-Mamadapur) of the Kaladgi basin the Saundatti Quartzite as well as the Salgundi Conglomerate Members directly rests over the granites. The sedimentary cover rocks are stated to be mildly deformed in this part of the region and a homocline has developed with intervening normal faults; but no cleavage development. In their study, thin section observation of the detrital quartz grains within the Saundatti quartzites from the gently southward dipping beds at Bilgi, show no deformation of grain boundaries and no cleavage development, but many of the grains show sweeping undulose extinction

which is suggestive of intracrystalline deformation by dislocation creep. They conclude that the intracrystalline deformation in the detrital quartz grains at Bilgi was therefore partly inherited from the basement rocks comprising Peninsular Gneiss, Granite and Hungund Schist Belt during deposition and is not completely due to deformation of the cover rocks.

Govinda Rajulu *et al.*, (1968) studied the authigenic growth of the tourmaline over detrital tourmaline cores with respect to morphology, origin and significance of the different varieties of tourmalines occurring in the lower Saundatti Quartzite Member. According to them the diagenetic changes resulting in the growth of the varieties of tourmalines are controlled neither by the chemical composition of the detrital grains nor the host tourmaline grains. The tourmalines studied viz; schorlite and elbaite, constituted 60% to 50% respectively among the host grains and as overgrowths. The clear cut difference between the host grains and the overgrowths indicate that the authigenic tourmalines grew independently of the chemical composition of the detrital core. The study of such tourmaline can thus be used in tracing relationships between different horizons within the basin and elsewhere. It may also help in solving problems like classification and correlation of sediments and reconstruction of paleogeographic conditions. The growth and development of authigenic minerals helps in understanding physico-chemical environment that prevailed during the time of deposition and in understanding the boundary limit of diagenesis.

CHAPTER 3

GEOLOGY AND STRATIGRAPHY

3.1 Introduction

Even though the geology of Karnataka spans over the Archean, Proterozoic, Mesozoic and Cenozoic Eras, it is more extensively covered by rocks of Archean age. The state hosts the oldest cratonic rocks that include Gorur gneisses dating about 3.3Ga. The craton is extensively intruded by granites and granitoids ranging in age from 2.6 to 2.5Ga. The Precambrian rocks are divided into the older Sargur supracrustals (3.3 to 3.0Ga) and the younger Dharwar Supergroup (3.0 to 2.6Ga). The Dharwar Supergroup is further subdivided into the older Bababudan Group (3.0 to 2.7Ga) and the younger Chitradurga Group (2.7 to 2.5Ga). Towards the northern part of the craton lies the intracratonic sedimentary basin constituting the Kaladgi Supergroup of Mesoproterozoic age. A substantial part of the northern Karnataka is covered by Deccan basalts of Cretaceous-Tertiary age. A detailed account of the Kaladgi-Badami basin is as follows.

3.2 Geological setting of Kaladgi-Badami basin

The Kaladgi basin lies in south-west India in the state of Karnataka constituting a part of the northern Dharwar craton (Fig.3.1). The basin trends East-West with an irregular ovoidal outline having an extent of about 500kms and covering an area of about 8330km^2. The basin is intracratonic since it lies within a stable continental interior with the older Archean continental rocks/supracrustal rocks of the Dharwar craton serving as a basement. Resting above the Archean basement with a prominent unconformity of 4500m is a thick pile of sedimentary rocks constituting the Kaladgi Supergroup of rocks. This

Mesoproterozoic sedimentary sequence is in turn unconformably overlain by younger Neoproterozoic sedimentary rocks. The Deccan flood basalts of the Cretaceous-Eocene age overlap the Kaladgi Supergroup of rocks (Jayaprakash *et al.*, 1987; Dey, 2015; Mukerjee *et al.*, 2016).

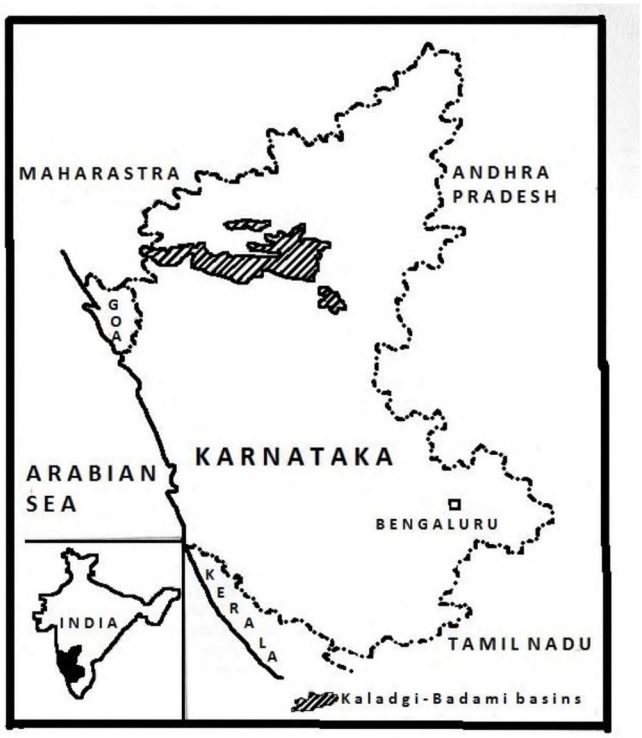

Figure 3.1 Sketch of the Kaladgi-Badami basin and its location in Karnataka (not to scale).

The basin is surrounded towards the south by Peninsular Gneissic Complex (PCG), towards the east is the Hungund Schist Belt (HSB) whereas towards the northern, central and south-east the Closepet Granite serves as a basement rock (Fig. 3.2).

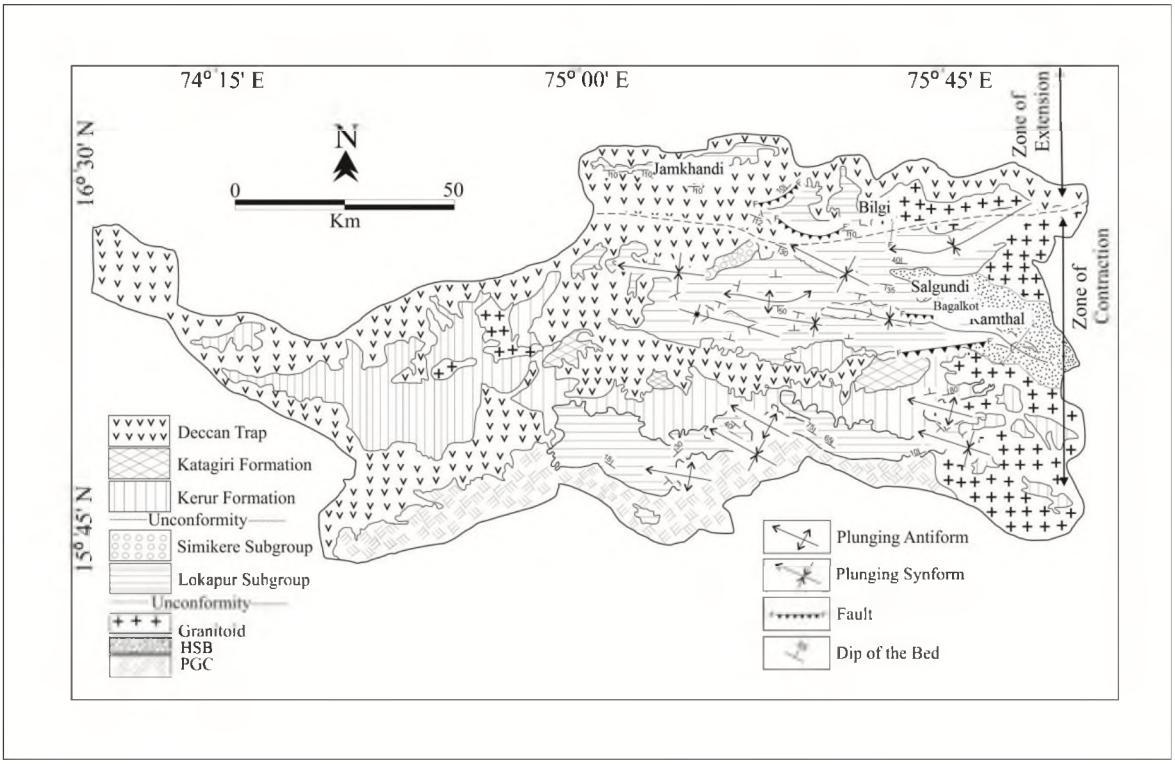

Figure 3.2 Geological and structural map of the Kaladgi-Badami Basin (*after* Mukerjee *et al.*, 2016).

PAGE 13

3.2.1 Composition of the basement rocks

- *Peninsular Gneissic Complex (PGC)*

Based on Rb-Sr and Pb-Pb methods (Bhaskar Rao *et al.,* 1991; Naha *et al.,* 1993) the age of the PGC is reported to be about 3.3 to 3.4Ga whereas recent U-Pb zircon dating gives a range from 3.5 to 3.6Ga (Meert *et al.,* 2010) with a Tonalite-Trondjhemite-Granodiorite (TTG) composition. The PGC, the oldest rocks of India have undergone a long history of evolution ranging from 3.3 to 2.5Ga approximately (Beckinsale *et al.,* 1980; Beckinsale *et al.,* 1982; Jayananda *et al.,* 2000). These well foliated rocks constitute thin bands of alternating light and dark compositional layers composed of quartz-plagioclase, Biotite(+/-hornblende) and Fe-Ti oxides. They occupy a major portion of the Dharwar craton and have undergone several cycles of deformation and migmatisation. The repeated cycles of deformation, metamorphism and partial melting lead to the obliteration of identity of the early events through which the rocks underwent.

- *Hungund schist belt (HSB)*

The HSB exposed towards the eastern part of the Kaladgi basin serving as a basement for the sedimentary cover rocks is about 400kms long, trending NNW–SSE (Naqvi *et al.,* 2006). It constitutes an assemblage of rocks mainly consisting of metabasalts with metaultramafics, metasediments with minor metavolcanics and greywackes with intercalated Banded Iron Formation (BIF) (Roy, 1983).

Rocks like amphibolites, hornblende-tremolite-actinolite schist, hornblende-plagioclase schist and hornblende-chlorite schist represent the metabasalts of HSB. The metapelites

occurring as thick horizons are interlayered with metavolcanics and consist of quartz-chlorite schists, chlorite schist, and carbonaceous phyllites. The Iron Formations are about 50-100km thick and alternate with the metapelites. Banded hematite quartzite, chert and banded hematite jasper, ferruginous meta-argillites make up the framework clasts within BIF. Minerals like muscovite, chlorite and quartz make the metapelites and occur as thick horizons. Polymictic conglomerate also occurs along with the metapelites. Massive dykes of gabbro about 5-10m intrude the HSB and trend E-W.

- *Closepet Granite*

The Closepet granitic batholith trending N-S is about 400 km long and 20–30 km wide, with its margins sheared (Meert and Pandit 2015). It serves as a basement rock for the overlying sedimentary cover rocks towards the northern as well as south-eastern part of the basin. This leucocratic body is two-feldspar granite composed essentially of quartz, plagioclase, microcline, and biotite along with accessory sphene, schorl, apatite, zircon, magnetite, pyrite, and anatase. The medium grained granite is characterised by larger grains of quartz, microcline and plagioclase forming a hypidiomorphic composite. The poikilitic texture is marked by the presence of euhedral plagioclase, rounded to sub-rounded grains of quartz and biotite mica included within the relatively larger anhedral to subhedral grains of microcline. Medium grained plagioclase exhibits normal zoning. At places the plagioclase is sericitised. Intergrowth of myrmekites and flame perthites are common. Compositional variation of the granite ranges from granodiorite to monzogranite (Dey *et al.,* 2009). Being referred to as a 'stitching pluton' (Ramakrishnan and Vaidyanadhan, 2008; Meert and Pandit, 2015), this granitic body has been dated as of 2513 ± 5 Ma (Friend and Nutman, 1991) and is considered to be a part of the Neo-Archean phase of plutonism (Mojzsis *et al.,* 2003; Maibam *et al.,* 2011; Jayananda *et al.,*

2013), formed during the suturing of the eastern and western cratons. It is known to mark the stabilisation age for both the eastern and western Dharwar craton (Meert *et al.*, 2010). The granites have a low-Al TTG affinity and high SiO_2, Na_2O content with moderate to high concentrations of Cr and Ni; also present within are a large number of amphibolite xenoliths and microgranular enclaves (Dey *et al.*, 2009).

3.2.2 Composition of the sedimentary cover rocks

The Kaladgi Supergroup is divided into two Groups; an older Mesoproterozoic Bagalkot Group and a younger Neoproterozoic Badami Group separated by a distinct angular unconformity. On the basis of a disconformity and the presence of a basal conglomerate the Bagalkot Group is further divided into two Subgroups namely the older Lokapur and younger Simikeri Subgroup. The Subgroups are based on the difference in facies which ranges from clastic coarse to fine gain size grading into nonclastic chemogenic. This oscillatory cyclic type of deposition is attributed to a sinking type of cratonic basin which witnessed repeated episodes of marine transgression (Kale and Phansalkar, 1991). The Lokapur Subgroup comprises of five Formations namely Ramdurg as the oldest followed by Yargatti, Yendigeri, Muddapur, Yadhalli. The lithounits on which this study is based form a constituent of the basal Ramdurg Formation which is about 475m thick. Outcrops of these units are well exposed at Bilgi, Jamkhandi, Salgundi and Ramthal. The Formation comprises of three Members: the Salgundi Conglomerate, Saundatti Quartzite and Manoli Argillite in ascending order (Jayaprakash *et al.*, 1987; Bose *et al.*, 2008). The general lithostratigraphy of the Kaladgi Supergroup is presented in Table 3.1.

Of the two Subgroups that are separated by a disconformity, the older Lokapur Subgroup is the thickest (3.1km) and occurs throughout the basin. The younger Simikeri Subgroup on the other hand is confined towards the east-central parts of the basin. The Mesoproterozoic Bagalkot Group hosts a variety of rocks which include coarse siliciclastic rocks like conglomerate, arkose as well as cherts along the basin margins that give way to the argillites and carbonate rocks towards the basin interior (Kale and Phansalkar, 1991; Pillai and Kale, 2011). The coarse siliciclastic facies formation is attributed to marginal marine to shallow water depositional environments which include braided delta fronts and long linear beach representing a paleocoast (Bose *et al.,* 2008; Pillai and Kale, 2011). The siliciclastic facies grade laterally and vertically into argillite facies. These are parallel laminated, fissile and reflect a tidal flat environment of deposition. Towards the interior of the basin the argillite facies grade into carbonate facies. The carbonate facies occur as thin bedded laterally extensive deposits formed to reflect waves and tide dominated mud and carbonate flats with a gentle slope (Jayaprakash *et al.,* 1987; Kale *et al.,* 1996; Jayaprakash, 2007)

The younger undeformed Neoproterozoic horizontal Arenites of Badami's extend E-W for a stretch of about 200 km and unconformably overlie the Archaean basement rocks and the Bagalkot Group of rocks. This Badami Group is separated from the Simikeri Subgroup of the older Bagalkot Group by an angular unconformity. In the southern part of the basin it overlies the Lokapur Subgroup and at places the Archean basement rocks. They are moderately well to poorly sorted subarkose to arkosic wacke in composition consisting of quartz and feldspars forming the dominant framework clasts with considerable amount of sericitic matrix. The arenite at places contains fragments of the rocks from the older Bagalkot Group indicating recycling (Dey, 2006).

3.2.3 Structure of the Kaladgi-Badami Basin

The Kaladgi basin strikes E-W along its longer axis which is at an angle to the basement rocks which strike NNW-SSE. This means the basement rocks and the orientation of the sedimentary cover rocks is highly contrasting and therefore the older basement must have not participated in the deformation process of the younger rocks or its deformation has not been later than the younger rocks.

Two distinct unconformities are defined within the Kaladgi Supergroup (Table 3.1). Towards the North of the basin, the sediments overlie a tectonically undeformed granite forming non-conformity whereas towards the east an angular unconformity separates the sedimentary sequence from the older Hungund Schist Belt (Kale and Pillai, 2011; Mukherjee *et al.*, 2016).

3.2.4 Age of Kaladgi-Badami sedimentary sequence

No isotopic data is available on the Kaladgi sediments. The pervious suggestion that the Bagalkot Group belongs to the Late Paleoproterozoic age based on stromatolitic studies (Sharma *et al.*, 2012) is supported further by geochronological studies indicating a Mesoproterozoic age for the Group that was deposited around 1800 $\pm$ 100Ma (Padmakumari *et al.*, 1998; Balesh Kumar *et al.*, 1999). Based on lithostratigraphy, Kale and Phansalkar (1991) have correlated the Kaladgi Supergroup of rocks with the unmetamorphosed Mesoproterozoic and Neoproterozoic succession of similar other supracratonic Purana basins of Peninsular India.

3.2.5 Deformation of the Kaladgi-Badami sedimentary sequence

As reported, the sedimentary cover occupying the northern portion of the Kaladgi basin (*e.g.* Bilgi and Jamkhandi) remained undeformed whereas the south-central part of the basin (*e.g.* Salgundi and Ramthal) is highly deformed (Jayaprakash et al., 1987; Jayaprakash, 2007; Mukerjee et al., 2016). The deformation is observed in the form of elongated regional dome and basin patterns oriented WNW-ESE to E-W. This deformation is explained to have occurred as a result of gravity gliding of the sedimentary rocks from north towards south over the underlying basement leading to decoupling between them. The unconformity separating the older basement rocks from the younger sedimentary cover, itself serves as the detachment surface along which the sliding occurred. The compressive stresses during the terminal phase of the Sausar Mobile Belt (SMB) and Eastern Ghat- Rayner (EGRY) orogeny around~ 1000 – ~ 800 Ma produced a mild flexure of the crust that resulted in the upliftment of the basement rock towards the northern part of the basin. This subsequently led to the sliding of the sedimentary cover rocks over the basement rock from the northern side under the influence of gravity. Also, the sedimentary cover rocks from the northern and south-central section are spatially related as a part of a single deformational event (Mukerjee *et al.*, 2016).

3.3 Stratigraphy of the Kaladgi Supergroup

3.3.1 Bagalkot Group

The Bagalkot Group is divided into two Subgroups, namely the older Lokapur and younger Simikeri Subgroup. The Lokapur Subgroup consists of five Formations namely the Ramdurg, Yargatti, Yendigeri, Muddapur and Yadhalli whereas the Kundargi,

Arlikatti and Hoskatti are the three Formations belonging to the younger Simikeri Subgroup. As compared to the Simikeri Subgroup the areal extent of the Lokapur Subgroup is larger.

3.3.1.1 Lokapur Subgroup: This Subgroup consists, mainly of arenaceous to argillaceous facies of rocks towards the margins of the basin whereas towards the centre they are non clastic carbonate facies of rocks. There are thirteen Members belonging to the five Formations in this Subgroup as follows

- **Ramdurg Formation:** consists of arenaceous and argillaceous sediments with a prominent basal conglomerate.

i. *Salgundi Conglomerate Member*: The base of the Kaladgi Supergroup is marked by a distinct conglomerate resting unconformably over the Archean basement rocks. This lithounit is best exposed at Salgundi and Ramthal. Wherever the conglomerate rests over the schistose rocks the pebbles and cobbles are of banded haematite quartzite, vein quartz, chert and wherein the basement is of granitic rocks the conglomerate is oligomictic, with well-rounded pebbles of vein quartz, quartzite, chert, jasper, and fresh feldspars.

ii. *Saundatti Quartzite Member*: wherever the basal conglomerate is insignificant the quartzitic Member forms the lowermost Member of the Subgroup. The Saundatti Quartzites form a marker horizon and demarcates the basin boundary of the Bagalkot Group forming linear ridges. The thickness of the Member is 370m with composition varying from quartz arenite, feldsarenite, subfeldsarenites to quartzwacke. This Member is seen exposed at Bilgi and Jamkhandi.

iii. *Manoli Argillite Member*: Immediately above the quartzites and with a gradational contact the Manoli Argillite occurs as a thin band. The argillite is brown to purple in colour with prominent bedding fissility.

- **Yargatti Formation**: is essentially made up of chert breccia, argillite and dolomite Members.

i. *Mahakut Chert breccia Member*: occurs as lensoidal bodies with a maximum thickness of 133m. It is composed of pink, fine-grained, cryptocrystalline to microcrystalline, tough matrix in which angular fragments of chert are welded.

ii. *Muttalgeri Argillite Member*: is one of thickest Member of the Bagalkot Group. As a result of facies variation argillite are locally carbonate-rich and due to weathering generate kankar.

iii. *Chitrabhanukot Dolomite Member*: near the core of the basin this Member forms a circular dome. Colour of the rock varies from grey, blue-grey to dark grey. Presence of stromatolite is reported from this Member.

- **Yendigeri Formation**: is represented by smoky blue argillite, limestone and black dolomite Members.

i. *Hebbal Argillite Member*: is soft, friable, smoky-blue Argillite best exposed at Hebbal and is often intruded by small quartz veins parallel to the bedding.

ii. *Chikshellikeri Limestone Member*: The member is more than 800m thick and is informally divided into (a) variegated limestone and (b) grey limestone. This Member shows intricate fold patterns.

iii. *Naganur Dolomite Member*: has maximum thickness of around 100m and the black colour of the dolomites is attributed to organic matter.

➢ **Muddapur Formation**: The lithological constituent of this Formation is similar to Yendigeri Formation except that the dolomite Member attains a maximum thickness of 400m and is stromatolite-bearing.

i. *Jalikatti Argillite Member*: This unit serves as a marker horizon in the repeated dolomite and limestone sequences of the Bagalkot Group. Exposures' ranging from black to black in colour, this unit is well developed in the central part of the basin. The rock is phyllitic and has prominent cleavage parallel to the bedding plane.

ii. *Petlur Limestone Member*: has limited areal extent and thickness and is subdivided into (a) variegated limestone and (b) grey limestone.

iii. *Bamanbudai Dolomite Member*: the rock unit is light grey in colour with low magnesia. The Formation includes two argillite bands of more than 5m thickness. They are disconnected and impersistant over longer distances suggesting frequent facies variation.

➢ **Yadhalli Formation:** Argillite, smoky blue to purple coloured soft, fissile to massive rock units form the uppermost Member of the Lokapur Subgroup.

Disconformity: After the deposition of the Lokapur Subgroup, the sedimentation process appeared to have ceased with the retreat of the sea for a short period and upliftment, weathering and erosion of the Formation occurred to some extent. On the denuded surface of the Yadhalli Formation, deposition of the Simikeri Subgroup began with a conglomerate horizon lying in disconformity to the preceding sequence.

3.3.1.2 Simikeri Subgroup: This Subgroup is composed of rocks similar in composition to Lokapur Subgroup, but with smaller areal extent. This Subgroup of sediments is confined to the central portion of the basin and occurs as elongated, doubly plunging synclines and anticlines of different dimensions with the long axis trending in the east-west direction. It includes three Formations and seven Members which are as follows.

- **Kundargi Formation**: includes three Members of arenaceous and argillaceous components that are identical to Ramdurg Formation of Lokapur Subgroup.

i. *Bevinmatti Conglomerate Member*: occurs as discontinuous lenses, developed with maximum thickness of 15m. At places, the clasts are elongated or stretched parallel to the bedding plane.

ii. *Muchkundi Quartzite Member*: has a maximum thickness of 200m; medium to thickly bedded and well sorted. The original texture is obliterated by secondary growth.

iii. *Govindkoppa Argillite Member*: is resistant with exposures subdued by the underlying and overlying units. Repeated purple and brick red coloured fine lamellae are common.

- **Arlikatti Formation**: Heamatite schist Member sandwiched between non clastics constitutes this Formation wherein hematite schist occurs as discontinuous beds of varying thickness. Unlike the Chert breccias from Lokapur Subgroup these do not stand out prominently forming ridges.

i. Niralkeri Chert-breccia Member: this lowermost member is about 10 to 15m thick, white with massive chert beds. They show sharp contact with the underlying argillite. It formed as a result of chemical precipitation and is dull and tough showing oolitic texture. The Member forms smooth to flat topped linear ridges along quartzites.

ii. *Kerkalmatti Hematite schist Member*: this Member is in sharp contact with the underlying and overlying units. Despite its irregular thickness and limited areal extent, it is

distributed throughout the basin in disconnected patches. Hematite is massive with thin bands of chert, jasper and quartzite; compositionally the schist is argillaceous or siliceous.

iii. Lakshanhatti Dolomite Member: This dolomite is grey to smoky blue in fresh cuttings and deep grey on weathered surfaces, with interbedded dark brown, black and white cert ribbons.

- **Hoskatti Formation**: This Formation is similar to the Yadhalli Formation but there is only one argillite Member exhibiting a series of minor folds.

i. *Dadanhatti Argillite Member*: This is the youngest lithounit in sedimentary sequence of Bagalkot Group. Since this Member forms the core of the basin, it has suffered higher degree of deformation, as a result of which the beds display a series of minor folds.

ii. *Mallapur Intrusives*: Rocks of Bagalkot Group are intruded with both acid intrusives consisting of quartz vein and pegmatite veins of hydrothermal origin parallel to the bedding plane as well as basic intrusives represented by dolerite dykes. Nowhere these dykes intrude the younger Badami Group of rocks.

3.3.2 Badami Group

The Badami Group of sediments overlie the sediments of the Bagalkot Group as well as basement granitoids with a distinct angular unconformity and is marked by the presence of a conglomerate. The Group includes two Formations and six Members.

- **Kerur Formation**: consists of four Members, mostly arenaceous in character. The basal conglomerate member has great stratigraphic value in separating the Bagalkot Group from the younger Badami Group of rocks.

i. *Kendur conglomerate Member*: The conglomerate with a thickness of 5m is seen overlying the granitoids, metasedimentaries and a few members of Bagalkot Group thus suggesting a major unconformity and hiatus heralding the deposition of a new group of sediments.

ii. *Cave-temple Arenite Member*: with a maximum thickness of 150m; this member is well developed and forms flat topped barren hillocks with vertical scarps or small mounds and elevated grounds.

iii. *Halgeri Shale Member*: with a thickness of m this Member is constituted of beds of shales which are bottle green to greenish yellow in colour, friable with convolute laminations and rich in micaceous minerals. This shale acts as a key bed to separate the arenite members in the Badami Group.

iv. *Belikhindi Arenite Member*: is in sharp contact with the underlying unit. These arenites lack ferruginous matter and have peculiar geomorphic expression i.e. forming smooth hills with a lighter tone and a thin soil cover supporting thorny bushes. While primary sedimentary structures like cross bedding, ripple marks, casts and convolute lamination are present in cave temple Arenite member, these are rarely recorded in this Member.

- **Katgeri Formation**: Shale having an larger areal extent and younger limestone which is flaggy are the two Members representing this Formation.

i. *Halakurki Shale Member*: The rock is chocolate brown to dark brown in colour, finely laminated distinctly bedded with prominent bedding fissility.

ii. *Konkankoppa Limestone Member*: is the youngest Member of the Kaladgi Supergroup with gradational contact with the underlying shale. The limestone is flaggy, medium-

bedded, bottle green, cream, buff and pale grey with frequent partings and fine colour banding.

3.3.3 Younger rocks

Deccan Traps: partly cover and conceal the Kaladgi Supergroup of rocks in different areas. A total of 3 flows are recognised of slab pahoehoe type. At places red bole beds mark the contact, intertrappean beds of immature argillaceous and carbonate bearing sandstone are also recorded.

Table 3.1 Lithostratigraphy of the Kaladgi Basin (*modified after* Jayaprakash, 2007).

Supergroup	Group	Subgroup	Formation	Member	Thickness (m)
Kaladgi	Badami (Neoproterozoic)		Katageri	Konkankoppa Limestone	85
				Halkurki Shale	67
				Belikhindi Arenite	39
			----------	----------*Sharp contact* ----------	----------
			Kerur	Halgeri Shale	03
				Cave Temple Arenite	89
				Kendur Conglomerate	03
	----------	----------	----------	*Angular unconformity* ----------	----------
	Bagalkot (Mesoproterozoic)	Simikere	Hoskatti	Argillite	695
			----------	----- *Transitional contact* ---------	----------
			Arlikatti	Lakshanhatti Dolomite	87
				Kerkalmatti ferruginous member	42
				Neralkeri Chert	39
				Govindkoppa argillite	80
			----------	------- *Transitional contact* ---------	----------
			Kundargi	Muchkundi Quartzite	182
				Bevinmatti Conglomerate	15
		----------	----------	*Disconformity* ----------	----------
		Lokapur	Yadhalli	Argilite	58
			----------	*Transitional contact* ----------	----------
			Muddapur	Bamanbudni Dolomite	402
				Petlur Limestone	121
				Jalikatti Argillite	43
			----------	------- *Sharp contact* ----------	----------
			Yargatti	Nagnapur Dolomite	93
				Chikkashellikere Limestone	883
				Hebbal Argilite	166
			----------	------- *Transitional contact* ----------	----------
			Malprabha	Mahakut Chert	133
				Manoli Argillite	61
			----------	------- *Transitional contact* ----------	----------
			Ramdurg	Saundatti Quartzite	383
				Salgundi Conglomerate	31

----------Non-conformity----------

Basement Rocks (Archaean) Granitoids, Gneisses, and Schist belts

3.4 Location of the study areas

To understand the relationship between the Mesoproterozoic cover rocks and the underlying basement, this study focuses on the lowermost Member of the Ramdurg Formation. The lithounits representing it have their outcrops extensively exposed at Bilgi, Jamkhandi, Ramthal and Salgundi.

These four areas lie round the town of Bagalkot in the state of Karnataka and encompass a part of the Mesoproterozoic sedimentary cover. Since the lithounit studied at these places is the oldest Member, its serves to correlate the composition with the basement rock and also, to understand the deformational history in relation to the basement rock. Tors of pink Granite which form one of the basement rock is well exposed along hill slopes at Bilgi (Karnataka) between latitude $16^0$20'00"N to $16^0$20'29"N and Longitude $75^0$26"22' E to $75^0$37'48"E. (Fig. 3.3). At Jamkhandi the younger Mesoproterozoic sedimentaries are very well exposed supposedly resting over Closepet Granite. The exposures of the outcrops lie between latitude 16°30'00"N to 16°30'30"N and longitude 75°16'00"E to 75°16'50"E. These sedimentaries same as at Bilgi stratigraphically belong to the Lokapur Subgroup of the Bagalkot Group of the Kaladgi basin (Fig 3.4). The study area of Salgundi is located between latitudes 16°12'20"N to 16°12'39"N and longitude 75°43'0"E to 75°43'20"E (Fig. 3.5); and Ramthal between latitude 16°05'00"N to 16°05'15"N and longitude75° 52'20"E to longitude75° 52'30" E (Fig. 3.6) are chosen as representative areas for the study since the rocks representing the lower part of the Kaladgi sequence are well exposed and represented here. While, exposures at Ramthal are over a small hillock with scanty vegetation; at Salgundi; the rocks are exposed over a ridge trending E-W.

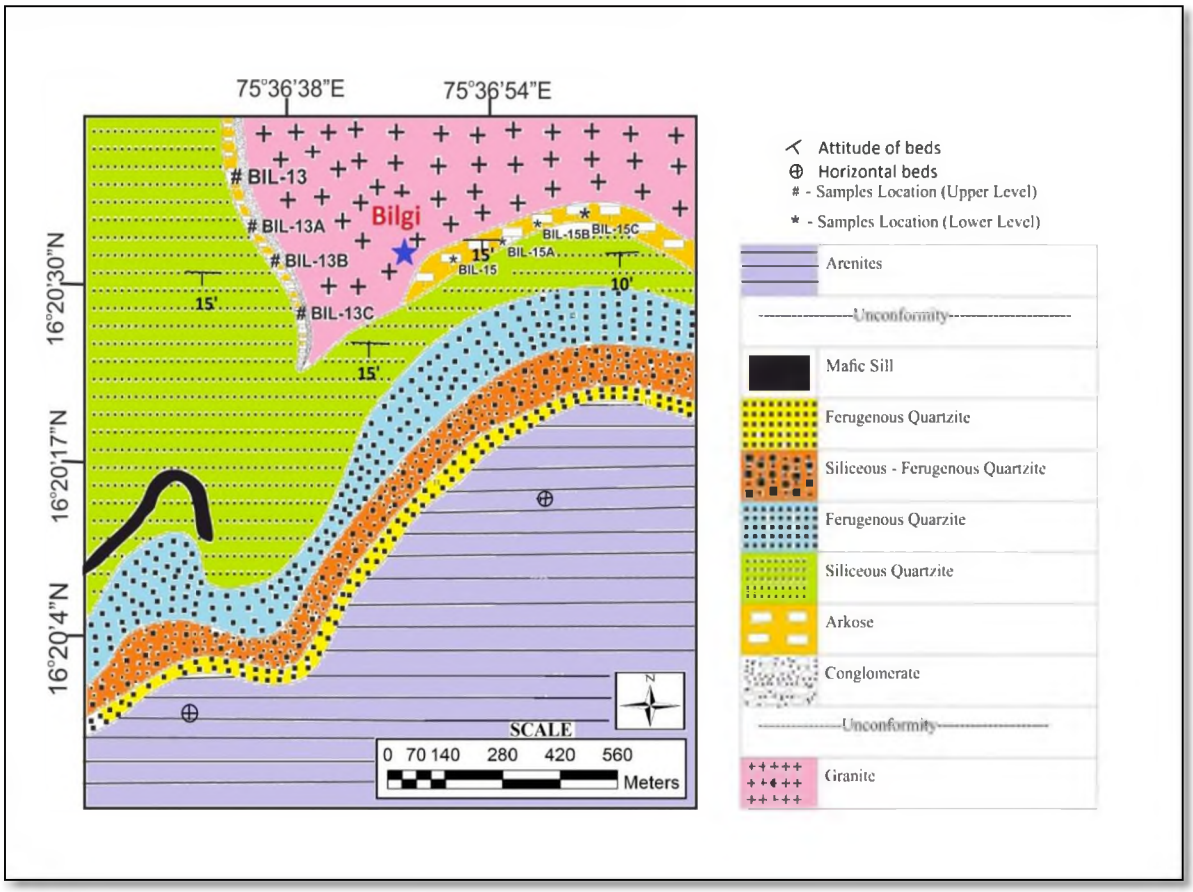

Figure 3.3 Geological map along with sample locations at Bilgi.

PAGE 29-32

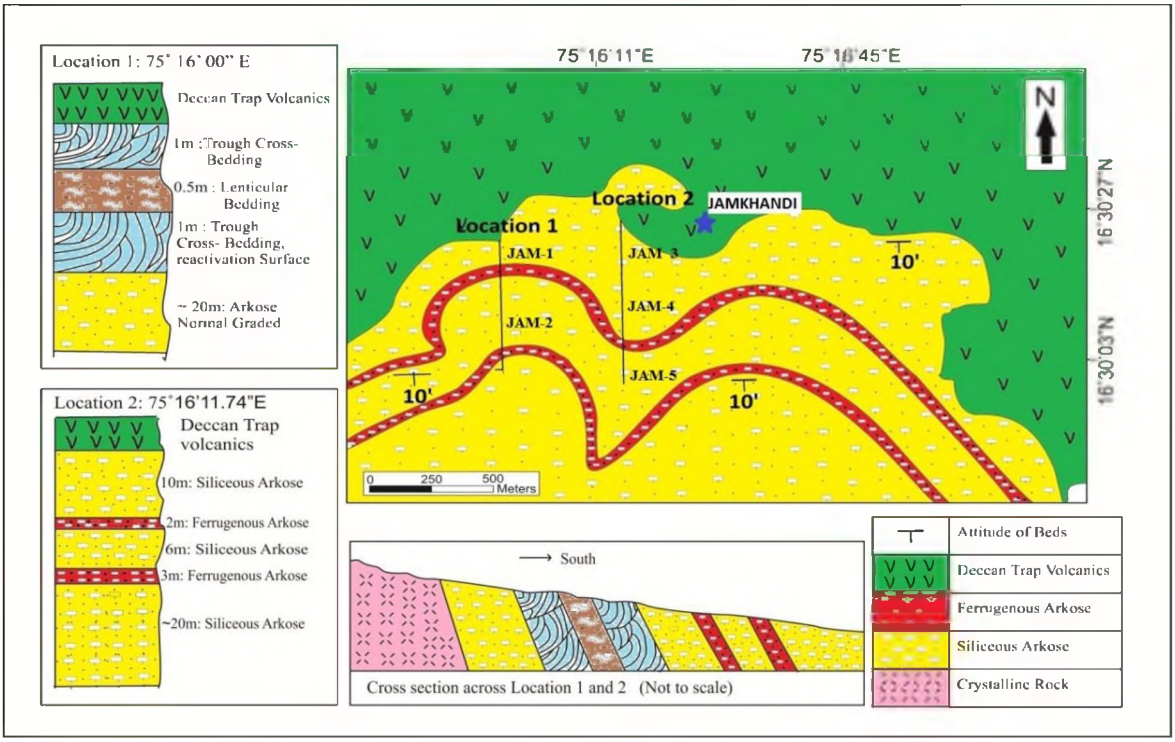

Figure 3.4 Geological map along with sample locations at Jamkhandi.

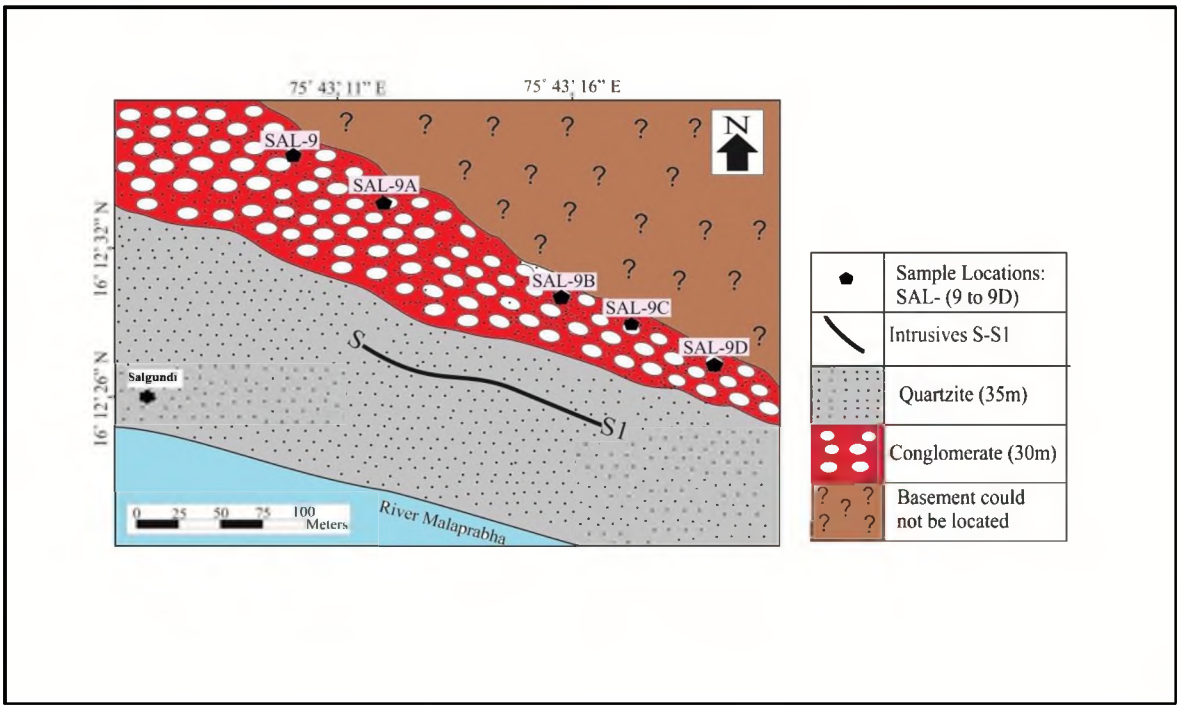

Figure 3.5 Geological map along with sample locations at Salgundi.

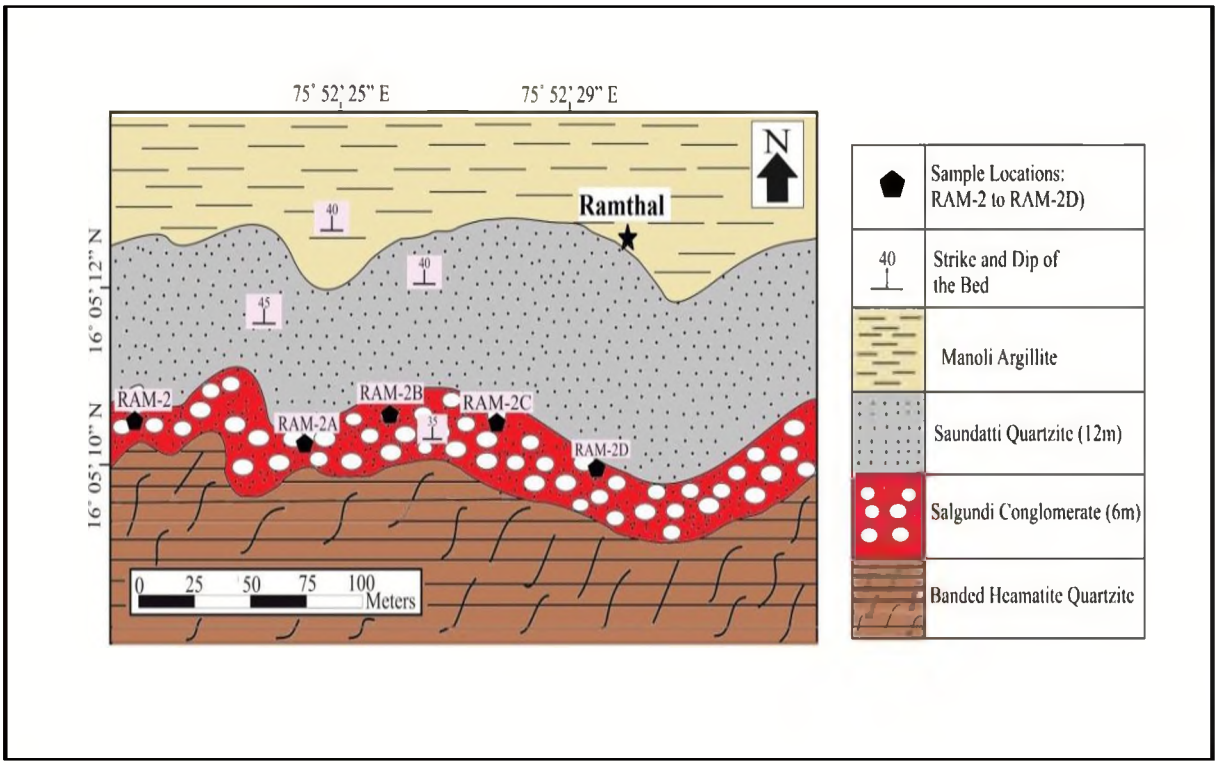

Figure 3.6 Geological map along with sample locations at Ramthal

CHAPTER 4

FIELD OBSERVATIONS AND ANALYTICAL METHODS

4.1 Introduction

As the focus in this research has been laid in establishing and understanding the relation between the lowermost rock units of the Ramdurg Formation and the underlying basement the study in a reconnaissance survey and a review of earlier literature had marked out Bilgi Jamkhandi Ramthal and Salgundi as the representative areas. Outcrops of these rocks are well exposed besides being easily accessible in these areas. The outcrops here representing the lower Lokapur Subgroup of the Bagalkot Group range from coarse to fine siliciclastic rocks. An intensive field study was since carried out covering these representation areas that involved collecting rock samples and noting of outcrop features on megascale.

This chapter also provides an account of the several laboratory techniques employed as a part of the research. At the first stage the rock samples collected in the field were cleaned and subjected to systematic laboratory procedures that involved preparation of microsections from chips and breaking and crushing of each of the sample to powder to be used for geochemical analysis. Microsections were used to identify presence of microstructures if any besides petrographic studies and in making modal calculations. As detailed investigations were needed of individual grains the microsections were also observed under a Scanning Electron Microscope, and subjected to Energy Dispersive Spectroscopy (SEM-EDS).

The crushed samples were utilised for geochemical analysis involving X-Ray Fluorescence (XRF) for determining major oxide compositions and Inductively Coupled Plasma-mass Spectrometry (ICP-MS) for determining trace and Rare Earth Elements concentrations in the bulk rock samples.

4.2 Field Observations: Geology of the study areas

4.2.1 Bilgi

- *Location and Topography*

The town of Bilgi is about 24kms North of Bagalkot along the Bijapur-Raichur highway. A range of hills with elevation in excess of 600m strikingly mark the topography of the town. This range of hills bordering the town show steep escarpment on one side, while the other exhibits a gentle dip slope. This pattern is very distinctive forming narrow, V-shaped valleys that are drained by seasonal streams. The hills are sparsely vegetated with thorny bushes. The jointing pattern in the rocks probably supports the vegetation in a semi-arid climate. The exposures here lie between latitude $16^{0}20'00"N$ to $16^{0}20'29"N$ and Longitude $75^{0}26'22"E$ to $75^{0}37'48"E$. A 25m thick arkosic sequence belonging to the Mesoproterozoic Salgundi Conglomerate Member of the Ramdurg Formation of the Bagalkot Group is well exposed all along the foot hills. The sequence rests unconformably over the pink Closepet Granite with a non-conformity marked by the arkosic bed (Fig. 4.1). The rocks strike E-W with dips of 15°S. Inliers of Neoproterozoic Badami cave arenites are found here to overlie the Mesoproterozoic sedimentary cover.

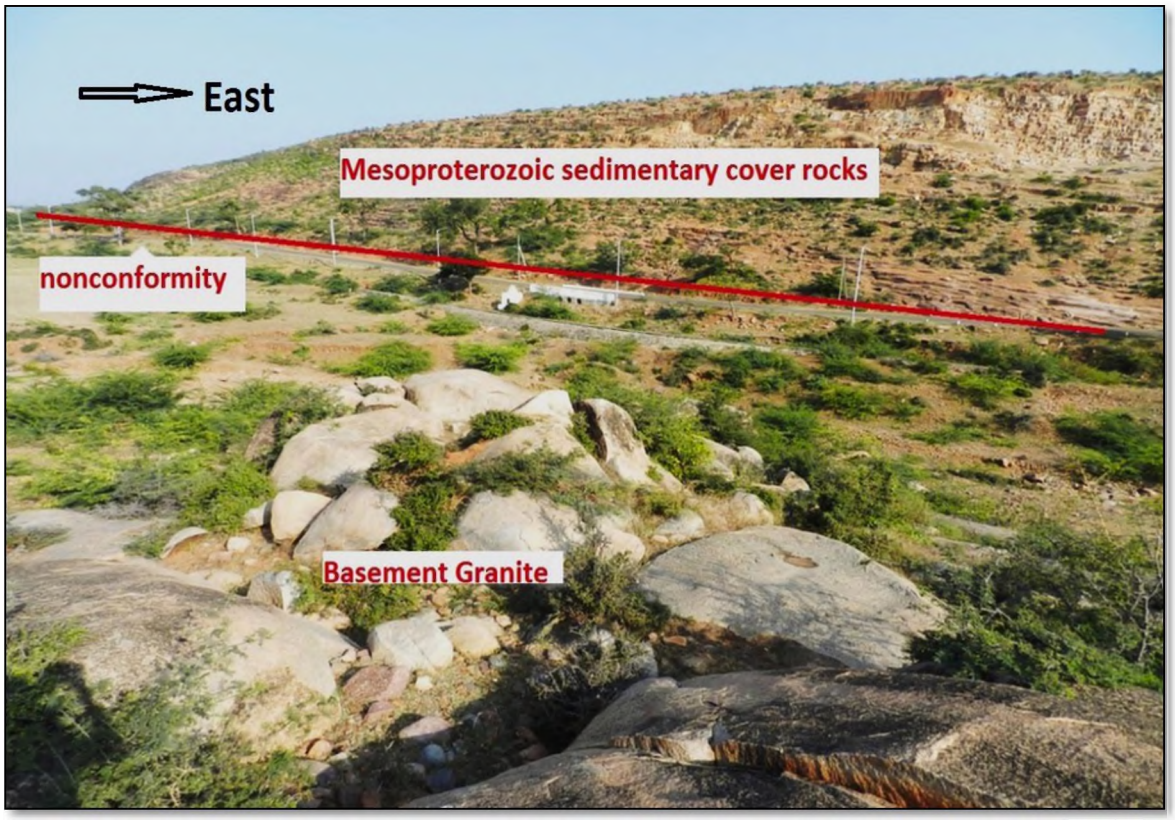

Figure 4.1 Mesoproterozoic sedimentary cover separated by nonconformity from Closepet Granite.

➢ *Basement rock at Bilgi*

The Closepet Granite that separates the eastern from the western Dharwar craton intruded during the late Archean times represents the basement rock for the overlying sedimentary sequence at Bilgi. Good large exposures of the rock are seen at the foot of the hills in the form of tors. It is reported to vary from granodiorite to monzodiorite in composition and is characterised by the inclusions of several amphibolite xenoliths and microgranular enclaves (Dey *et al.*, 2009). It is considered to mark the stabilisation age for the two cratonic parts of the Dharwar craton (Meert *et al.*, 2010). Pink coloured alkali feldspar and some plagioclase along with quartz constitute the groundmass as well as the phenocrysts of this leucocratic body. The accessory minerals include biotite, schorl, zircon, sphene and

opaque minerals. Very prominent are a number of intervening pegmatitic veins restricted within the granitic body while no such quartzofeldspathic vein is noticed to intrude both the granites as well as the sediments (Fig. 4.2).

This two-feldspar Granite shows inconsistent compositional layering of alternating felsic and mafic minerals. Undeformed as it has remained it is devoid of any visible preferred orientation of minerals that would indicate penetrative tectonic fabric. Only exception is the undulose extinction exhibited in thin sections which is attributed to post-solidification microstructural adjustment during cooling (Mukerjee *et al.*, 2016). The Mesoproterozoic sedimentary sequence here comprising of the arkose at the bottom followed by quartzitic sandstones unconformably overlies this granitic body.

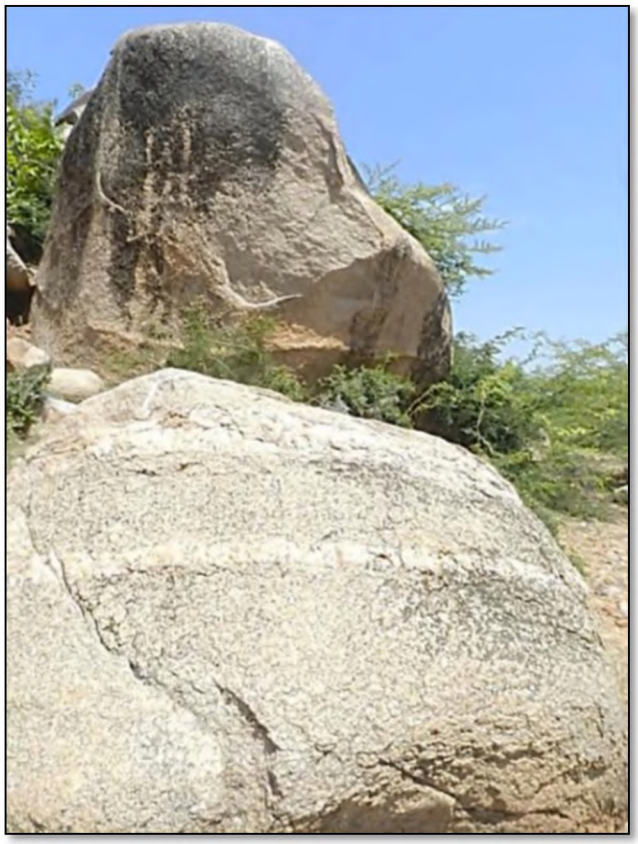

Figure 4.2 Tors of Closepet Granite intervened by pegmatitic veins

- *Mesoproterozoic sedimentary cover at Bilgi*

The arkosic rock that is superposed over the Granite is composed partly of siliceous to argillaceous and partly ferrugenous matrix. Framework clasts of subrounded quartz and angular feldspars enclosed within appear matrix supported. The clasts of quartz range between 2cm – 10cm in length, while the feldspars are up to 3cms long. The feldspars are pink and relatively fresh presumably derived from the underlying basement (Fig. 4.3). Depositional grading has resulted in larger fragments at the bottom followed successively by smaller sizes. An increase in percentage of quartz content is observed with a concomitant decline in feldspars from the bottom towards the top of the section indicating mineralogical maturity. Some of the feldspars show a pitted appearance.

Exposures of the arkosic rock show deformative characters in the form of penetrative features in the field. The bedding plane markedly denotes the S_0 foliation having E-W strike with dips varying from 10° to 15°S. The clasts are stretched, elongated and flattened (Fig. 4.3) representing solid-state deformation imparting the S_1 foliation to the rock (Fig. 4.4). The S_1 has strongly developed sub parallel to S_0 as a set of closely spaced planes and is penetrative on outcrop scale. The S_0 and S_1 are transacted by a steeper set of relatively widely spaced cleavage planes representing S_2 in the rock. Reorientation of S_0 and S_1 grains and new grain development can be observed along the S_2 trending almost SE (Fig. 4.4).

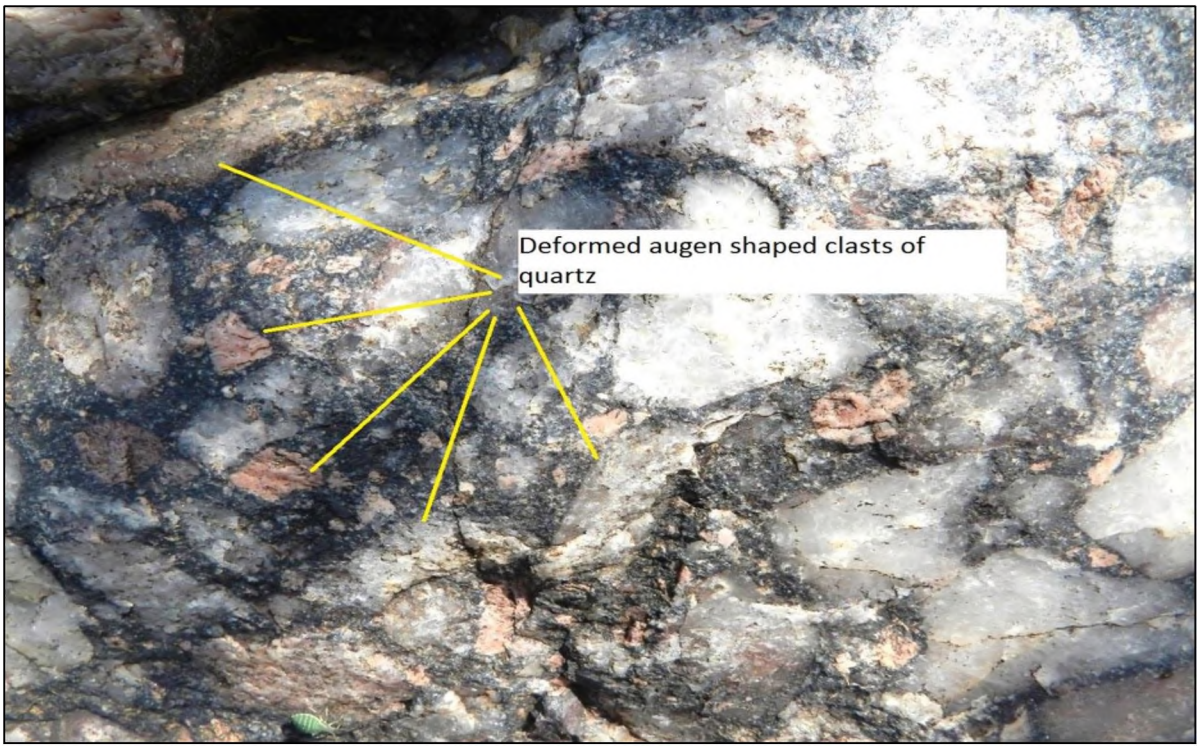

Figure 4.3 Deformed clasts of quartz and K-Feldspar within the arkosic sandstone.

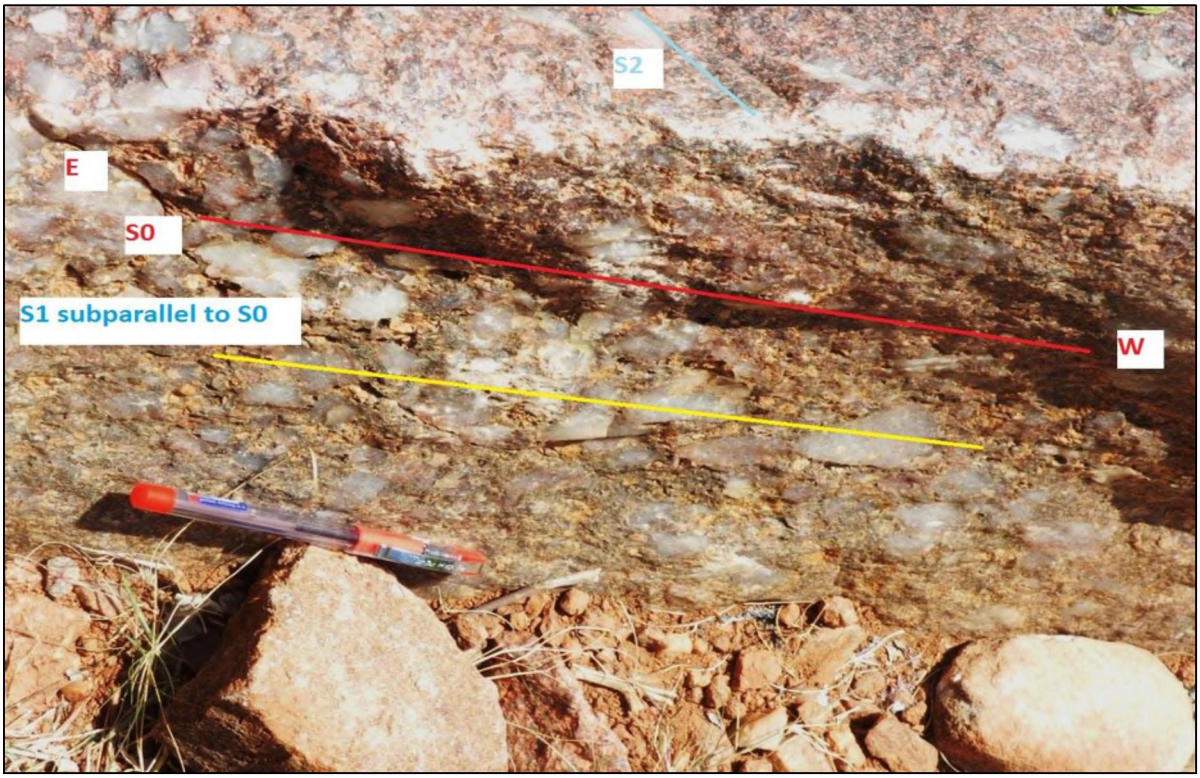

Figure 4.4 Reorientation of S_0 and S_1 grains and a new grain development along the S_2 in the arkosic rock.

The quartzitic sandstones that conformably follow the arkosic rock are exposed from an elevation of 564m above msl. Though dominantly siliceous at the bottom, their matrix is more ferruginous upwards, displaying a rhythmic alternation of siliceous and ferruginous character further on. The exposures are massive and the rock is compact maintaining the same E-W strike and 15°S dip as the underlying arkose. Of the three prominent joint sets, two are vertical trending E-W and N-S respectively, while the third is the bedding joint. Leaching of iron has caused the formation of a layer of incrustation on the joint face giving a leopard skin appearance (Fig. 4.5a). Also, secondary quartz mineralisation is commonly noticed filling some of the fractures displaying clear, singly terminated crystals of quartz. Current bedding, well exhibited in the upper levels of the exposure have their cross-beds inclined towards east (Fig. 4.5b). The current ripples on the surface have wavelength ranging between 5-7cms with a trough depth of up to 3cms (Fig. 4.5c). Dendritic algal secretion on the joint surfaces and convolute bedding in some of the layers is quite noticeable (Fig. 4.5d). A mafic sill along with several offshoots is found invading the fractures (Fig. 4.5e).

Remnants of horizontally bedded Badami rocks are exposed as inliers at elevations of >611m above msl. Here, the Bagalkot Group of rocks being more resistant stand at a higher elevation and are surrounded by the Badami Group of rocks (Fig. 4.5f). The Badami rock is an Arenite, displaying current bedding and showing low angle dips of about 5°. The cross layers are more ferrugenous while the arenite is less compact and breaks more easily.

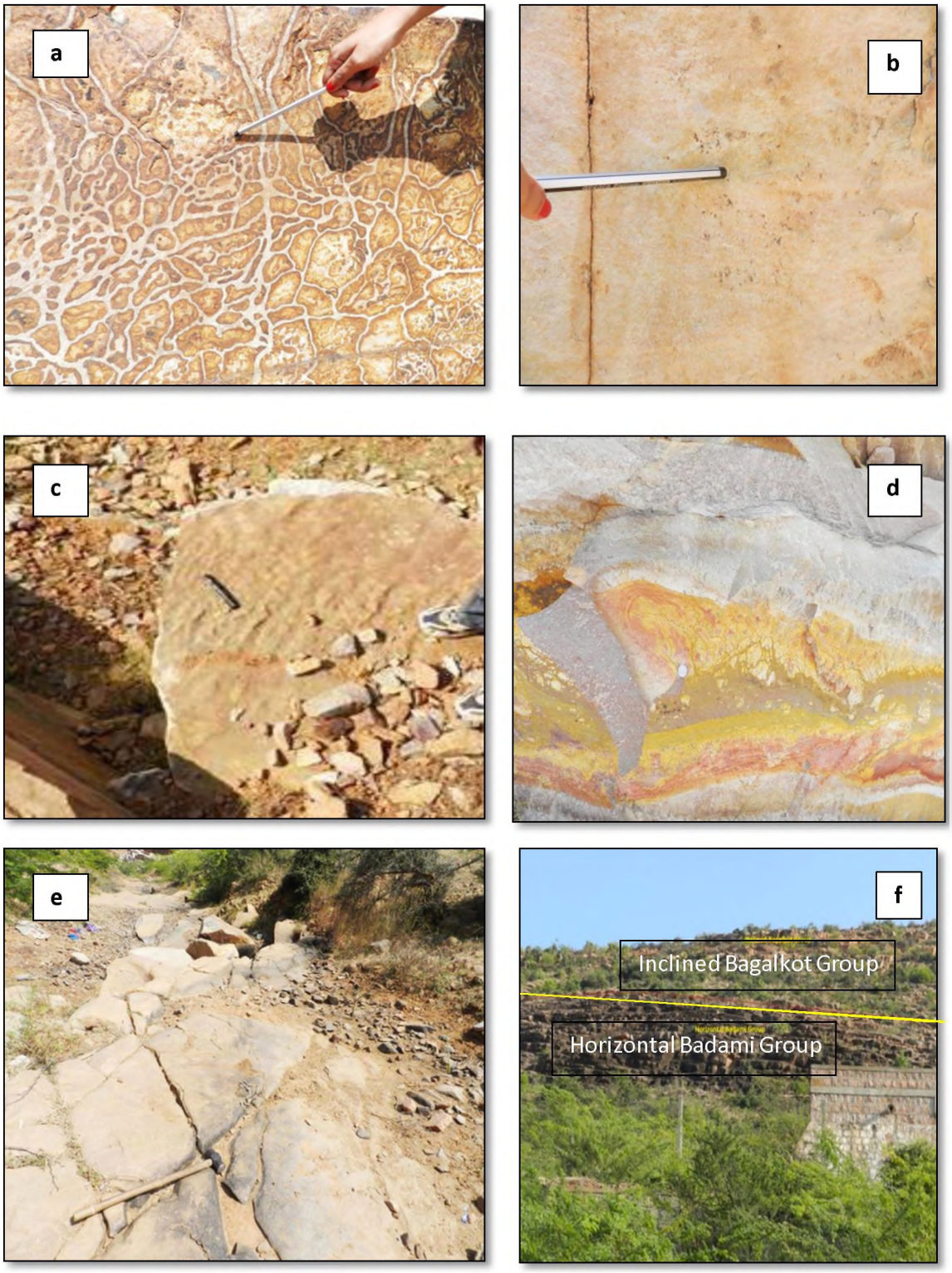

Figure 4.5 (a) Leaching of iron along joint planes in quartzitic sandstone **(b)** cross-bedding inclined towards east in quartzitic sandstone **(c)** current ripples **(d)** convolute bedding **(e)** Intrusion of mafic sills **(f)** Bagalkot Group of rocks exposed as outliers, Bilgi

4.2.2 Jamkhandi

- *Location and Topography*

Jamkhandi is situated about 80kms North of the Bagalkot town between latitude 16°30'00"N to 16°30'30"N and longitude 75°16'00"E to 75°16'50"E. A number of hillocks having elevation of about 600m above msl rise above the surrounding low lands. The hills present a cuesta structure with a steep escarpment slope and a gentle dip slope (Fig. 4.6a & 4.6b). A semi-arid climate has induced sparse vegetation with sporadic thorny bushes.

Figure 4.6 (a) Independent hills surrounded by peneplain **(b)** hills forming a cuesta with a steep escarpment slope and a gently dipping dip slope.

- *Field Observations*

The younger Mesoproterozoic sedimentaries stratigraphically belonging to the Lokapur Subgroup of the Bagalkot Group are well exposed. As reported, these unconformably overlie the Closepet Granite, though no exposures of the same are visible. As at Bilgi, here too the sedimentary cover rocks are composed of a brecciated arkose at the base followed up by partly siliceous and partly ferruginous quartzitic sandstone. They strike East – West with dips varying between 10^0S- 15^0S with a thickness of about 35m.

The brecciated arkose has angular to sub angular pink feldspar and rounded to sub-rounded quartz grains spans the whole thickness (Fig 4.7a). The feldspars are sub-vitreous, with some grains maintaining the original shape, exhibiting two sets of cleavage. They are well preserved and fresh. The quartz is granular and colourless. Both of these form the dominant framework clasts, intermingled within which are pistachio green epidote and smoky brown quartz. While, the grains of quartz and feldspar are relatively much larger in the lower part of the unit; an increase in the content of feldspars is noticeable in the upper parts. Though the matrix is siliceous in general; it includes thin bands of ferruginous matter towards the top (Fig. 4.7b). The rock is poorly sorted, oligomictic and matrix supported.

Figure 4.7 (a) Clasts of feldspar and quartz in arkosic sandstone, Jamkhandi **(b)** Interbedding of ferruginous layers within siliceous quartzite, Jamkhandi.

The succeeding quartzitic sandstones display cross-bedded structures, on the surface as several sets. The cross beds range in thickness between 6cm – 8cm with a height exceeding 6cms. In a three dimensional view cross-stratified units can be of two types: Tabular, where the inter–set boundaries are planar and maintaining an angular to tangential contact with the base; and, Trough cross-strata, where the inter-set boundaries are scoop-shaped and maintaining a tangential contact with the base (Fig. 4.8a & 4.8b).

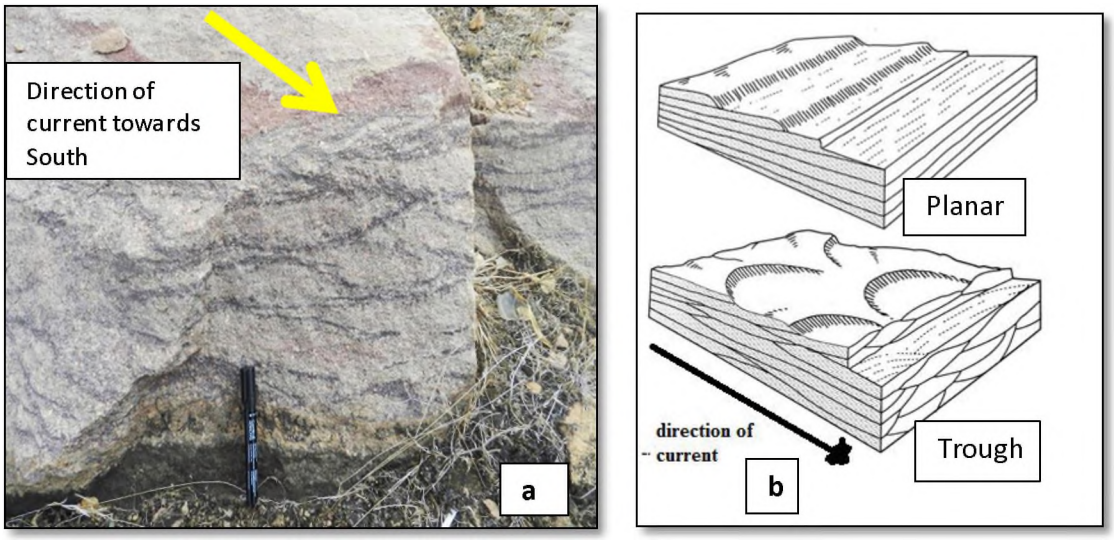

Figure 4.8 (a) Trough cross-stratification within quartzitic sandstone
(b) Block diagram of cross stratification, planar and trough (*Source*: Tucker, 2011)

The cross-bedding observed at Jamkhandi can be classified as trough cross- strata showing scoop-shaped inter-set boundaries; as they have tangential bases and a nested, curved appearance (Fig 4.8a). The indicative direction of paleocurrent depicted by the cross-stratification is towards South. The cross-bedded structures also exhibit lenticular bedding with discontinuous lenses of sand, both vertically and laterally (Fig. 4.9a). The climbing-ripple or chevron type laminations observed at Jamkhandi are of in-phase type suggesting they did not migrate (Fig. 4.9b).

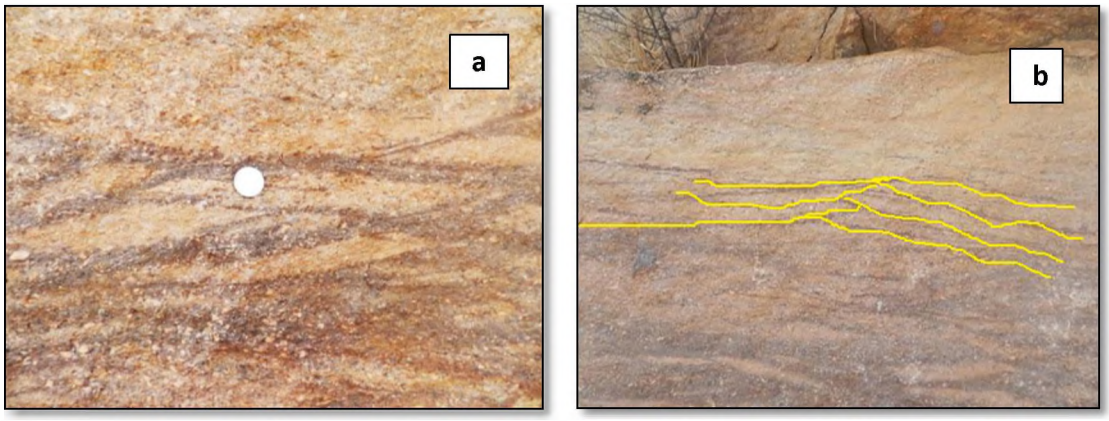

Figure 4.9 (a) Lenticular bedding: thin layers of cross-laminated siliceous lenses (sediment transport right to left) in quartzitic sandstone **(b)** Chevron type up-building (draping foreset) structure of ripples

In some cross-bed sets there are erosional surfaces observed cutting across the cross-strata. These are reactivation surfaces representing short term changes indicating change in flow direction leading to modification of previously formed ripples. These form whenever there is a change in the current direction or when there is a decrease in the depth of water. Such reactivation surfaces are associated with tidal current reversals or formed during storms (Fig. 4.10a & 4.10b).

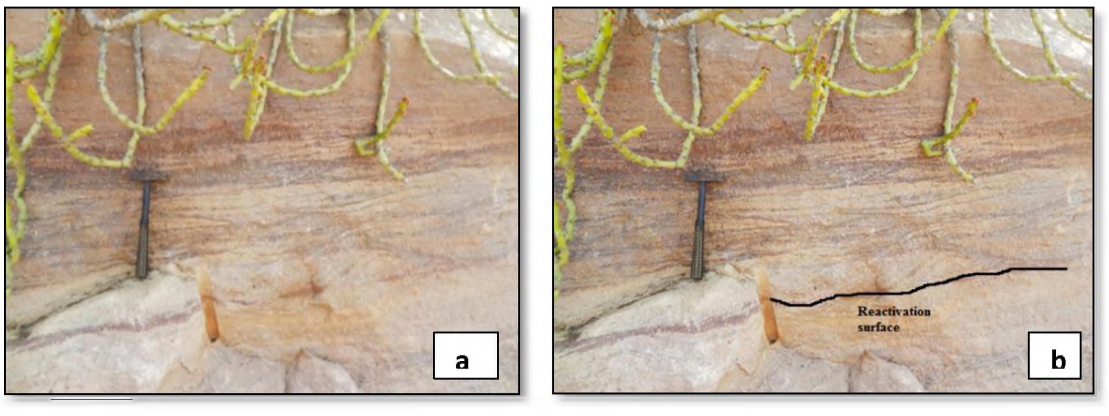

Figure 4.10 (a) Reactivation surface in cross-bedding, Jamkhandi **(b)** Reactivation surface, Jamkhandi.

4.2.3 Ramthal

- *Location and Topography*

The village of Ramthal, located about 20km from the town of Bagalkot lies between latitude 16°05'00"N to 16°05'15"N and longitude 75° 52'20"E to longitude 75° 52'30" E. The terrain is hilly and marked by thorny bushes. Thick beds of Banded Hematite Quartzites interbedded with ferruginous phyllites of the Hungund Schist Belt are exposed at the foot of a hill that rises to an elevation of about 600m above msl. This Archean sequence is steeply inclined representing the limb of a major fold. Overlying unconformity is a 7m thick Mesoproterozoic sedimentary cover comprising of conglomerates at the base followed by quartzitic sandstone at the top. The sequence is reported to belong to the Ramdurg Formation of Lokapur subgroup within the Bagalkot Group of the Kaladgi Supergroup (Jayaprakash *et al.*, 1987).

- *Field Observations*

The BHQ's forming the basement are characterised by distinct alternating bands of iron and silica and display secondary folds (Fig. 4.11a). The haematitic bands of iron are relatively softer than those of silica which exhibit minute displacement at localised spots. These along with the variegated phyllites being highly ferruginous suggest an oxidising environment at the time of deposition of the original protolith.

The unconformable conglomerate referred as Salgundi Conglomerate in the geologic literature on Kaladgi basin is about 6.3m thick. It strikes E-W with dips of 35°N. This orthoquartizitic, oligomictic conglomerate is composed of a mixture of crystalline and

cryptocrystalline varieties of silica such as quartz, jasper, chert, banded chert intermixed with varying sized fragments of Banded Hematite Quartzite (Fig. 4.11b). Large cobbles and pebbles of these constituents showing point and suture contact appear oriented with their longer axes parallel. This oligomictic orthoconglomerate with its intact framework is bound by ferruginous matrix. The constituents occur both as large clasts and as detrital grains in the matrix. A noteworthy feature is the imbrication displayed by the pebbles (Fig. 4.12a). It is a primary depositional feature consisting of aligned pebbles such that they overlap one another in a consistent manner. At Ramthal, this is found to indicate the upstream side towards east while the currents (palaeo) flowed towards the west. The paleocurrents indicated by imbrications are upstream on river-beds and sea wards on beaches (Tucker, 2011). Two sets of prominent vertical joints intersecting at right angle cut through the clasts of cryptocrystalline silica displaying smooth, planar surfaces. Minor structure of matrix folding around the pebbles is also noticed (Fig. 4.12b).

The overlying ferruginous quartzitic sandstones about 12m thick are conformable but mark a sharp contact with the conglomerate below. They maintain the same structural attitude as the underlying conglomerate and are found to display current beddings. These shallow water structure have their cross-beds inclined towards west (Fig.4.12c) suggesting a westward flow of paleocurrents; while occasional turbulence in the currents have resulted in developing torrential beddings.

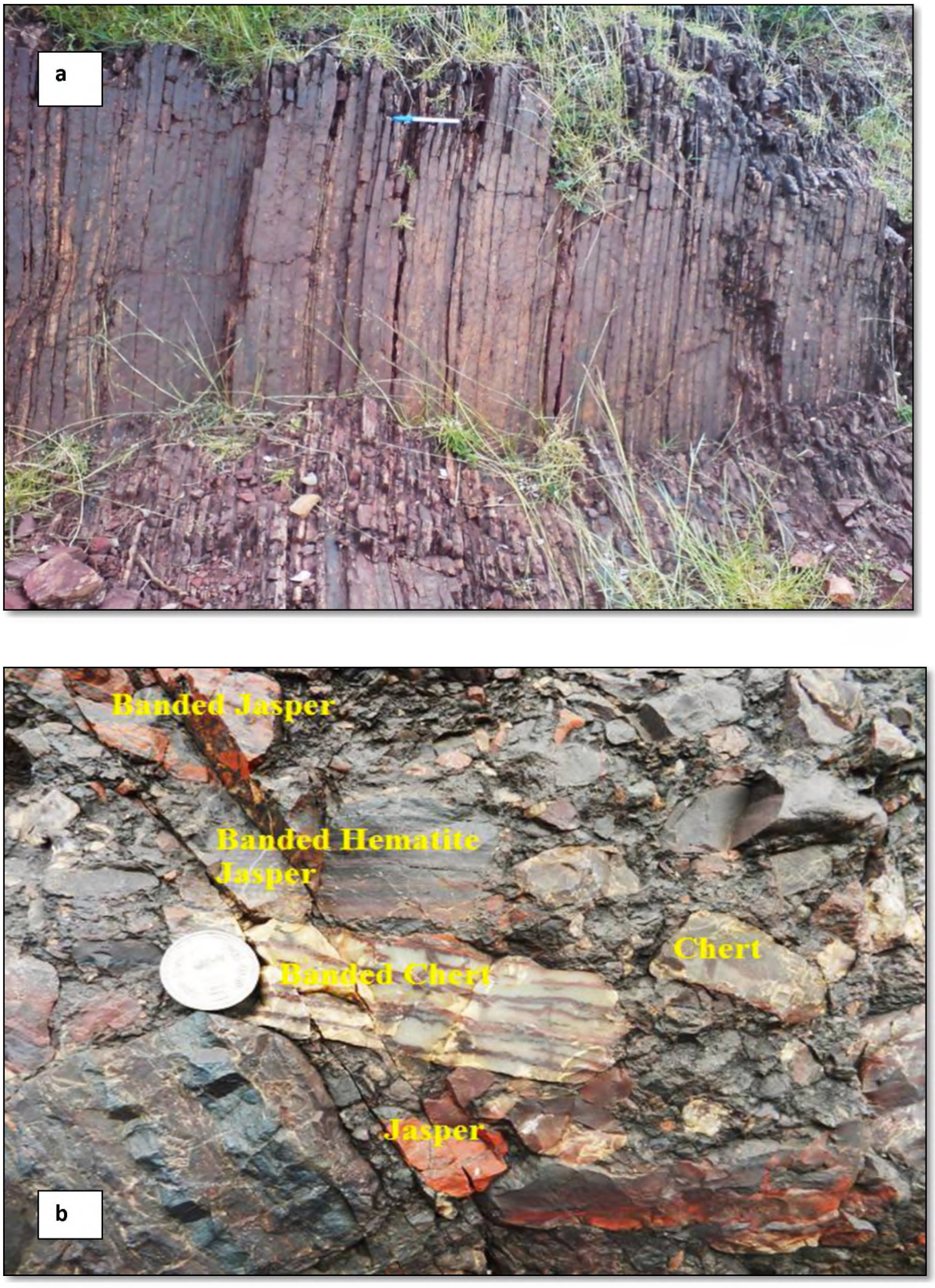

Figure 4.11 (a) Basement Banded Hematite Quartzite, Ramthal **(b)** Polymineralic conglomerate, Ramthal

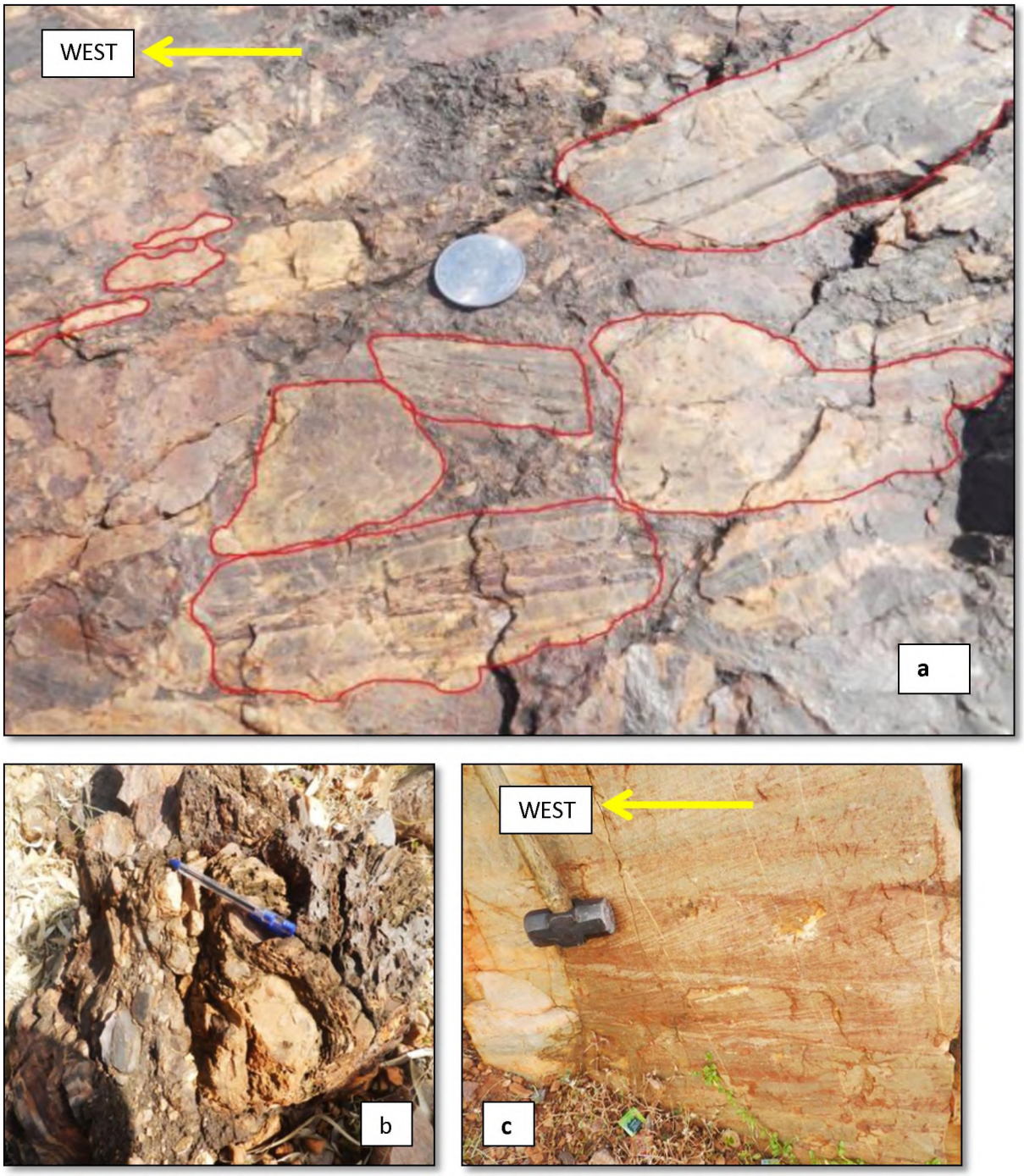

Figure 4.12 (a) Imbrication displayed by the pebbles with upstream side towards East **(b)** folding of the matrix material around the framework clasts **(c)** current bedding with cross-beds inclined towards west.

4.2.4 Salgundi

- *Location and Topography*

A range of hills here rise to a height of about 110m. The dip slope is at a high angle while it is barren lower down and covered with scree all along. Thick, thorny bushes cover the upper parts of this slope. The escarpment slope in contrast is very steep with River Malaprabha sinuating at the foot hills.

- *Field Observations*

The rocks that belong to the Ramdurg Formation as at Bilgi, Jamkhandi and Ramthal are exposed all along the slopes of the hills at Salgundi. The lowermost bed of conglomerate, herein represents the type area for the stratigraphically recognised Salgundi Conglomerate within the Kaladgi Supergroup of rocks. (Fig. 4.13). This polymictic lithounit is about 30m thick, supposedly overlying Archean basement, outcrops of which are visibly exposed around. The rock is composed of rounded to sub-rounded cobbles and pebbles. A long travel has brought in rounding of these pebbles and cobbles which range from 0.1cm to 18cms along their long axis. The clasts admixed in a siliceous matrix give a matrix-supported texture to the rock. They are well rounded but lack sphericity exhibiting ellipsoidal shapes. The long axis of the elongated clasts appear oriented parallel to the E-W strike direction of the bed which, unlike Ramthal has a 40° dip towards South (Fig. 4.14a). An overlapping positioning of the pebbles signifying imbrication is displayed on the vertical surface and suggests a westward upstream end, while the inferred flow of paleocurrents was towards the east (Fig. 4.14b). The rock is compact, massive but exhibits bedding joints. Overlying conformably and following the same E-W strike and 40°-45° dip due South are massive, quartzitic sandstones (Fig. 4.15a). Conspicuously these are

intervened by a thick quartz vein, offshoots of which are spread all around. A mafic sill (Fig. 4.15b) has subsequently intruded both the country rocks as well as the vein of quartz as evidenced by their shearing along the margin. The shearing has caused minor faults and en echelon fractures (Fig. 4.15c) within the county rock which, subsequently have been filled by secondary mineralisation of quartz. The quartzitic sandstone is intensely jointed and large boulders are caught up in the sill. Erosive activity has created accumulation of scree all along the slope.

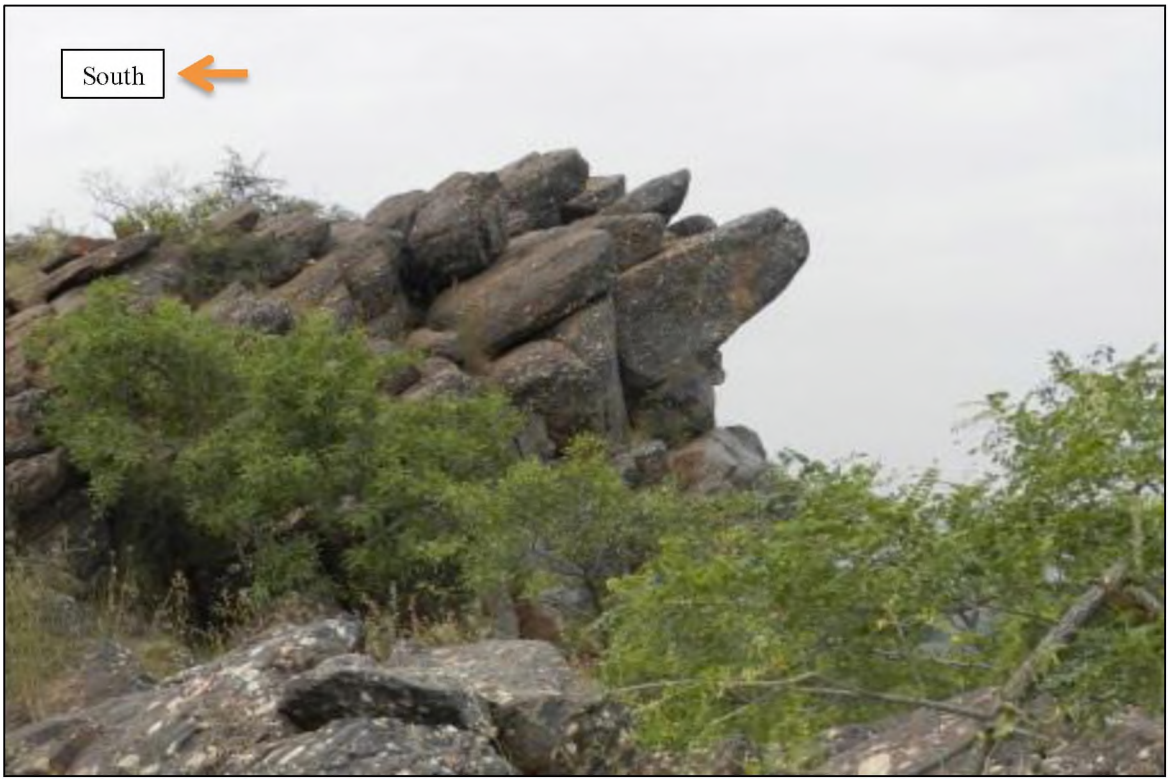

Figure 4.13 Salgundi Conglomerate, Salgundi

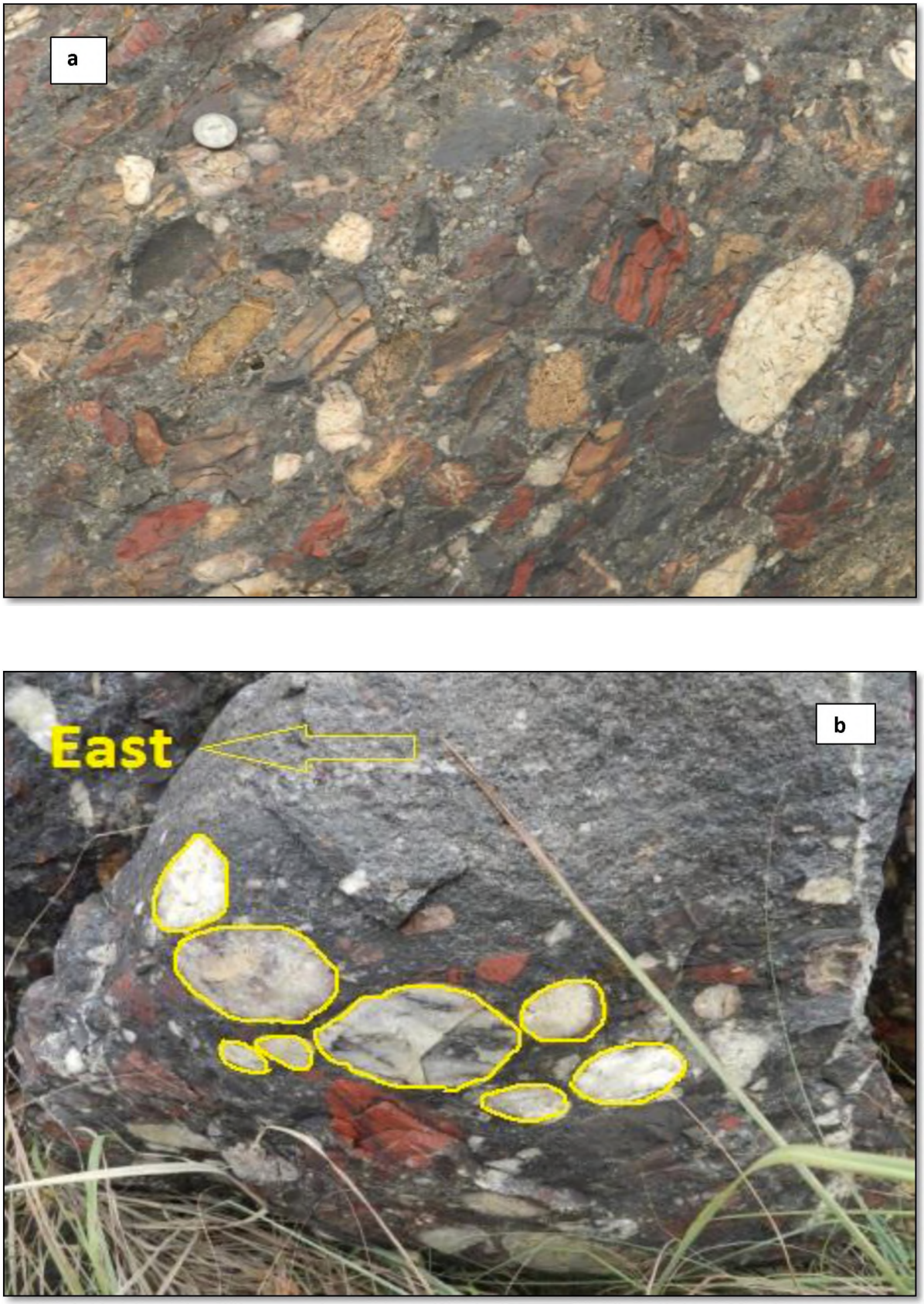

Figure 4.14 (a) Parallel orientation of the pebbles **(b)** Imbrications of pebbles with upstream towards west.

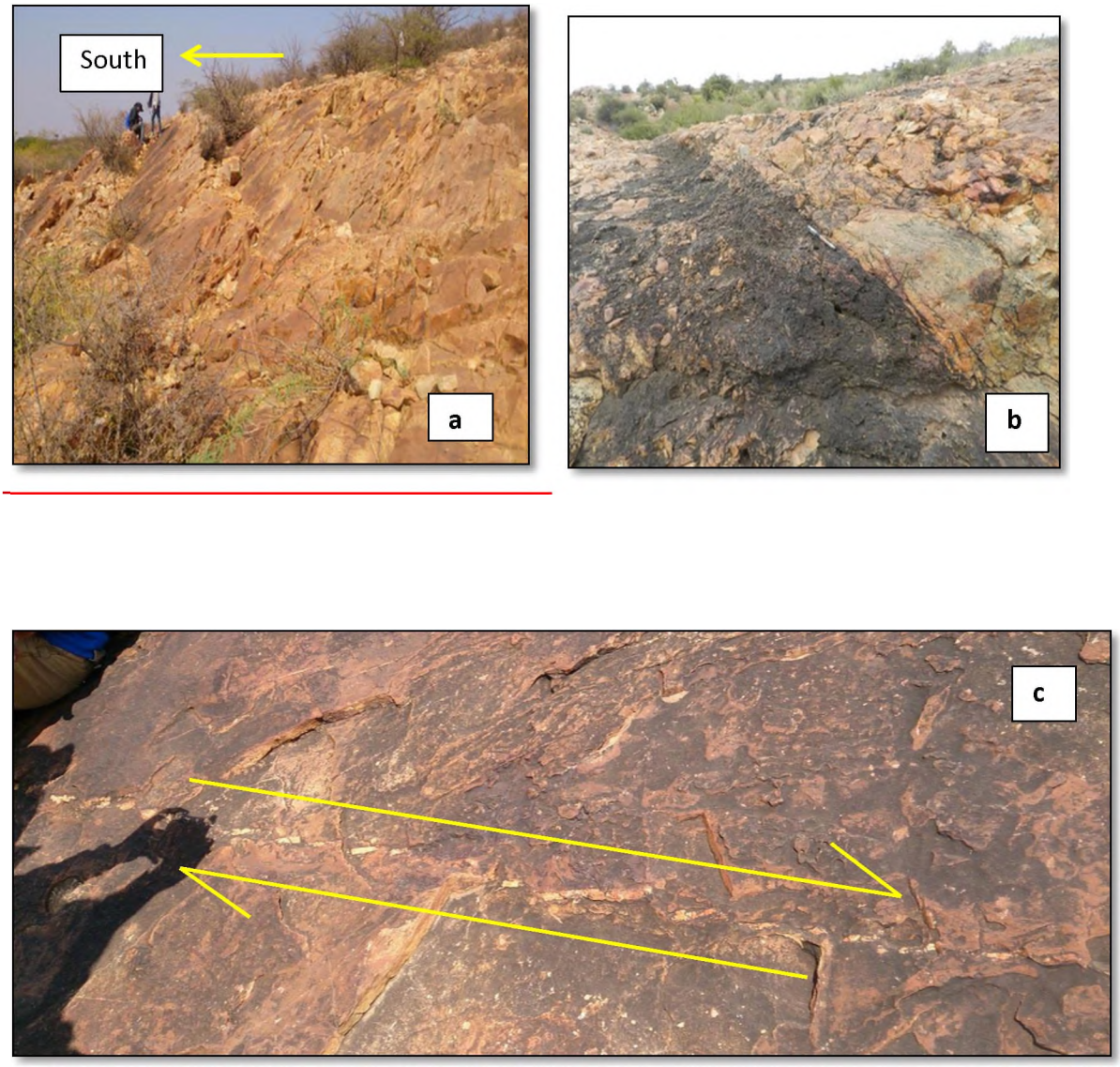

Figure 4.15 (a) Massive quartzitic sandstone dipping South **(b)** Intrusion of mafic sill **(c)** en echelon fractures in quartzitic sandstone at Salgundi.

4.3 Sampling and Analytical methods

Observation of the exposures in the field revealed fragment changes in lithology, textures and structural features. Taking view of the same samples were collected systematically at intervals of 10 – 15m horizontally as well as vertically as a variation in mineralogy, texture or structure was noticeable. The collected field samples were cleaned with distilled

water and dried further to prevent dust contamination as they were to be used for the purpose of laboratory analytical studies.

4.4 Studies based on Microsections

Microsections were prepared of fifteen rock samples each from all of the areas under study viz. Bilgi, Jamkhandi, Salgundi and Ramthal respectively. They were observed for petrographic studies under Petrological microscope Model: NIKON Eclipse E200 at the Department of Earth Science Goa University. Studies based on observation of these sections involved mineralogical and qualitative modal analysis and identifying petrological characters and microstructures. They were also utilised for the study of back scattered electron images and for the purpose of obtaining chemical analysis of mineral on Scanning Electron Microscope.

Scale of the thin section photographs

4x= 5.87mm base of the photograph

10x = 1.54mm base of the photograph

20x = 1.15mm base of the photograph

40x = 0.57mm base of the photograph

From each of the fifteen samples observed under the microscope a qualitative modal analysis from the base towards the top of the exposed sections was done. Most samples were realised to have given similar results. As such sample numbers BIL-13, lower level and BIL-15 from the upper level of the section at Bilgi; JAM-1 from Jamkhandi; SAL-9 from Salgundi and RAM-2 from Ramthal are presented in table 4.1 for representative results.

Table 4.1 Average modal composition in volume % of the studied samples

Sample No	BIL-13	BIL-15	JAM-1	SAL-9	RAM-2
Locality	Bilgi	Bilgi	Jamkhandi	Salgundi	Ramthal
Rock type	Arkose	Arkose	Arkose	Conglomerate	Conglomerate
Framework clasts					
Quartz (Monocrystalline)	20	22	20	33	30
Quartz (Polycrystalline)	19	19	17	40	43
Microcline feldspar	10	11	19		
Orthoclase feldspar	07	05	10	01	01
Plagioclase feldspar	02	02	02		
Muscovite mica	Trace	Trace	Trace		
Biotite mica	Trace	Trace	Trace		
Apatite	Trace	Trace	Trace		
Sphene	Trace	Trace	Trace		
Opaque	07	09	03	09	08
Lithic fragments	03	02	03	03	05
Matrix					
Sericite clay	✓	✓	✓		
Siliceous	✓	✓	✓	✓	✓
Ferruginous				✓	✓
Authigenic/ Cement					
Overgrowth of silica	06	07	06	05	05
Overgrowth on feldspar	04	06	09		
Tourmaline	07	12	03		
Iron oxide	03	02		04	03

4.5 Studies based on Scanning Electron Microscope

Analytical study of the micro sections of the samples under Scanning Electron Microscope - Energy Dispersive Spectroscopy (SEM – EDS) was done at National Centre for Antarctica and Ocean Research (NCAOR), Vasco-Goa using Zeiss EVO 18 (Fig. 4.16a) and at Department of Electronics, Goa University using JOEL JSM-6360LV (Fig. 4.16b).

On the Scanning Electron Microscope - Energy Dispersive Spectroscopy (SEM – EDS) using 70μm magnification, studies were carried exclusively on the prismatic grains of tourmaline present within the matrix because of the difficulty to separate out independent grains from the whole rock.

Figure 4.16 (a) Zeiss EVO 18 for SEM-EDS **(b)** JOEL JSM-6360LV for SEM (*Courtesy*: National Centre Antarctica and Ocean Research, NCAOR)

- *Principle*

Scanning Electron Microscope helps in the visual observations of the sample under study in a very different way from that of Polarising Microscope. Instead of using light, a Scanning Electron Microscope uses electrons to produce an image of a mineral. It scans an electron beam over the surface of the mineral sample under study wherein the beam interacts with the sample, producing various signals that can be used to obtain information

about the surface topography and its composition. The first successful Scanning Electron Microscope (SEM) was developed by Oliver C. Wells, Thomas E. Everhart and R K Matt in 1963.

- *Working*

The scanning electron microscope consists of a source of electrons; lenses for focussing them to a fine beam; facilities for sweeping the beam in a raster; arrangements for detecting electrons emitted by the specimen; and an image-display system (Fig. 4.17). Secondary-electron (SE) images, which show topographic features of the specimen, are the most commonly used type. Backscattered-electron (BSE) images are principally used to reveal compositional variations. SEM examines the sample under study at extremely high magnifications to produce electron and back scattered electron images of high resolution and detailed depth of field. BSE images in the SEM display compositional contrast that results from different atomic number elements and their distribution. EDS allows identifying what those particular elements are and their relative proportions.

Energy dispersive Spectrometer (EDS) is used to obtain semi-quantitative elemental results about very specific locations within the area of interest. It is not a surface analysis technique. It makes use of X ray spectrum emitted by solid sample bombarded with a focussed beam of electron to obtain a localised chemical analysis. All elements from atomic number 4 (Be) to 92(U) can be detected in principle, though not all instruments are equipped for light element ($Z<10$). Determination of the concentrations of the elements present requires measuring line intensities for each element in the sample and for the same elements in calibration standards of known compositions. A specimen under study is placed within the vacuum chamber located at the bottom of the SEM column. An electron

source located at the top of the column produces electrons, which pass through the column and are incident upon the specimen. The electron beam is directed and focussed by magnets and lens inside the SEM column as it approaches the specimen. The ebam 'swings' across the sample causing some of the electrons to be reflected by the specimen and some to be absorbed.

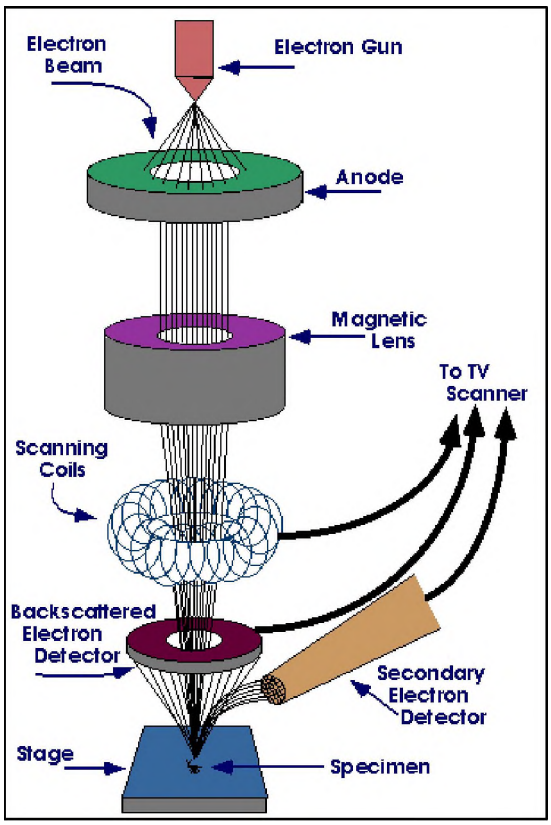

Figure 4.17 Working of SEM

- *Accuracy and sensitivity*

For major elements it is usually not difficult to obtain a precision of better than ±1% but the overall analytical accuracy is near ±2% owing to other factors such as uncertainties in the compositions of the standards and errors in the various corrections which need to be applied to the raw data.

- *Spatial resolution*

It is governed by the penetration and spreading of the electron beam in the specimen and is a function of density. In case of silicates the nominal resolution is about 2μm under normal conditions, but for quantitative analysis a minimum grain size of several micrometres is desirable. The units of spatial resolution are microns and not nanometers. This is due to the fact that X-rays are generated from very deep in the interaction volume. Size of interaction volume increases with accelerating voltage.

- *Sample preparation*

Since the electron probe analyses only a shallow depth, specimens should be well polished so that surface roughness does not affect the results. For transmitted light viewing, polished thin sections on glass slides meet the requirement but opaque samples maybe embedded in epoxy resin blocks. Specimens of any shape and size can be analysed. Since rock specimens are electrically non-conducting, a conducting surface coat must be applied to provide a path for incident electrons to flow to ground. This is done by using a device called 'sputter coater'. The sputter coat uses an electric field and argon gas. The sample is placed in a small chamber that is a vacuum. Argon gas and an electric field cause an electron to be removed from the argon, making the atoms positively charged. The usual coating material is vaccum-evaporated carbon (app. 10nm thick) which has a minimal influence on X-ray intensities on account of its low atomic number and unlike gold (which is commonly used) does not add unwanted peaks to the X-ray spectrum. The argon ions knock gold atoms from the surface of the gold foil. These gold ions fall and settle onto the surface of the sample producing a thin gold coating.

- *Limitations*

Energy resolution 130eV at Mn Kα

Limits of detection: 1000-3000ppm; >10 % weight

Elements identified: Elements heavier than Be.

Spatial resolution: Low atomic number (Z): 1-5um^3; high Z= 0.2-1um^3

Precision (the closeness of agreement between randomly selected individual measurements): approximately ±0.1%

Accuracy (the closeness of agreement between an observed value and an accepted reference value): 95% analysis

±1% for polished bulk target, pure standards on site.

+2% for polished bulk target, standards collected on another SEM and then corrected for the geometry and settings of the present microscope (without standards)

±5% for particles and rough surfaces 'without standards'

4.6 Geochemical analysis

Twenty three bulk rock samples (*08 from Bilgi, 05 from Jamkhandi, 05 from Salgundi, 05 from Ramthal respectively*) were selected for the purpose of geochemical studies. Part of the matrix portion of selected rock samples was crushed using a brass pestle and powdered to < 0.004mm size using an agate mortar and pestle. Enough care was taken to avoid the larger clasts inorder to attain uniformity for the detection of major, trace and rare earth elements.

4.6.1 X-Ray Fluorescence (XRF)

The twenty three selected bulk rock samples from the four areas; (Bilgi, Jamkhandi, Salgundi and Ramthal) were analyzed for major oxide detection using Model Axios, PAN Alytical with the fused bead method given by Yamada Y., 2010 at the XRF Laboratory, National Institute of Oceanography (NIO, Goa) Final concentration for the major oxides thus determined is given in percentage (%).

- *Procedure - The Fused Bead Method*

The bulk rock samples were crushed to fine powder with the help of mortar and pestle. 0.5gms of the dry powdered sample was weighed using an electronic balance. 5gms of Lithium Metaborate flux was added to the sample in a platinum crucible. The flux was used to lower the temperature of melting of the sample. The sample was mixed thoroughly and then heated to a temperature of 250°C for 2minutes with the help of MiniFuse 2 (Fig. 4.18a). This is to ensure thorough mixing of the melt. Later, on increasing the temperature by 450°C and heating for about 7minutes, the sample is ensured to have melted completely. It was immediately poured into a platinum dish and allowed to cool (Fig. 4.18b) to result in the formation of the glass bead (Fig. 4.18c). Chances of the glass bead to break remain if the sample is not powdered thoroughly. The glass bead is then kept in a desiccator to avoid absorption of moisture. The machine is calibrated in a way that it takes care of Loss on Ignition (LOI). The platinum crucible and the dish are heated in hydrochloric acid (HCl) for half an hour to continue the process for the next sample. After the glass beads are prepared for all the samples, they are analyzed for major oxides by placing in the XRF machine (Fig.4.18d & 4.18e). The automatized robot in the XRF machine, Model: Axios, PAN Alytical does the analysis for major oxide compositions.

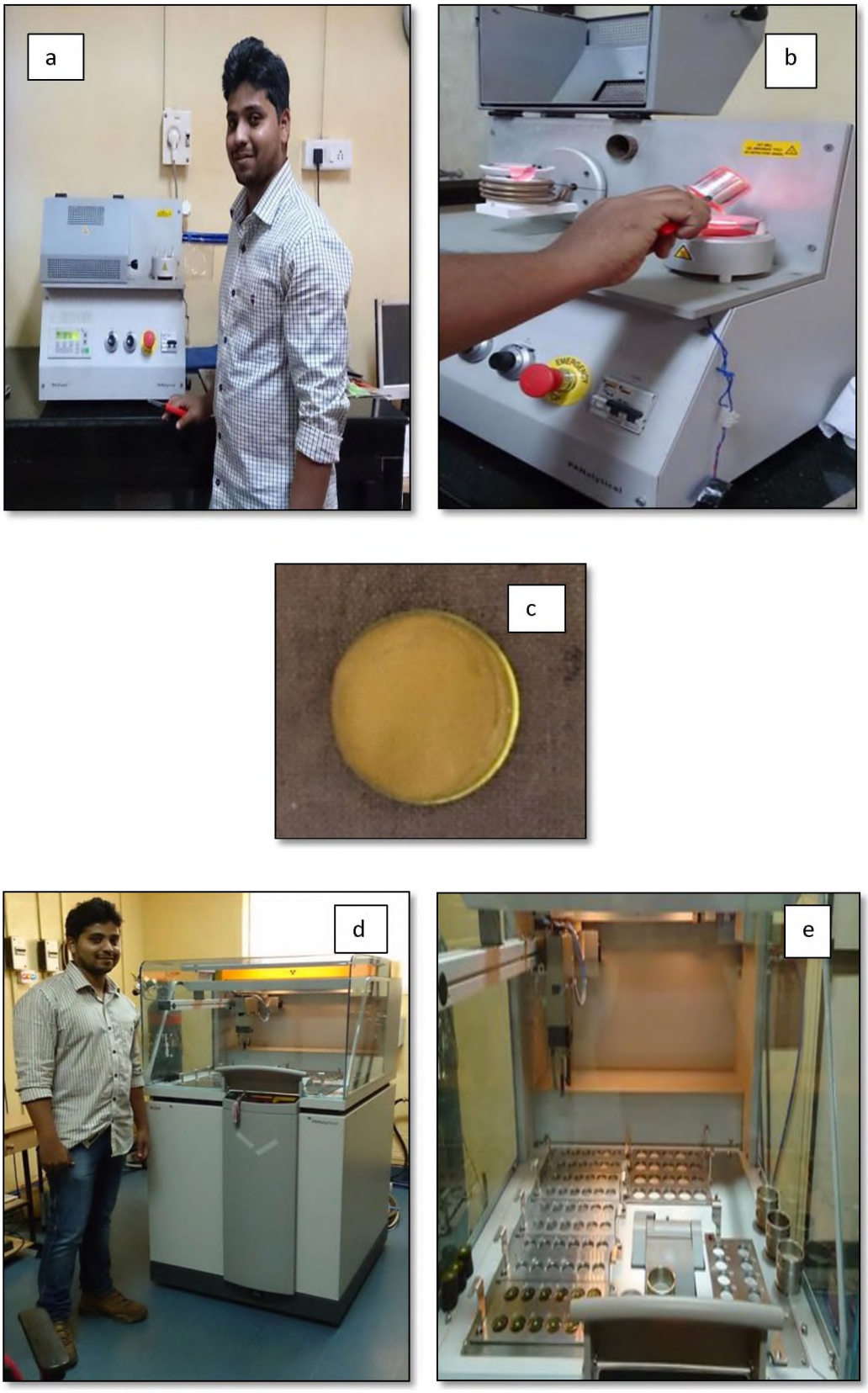

Figure 4.18 (a) MiniFuse2 to melt the dry powdered sample **(b)** Pouring of the melt from the platinum crucible to the platinum dish **(c)** The glass bead **(d & e)** XRF machine, Axios, PAN Alytical, National Institute of Oceanography (NIO), Dona Paula

The major oxides compositions are presented below in Table 4.2a, 4.2b, 4.2c, 4.2d & 4.2e for representative samples from Bilgi, Jamkhandi, Salgundi and Ramthal respectively.

Table 3.4a Major oxide compositions in weight percent (*wt. %)* for the Bilgi arkose with Chemical Index of Alteration (CIA, Nesbitt and Young, 1982).

Bulk rock sample	SiO_2	TiO_2	Al_2O_3	FeOT	Fe_2O_3*adj	FeOadj	MnO	MgO	CaO	Na_2O	K_2O	P_2O_5	**Total**	CaO^*	$SiO_2/20$
BIL-13	84.07	0.25	6.12	2.65	0.94	1.87	0.06	0.54	0.30	0.32	3.10	0.02	**97.44**	0.00197	4.2035
BIL-13A	84.44	0.24	6.13	2.77	0.97	1.95	0.01	0.53	0.25	0.35	3.10	0.02	**97.82**	0.00403	4.222
BIL-13B	85.77	0.23	5.98	2.32	0.81	1.62	0.01	0.61	0.23	0.33	3.45	0.02	**97.82**	0.00353	4.2885
BIL-13C	85.13	0.25	5.89	2.03	0.72	1.43	0.01	0.59	0.31	0.33	3.10	0.02	**97.76**	0.00553	4.2565
BIL-15	81.33	0.50	5.03	8.09	2.84	5.69	0.01	0.67	0.35	0.33	1.43	0.02	**97.74**	0.0053	4.0665
BIL-15A	81.87	0.52	5.12	7.65	2.68	5.37	0.01	0.87	0.25	0.31	1.51	0.02	**98.12**	0.00403	4.0935
BIL-15B	82.13	0.50	5.19	8.13	2.83	5.66	0.01	0.79	0.31	0.33	1.42	0.02	**98.83**	0.00553	4.1065
BIL-15C	81.30	0.52	6.10	8.12	2.82	5.65	0.00	0.69	0.32	0.32	1.50	0.01	**98.89**	0.00523	4.065
UCC[$]	65.89	0.50	15.17	4.49	-	-	0.07	2.20	4.19	3.89	3.39	0.20			
Avg Arkose (Pettijohn, 1963)	92.15	0.17	3.87	1.32	-	-	-	0.55	0.45	0.51	0.88	0.03	**99.93**		
PCS (Condie, 1993)	79.30	0.15	11.74	1.31	0.59	-	0.05	0.54	1.41	2.40	4.51	0.60			

Table 3.4a (*continued*) Major oxide compositions in weight percent *(wt.%)* for the Bilgi arkose with Chemical Index of Alteration (CIA, Nesbitt and Young, 1982).

Bulk rock sample	CIA	K_2O/Al_2O_3	K_2O/Na_2O	Na_2O/K_2O	SiO_2/Al_2O_3	$Fe_2O_3^*/K_2O$	Al_2O_3/SiO_2	Fe_2O_3*+MgO	K_2O+Na_2O	$TiO_2+Fe_2O_3$ +MgO	$Al_2O_3+Na_2O+$ K_2O
BIL-13	60.02	0.51	9.62	0.10	13.73	0.303	0.07	1.48	3.42	1.73	
BIL-13A	58.24	0.51	8.86	0.11	13.79	0.313	0.07	1.5	3.42	1.74	
BIL-13B	56.44	0.58	10.45	0.095	14.34	0.235	0.07	1.42	3.45	1.65	
BIL-13C	57.13	0.62	9.39	0.11	14.45	0.23	0.07	1.31	3.43	1.56	
BIL-15	66.2	0.28	4.333	0.23	16.17	1.99	0.06	3.51	1.76	4.01	
BIL-15A	66.64	0.30	4.87	0.21	15.99	1.77	0.06	3.55	1.82	4.07	
BIL-15B	66.55	0.27	4.30	0.23	15.82	1.99	0.06	3.62	1.75	4.12	
BIL-15C	45.01	0.25	4.69	0.21	13.33	1.88	0.08	3.51	1.82	4.03	

Table 3.4b Major oxide compositions in weight percent *(wt.%)* for the Jamkhandi arkose with Chemical Index of Alteration (CIA, Nesbitt and Young, 1982)

Bulk rock sample	SiO_2	TiO_2	Al_2O_3	FeOT	Fe_2O_3*adj	FeOadj	MgO	CaO	Na_2O	K_2O	P_2O_5	**Total**	$SiO_2/20$
JAM-1	81.56	0.30	6.28	3.09	1.10	2.19	0.14	0.12	0.06	5.51	0.05	**100.4**	4.078
JAM-2	81.36	0.34	6.89	3.10	1.08	2.16	0.14	0.11	0.06	4.99	0.05	**100.28**	4.068
JAM-3	81.46	0.37	7.25	3.24	1.14	2.27	0.15	0.12	0.06	4.46	0.05	**100.57**	4.073
JAM-4	80.95	0.29	6.80	3.01	1.07	2.14	0.15	0.12	0.06	5.40	0.05	**100.04**	4.048
JAM-5	81.41	0.40	6.98	3.16	1.10	2.21	0.14	0.12	0.07	4.50	0.05	**100.14**	4.07

Bulk rock sample	CIA	K_2O/Al_2O_3	K_2O/Na_2O	Na_2O/K_2O	SiO_2/Al_2O_3	Fe_2O_3*/K_2O	Al_2O_3/SiO_2	Fe_2O_3*+MgO	K_2O+Na_2O	$TiO_2+Fe_2O_3+MgO$
JAM-1	53.14	0.877	91.83	0.011	12.99	0.2	0.08	1.24	5.57	1.54
JAM-2	58.8	0.72	83.16	0.012	11.81	0.22	0.085	1.22	5.05	1.56
JAM-3	56.49	0.62	74.33	0.0135	11.24	0.26	0.09	1.29	4.52	1.66
JAM-4	52.48	0.79	90	0.011	11.90	0.2	0.08	1.22	5.46	1.51
JAM-5	55.61	0.64	64.29	0.016	11.66	0.24	0.09	1.24	4.57	1.64

Table 3.4c Major oxide compositions in weight percent *(wt.%)* for the conglomerate at Salgundi with Chemical Index of Alteration (CIA, Nesbitt and Young, 1982)

Bulk rock sample	SiO_2	TiO_2	Al_2O_3	FeOT	Fe_2O_3*adj	FeOadj	MnO	MgO	CaO	Na_2O	K_2O	P_2O_5	**Total**	$SiO_2/20$
SAL-9	83.32	0.187	3.981	8.21	2.92	5.83	0.00	0.48	0.09	0.26	0.28	0.03	**105.588**	4.166
SAL-9A	83.21	0.19	3.97	8.12	2.89	5.78	0.00	0.44	0.08	0.27	0.29	0.02	**105.26**	4.161
SAL-9B	83.28	0.182	3.892	8.19	2.92	5.83	0.00	0.48	0.08	0.26	0.25	0.03	**105.394**	4.164
SAL-9C	82.98	0.185	3.89	8.19	2.92	5.83	0.00	0.45	0.09	0.26	0.23	0.02	**105.045**	4.149
SAL-9D	83.54	0.179	3.67	8.21	2.92	5.83	0.00	0.50	0.08	0.26	0.24	0.03	**105.459**	4.177

Bulk rock sample	CIA	K_2O/Al_2O_3	K_2O/Na_2O	Na_2O/K_2O	SiO_2/Al_2O_3	$Fe_2O_3^*/K_2O$	Al_2O_3/SiO_2	Fe_2O_3*+MgO	K_2O+Na_2O	$TiO_2+Fe_2O_3^*+MgO$
SAL-9	72	0.07	1.077	0.929	20.93	10.42	0.048	3.4	0.54	3.587
SAL-9A	87	0.073	1.074	0.931	20.96	10.07	0.048	3.33	0.56	3.52
SAL-9B	72	0.064	0.96	1.04	21.40	11.68	0.0467	3.4	0.51	3.582
SAL-9C	88	0.059	0.885	1.13	21.33	12.70	21.33	3.37	0.49	3.555
SAL-9D	71	0.065	0.923	1.08	22.77	12.17	21.33	3.42	0.5	3.599

Table 3.4d Major oxide compositions in weight percent (*wt. %)* for the conglomerate at Ramthal with Chemical Index of Alteration (CIA, Nesbitt and Young, 1982)

Bulk rock sample	SiO_2	TiO_2	Al_2O_3	FeOT	Fe_2O_3*adj	FeOadj	MnO	MgO	CaO	Na_2O	K_2O	P_2O_5	**Total**	SiO_2/20
RAM-2	92.12	0.05	0.55	6.32	2.19	4.37	0.00	0.06	0.09	0.06	0.13	0.03	**99.40**	4.606
RAM-2A	92.12	0.04	0.55	6.29	2.18	4.36	0.00	0.06	0.10	0.05	0.13	0.01	**99.35**	4.606
RAM-2B	92.11	0.04	0.55	6.31	2.19	4.37	0.00	0.06	0.09	0.07	0.13	0.02	**99.37**	4.606
RAM-2C	92.12	0.05	0.54	6.29	2.18	4.36	0.00	0.05	0.09	0.05	0.13	0.01	**99.33**	4.606
RAM-2D	92.14	0.05	0.54	6.29	2.18	4.36	0.00	0.05	0.08	0.06	0.12	0.02	**99.35**	4.607

Bulk rock sample	CIA	K_2O/Al_2O_3	K_2O/Na_2O	Na_2O/K_2O	SiO_2/Al_2O_3	$Fe_2O_3^*/K_2O$	Al_2O_3/SiO_2	Fe_2O_3*+MgO	K_2O+Na_2O	$TiO_2+Fe_2O_3^*+MgO$
RAM-2	32	0.236	2.166	0.461	167.49	16.84	0.0059	2.25	0.19	2.3
RAM-2A	69	0.236	2.600	0.384	167.49	16.769	0.0059	2.24	0.18	2.28
RAM-2B	71	0.236	1.857	0.538	167.47	16.846	0.0059	2.25	0.2	2.29
RAM-2C	70	0.240	2.600	0.384	170.59	16.769	0.0058	2.23	0.18	2.28
RAM-2D	73	0.222	2.000	0.5	170.62	18.166	0.0058	2.23	0.18	2.28

Abbreviations: The subscript 'adj' refers to adjusted data (anhydrous 100% adjusted basis); FeOT = Total iron expressed as FeO. Iron split using Fe_2O_3/FeO ratio after Middlemost (1989).
Chemical Index of Alteration (CIA, Nesbitt and Young, 1982)
CaO* = CaO in silicate phase;
Fe_2O_3* = Total Fe expressed as Fe_2O_3

4.6.2 Inductively Coupled Plasma - Mass Spectrometry (ICP-MS)

Only twenty one selected (*06 from Bilgi, 05 from Salgundi, 05 Ramthal, 05 from Jamkhandi*,) bulk rock samples were analyzed and data recorded for trace-element and Rare Earth Elements (REE) using Agilent 7700 Series *Inductively Coupled Plasma - Mass Spectrometry*, ICP- MS at Isotrace Laboratory , National Centre for Antarctica and Ocean Research (NCAOR, Goa) using method proposed by Jarvis (1988). Internal Standard Rhodium was added and recovery was almost 100%. Calibration was done by Inorganic Ventures Multielement Standard. Analytical precision for trace elements and REE is generally better than 5%. United States Geological Systems (USGS) three reference standards SGR-1b (Green River Shale), GSP-2 (Silver Plume Granodiorite) and NIST 688 (Basalt) were measured along with samples. Final Concentration for all trace elements is given in ppm, and for major elements it is stated in %.

Inductively coupled plasma mass spectrometer (ICP-MS) is highly a sensitive and state-of-art instrument capable of determining a range of metals and several non-metals at concentration below one part in 10^{15} across the periodic table on non-interfered low background isotopes. The special feature of ICP is its ease for sample introduction and quick analyses and that of MS is in its accurate and low detection limit, both of which are coupled in ICP-MS. It is capable of trace and multi element analysis at parts per trillion (ppt) levels. Ionisation of the sample is done by ICP whereas the MS separates and quantifies those ions. ICP-MS has a greater speed, precision and sensitivity and introduces many interfering species: argon from plasma, component gases of air that leak through cone orifices and contamination from glassware and cones.

➢ *Components of ICP-MS*

(1) Inductively-Coupled Plasma: The plasma used in the spectrochemical analyses is electrically neutral with equal number of ions and electrons inorder to make the gas electrically conductive. The temperature of plasma is very high; as high as 10,000K. It is kept in a torch consisting of three concentric tubes made of quartz; the end of the torch is placed in an induction coil which is supplied with a radio-frequency electric current (Fig. 4.19). A flow of argon gas is introduced between the two outermost tubes and an electric spark is applied to introduce free electrons to the gas stream. These electrons interacting with the radio frequency magnetic field of induction coil accelerates in one direction and later changes the direction as the field changes. These accelerated electrons collide with argon atoms which after some time results in the release of electrons from argon atom. These electrons also accelerate rapidly changing the magnetic field. The process continues until equilibrium is reached between rate of release of new electron and the rate of recombination of electrons with argon atoms. This produces a fire ball.

Since the ICP is kept in a quartz torch, the flow of gas between the outermost tubes keeps it away from the walls. The second flow is introduced between central tube and intermediate tube. The third flow is introduced in to the central tube. This gas flow passes through the centre of the plasma creating a channel which is comparatively cooler. Samples are introduced into this channel after passing through the nebulizer. The nebulizer sample after entering the central channel evaporates and the solids dissolved in the liquid vaporize and break down into atoms. And these atoms are ionized by losing the outermost electrons.

(2) Mass Spectrometer**:** For coupling to mass spectrometer the ions from plasma are extracted through a quadrupole. The ions are separated on the basis of their mass to charge ratio and a detector receives a signal proportional to the concentration. The concentration is determined by calibrating with certified reference material.

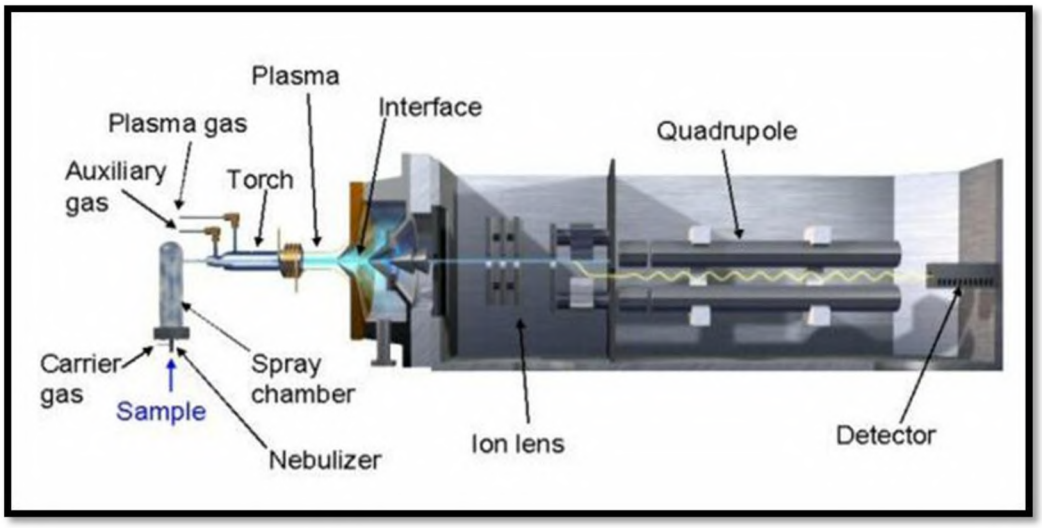

Figure 4.19 Schematic of ICP-MS

➢ *Instrument Description and Theory*

Samples are decomposed into neutral element in elevated temperature Argon plasma and analyzed. The analysis is based on the mass per charge ratio. The processes occurring in ICP-MS can be divided in to four parts (1) Sample introduction and aerosol generation (2) ionization by an argon plasma source (3) mass discrimination (4) detection. The diagram below depicts those processes (Fig. 4.20).

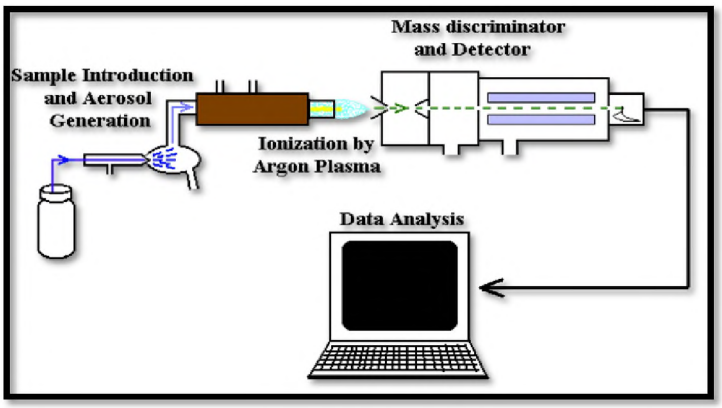

Figure 4.20 Schematic **of ICP-MS main processes**

Sample Introduction**:** ICP-MS can analyse both solid and liquid samples. Solid samples are introduced into ICP through a laser ablation system. Aqueous samples are introduced through a nebulizer. This device converts liquids into an aerosol. In this device, the sample passes through the high velocity Argon and it forms a mist. The aerosols pass into the spray chamber and large droplets are removed via a drain. It is found that only 2% of the original mist passes through the spray chamber. This process produces droplets which are small enough to vaporize in the plasma torch chamber. Many varieties of nebulizers are used including pneumatic, cross flow, ultra-sonic, and desolvating types. Auto samplers are used to make the process easier.

The ICP Torch- Making ions: The plasma generated in the ICP torch creates a very hot zone where the temperature is equal to the temperature at the surface of the sun. The aerosol produced by the nebulizer moves into the torch. The hot plasma removes any remaining solvent and causes sample atomization and ionization. The aerosols move in to the bottom of the torch body. At the top, there are two high quality quartz tubes and an inner alumina injector tube. The samples are first atomized. The atoms absorb more energy from the plasma and release one electron forming a singly charged ion. These ions exit plasma and enter the interface region.

The interface-Sampling Ions: This creates vacuum environment for MS. The entire Mass Spectrometer should be kept in vacuum so that the ions can easily move freely without colliding with air molecules. The ICP is maintained at atmospheric pressure .so a pumping system is needed to pull vacuum inside the spectrometer continuously. The interface consists of two inverted funnels like cones. They are the skimmer cone and the sampler cone. The sampler cone is located next to the plasma and the skimmer cone is located several millimeters behind the sampler cone. The ions pass through the opening that each cone has which is one mm in diameter. Between these cones a vacuum is maintained. As samples pass through ICP-MS materials will deposit on these cones and is needed to be cleaned occasionally. Behind the interface there is ion lens. This focuses ions into the quadrupole region. The irons produced by plasma are mostly positive charged .so they will be having a tendency to repel. So in order to get maximum amount of ions into the quadrupole region they have to be focused.

- *Sample Preparation and Digestion*

Dry samples of arkose from Bilgi (BIL) and Jamkhandi (JAM); (BIL-13, BIL-13A, BIl-13B from the lower elevation and BIL-15, BIL-15A, BIL-15B from the higher elevation; JAM-1, JAM-2, JAM-3, JAM-4, JAM-5), and of conglomerate from Salgundi (SAL-9, SAL-9A, SAL-9B) and Ramthal (RAM-2, RAM-2A, RAM-2B) were powdered using agate mortar and pestle and stored in pre-labelled vials. Prior to the usage of the vials they were soaked overnight in 2% HCl and thoroughly rinsed three times with ultrapure water to remove any contamination. The powdered samples were later weighed individually using a micro balance. All the acids used (HNO_3, HCl, HF and $HClO_4$ were of supra pure metal grade. Ultrapure water (Milli-Q element) was used in all the sample preparation

procedures. All glass wares, Teflon beakers and polypropylene bottles used in the experiment were cleaned by soaking them in acid bath (10% ultrapure HNO_3, 24h), rinsed several times with Milli-Q water and dried in oven at less than 60^0C.

About 30mg of powdered sediment sample was weighed in Teflon vial separately on an electronic balance along with three international standards of United States Geological Survey (USGS): GPS-2: Silver Plume Granodiorite; SGR-1b: Green River Shale and NIST 688: Basalt. The weighed samples were poured in dry high temperature Teflon viols for further analysis. Along with the samples a repeat sample (RAM-2) and a blank was also weighed. To all the dried samples, Hydrofluoric acid (HF acid), Nitric acid (HNO_3 acid), and Perchloric acid ($HClO_4$) were added in the ratio of 6: 3:1.5 into the vial and kept overnight for 12 hours at 120°C for digestion. Complete digestion of the samples ensures a thorough breaking of the bonds that would release the elements from the oxides/compounds. The samples were then heated in an acid kood the following day, with the temperature being increased gradually from 130°C to 200°C (Fig. 4.21a). The acids get completely vaporized by this process and helps in complete digestion of the samples. On observing that some powder had still remained undigested, the viols containing the samples were allowed to cool and the above process was repeated by altering the proportion of HF: HNO_3:$HClO_4$ = 3: 1.5: 0.75. The process was repeated further by decreasing the proportion of acids. HF helped in dissolving and eliminating Si whereas the purpose of $HClO_4$ was to dissolve the organic components and later to hasten the heating process. Further the quantity of HF and $HClO_4$ was increased and HNO_3 decreased (reason: HF helps in complete destroying and dissolving of Si whereas the purpose of $HClO_4$ now is not to remove the organic matter but to hasten up the heating process). The quantity of acids added was HF: $HClO_4$: HNO_3= 7: 3:1. The adding of acids in this

proportion was repeated four times until the samples got completely digested. After the complete digestion of the sample, 0.5ml HNO_3 was added in a numbered conical flask and made upto the mark of 50ml using MiliQ along with the dried sample from the vial. Sample BIL-13A, BIL-13B and BIL-15A required filtering because even after repeated adding of acids several times some undigested powder still remained. They were filtered using Waterman filter paper 4mm. 1ml of NHO_3 was pipetted and added to another conical flask and along with the sample made upto 10ml mark. The prepared samples was subjected for ICP-MS studies for trace element and Rare earth Element determination using the machine model Agilent 7700 Series at Isotrace Laboratory from National Centre for Antarctica and Ocean Research, NCAOR (Fig. 4.21b).

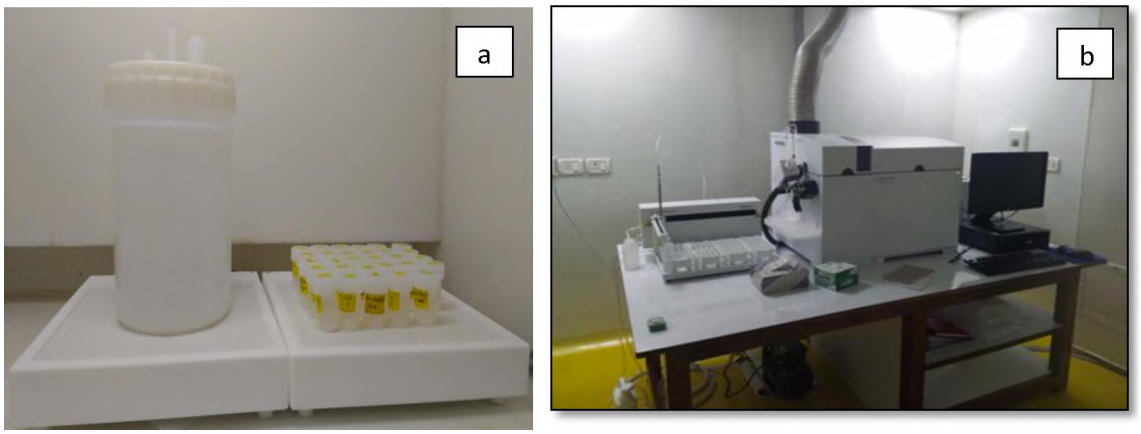

Figure 4.21 (a) Sediment digestion in Class 100 fume hood **(b)** ICP-MS determination for trace element and Rare Earth Elements using the machine model Agilent 7700 Series at Isotrace Laboratory from National Centre for Antarctica Ocean and Research, NCAOR.

Sediment Digestion

Weigh 100mg of powdered sample in to Teflon vial

↓

Add HF: HNO_3: $HClO_4$ mixture (7:4:1) & close the vial and digest overnight at 120°C

↓

Open the vial and dry the sample on hot plate (120°C)

↓

Add 3HCl:1HNO_3) and Dry the sample

↓

Repeat the above steps to finish the digestion

↓

Add 3ml HNO_3 and dry it out

↓

Take out the sample in 50 ml of 2% HNO_3 for ICP MS analysis.

- *Sample analysis and instrumentation*

Geochemical measurements were carried out using an Inductively Coupled Plasma Mass Spectrometer (ICP-MS – Agilent 7700x) at NCAOR, Goa. To check the accuracy and precision of measurements, three international standards of United States Geological Survey (USGS): GPS-2: Silver Plume Granodiorite; SGR-1b: Green River Shale and NIST 688: Basalt was digested along with the samples and run during the period of analysis. Several procedural blanks were also measured and to check the reproducibility of the data replicate samples were measured. Three standard solutions, freshly prepared multi

element stock solutions (ICP multi-element standard solution V1, Certipur, Merck) were used for calibration. The digested samples were further diluted 50 times for trace element and major element analysis respectively.

The analysis for trace elements (Table 4.3a, 4.3b, 4.3c, 4.3d & 4.3e) and Rare Earth Elements data (Table 4.4a, 4.4b, 4.4c & 4.4d) for representative samples from Bilgi, Jamkhandi, Salgundi and Ramthal respectively is presented in the tables below.

Table 4.3a Trace-element concentration (in ppm) for the standards

Sample #	Ag	Ba	Cd	V	Rb	Co	Cr	Ni	Cs	Ga	Mn	Pb	Sn	Th	U
$UCC_{\$}$	50	30	0.098	107	112	17	85	44	550	17		17	5.5	10.7	28
PCS[1]	ND	190	ND	29	30	2.8	24	11	ND	ND	ND	20	ND	4.2	1.2
Av. Arkose		190		29	30		24	11				20			

Subscript $ = Average Upper Continental Crust values, UCC (Taylor and McLennan, 1985, 1995)
HFSE: High Field Strength Elements (Ti, U, Th)
PCS[1] – Proterozoic Cratonic Sandstone (Condie, 1993).
Average Arkose (Pettijohn, 1963)

Table 4.3b Trace-element concentration (in ppm) for the arkose samples from Bilgi arkose using ICP-MS.

Sample #	Ag	Ba	Cd	V	Co	Cr	Ni	Cs	Ga	Mn	Pb	Sn	Rb	Sr	Th	U
BIL-13	1.08	358.52	0.43	15.12	1.32	12.87	17.73	0.85	5.02	12.72	137.38	34.98	59.00	3343	11.75	0.77
BIL-13A	0.75	292.25	0.22	9.60	1.12	10.60	18.98	0.67	4.12	9.27	122.12	35.45	45.93	30.267	8.62	0.73
BIL-13B	1.10	265.33	0.62	8.82	1.08	10.05	18.03	0.65	3.35	9.85	126.27	29.68	42.22	26.60	11.53	0.92
BIL-15	0.47	134.37	0.28	35.90	2.02	20.27	18.44	0.40	4.35	15.23	104.72	29.52	26.08	25.52	23.83	1.12
BIL-15A	0.48	20.28	0.13	3.82	0.45	1.65	20.35	0.10	0.63	1.97	15.47	32.52	3.68	16.08	2.47	0.25
BIL-15B	0.62	151.03	0.33	41.17	2.23	23.83	23.30	0.47	5.15	15.07	126.72	34.00	17.70	3.583	32.12	1.52

Sample #	Cr/Th	Cr/V	Th/U	Th/Co	La/Co
BIL-13	1.10	0.85	15.33	8.92	6.13
BIL-13A	1.23	1.10	11.75	7.72	6.40
BIL-13B	0.87	1.14	12.58	10.6	4.3
BIL-15	0.85	0.57	21.34	11.82	6.90
BIL-15A	0.67	0.43	9.87	5.48	3.81
UCC					

Table 4.3c Trace-element concentrations in ppm for the arkose samples from Jamkhandi using ICP-MS

Bulk rock sample	Ag	Ba	Cd	Ti	Co	Ni	Cr	Cs	Ga	Mn	Pb	Rb	Sn	Tl	Yb	Sr
JAM-1	2.57	396.47	1.13	0.49	2.10	40.63	55.83	0.77	6.52	19.77	244.93	74.97	72.42	0.3	3.90	35.42
JAM-2	1.38	640.23	0.60	0.21	0.92	31.82	27.00	1.27	8.17	8.42	202.42	114.12	54.37	0.47	1.63	52.00
JAM-3	1.03	765.58	0.53	0.17	3.63	30.70	47.35	1.23	9.57	72.22	174.40	112.25	38.08	0.54	1.82	73.20
JAM-4	1.60	576.13	0.58	0.067	1.02	34.34	17.33	0.93	6.67	7.88	236.33	99.08	66.37	0.43	1.58	49.57
JAM-5	0.85	518.97	0.35	0.15	0.77	12.98	26.22	1.12	7.00	7.08	136.57	96.08	15.56	0.43	1.78	43.52

Bulk rock sample	Th	U	V	Cr/Th	Cr/V	Th/U	Th/Co	La/Co
JAM-1	73.93	16.45	113.41	0.76	0.49	4.5	35.2	3.42
JAM-2	21.43	6.92	25.08	1.26	1.08	3.1	23.43	0.19
JAM-3	50.60	7.52	77.00	0.93	0.61	6.73	13.92	11.78
JAM-4	52.57	7.60	28.15	0.33	0.62	2.28	51.7	5.75
JAM-5	22.85	7.62	25.10	1.15	1.05	2.99	29.8	31.92

Table 4.3d Trace-element concentrations in ppm for the conglomerate samples from Ramthal using ICP-MS

Bulk rock sample	Ag	Ba	Cd	Ti (%)	Co	Ni	Cr	Cs	Ga	Mn	Pb	Rb	Sn
RAM-2	1.3167	15.200	0.2667	0.01867	0.4333	23.05281	6.3000	0.1000	1.5333	3.9333	148.5833	1.4333	43.54785
RAM-2A	1.0500	17.9233	0.5167	0.035874	0.4167	29.74832	6.7333	0.1167	1.4167	2.9167	182.5500	1.7000	58.28859
RAM-2B	0.6167	17.1833	0.3333	0.016674	0.4167	28.11075	6.7333	0.1000	1.3333	2.9833	201.4667	1.6667	58.82736
RAM-2C	1.0833	17.3500	0.4833	0.02911	0.5333	30.36667	7.2167	0.2333	1.7000	3.4167	210.7167	1.8333	64.28333
RAM-2D	1.0278	17.4562	0.4537	0.03525	0.4125	29.3612	6.7834	0.1341	1.5646	3.5923	195.673	1.6789	58.7842

Bulk rock sample	Yb	Sr	Th	U	V	Cr/Th	Cr/V	Th/U	Th/Co	La/Co
RAM-2	0.082508	6.5833	1.5333	0.4500	2.4500	4.1087	2.571	3.407	3.538	3.807
RAM-2A	0.167785	8.4833	1.8333	0.5167	2.8333	3.6727	2.376	3.548	3.679	4.039
RAM-2B	0.09772	8.0500	1.5667	0.5167	2.7833	4.2977	2.419	3.032	3.759	3.959
RAM-2C	0.23333	8.2167	2.2667	0.6833	3.1000	3.1838	2.327	3.317	4.250	5.312
RAM-2D	0.09356	8.2011	2.1978	0.5280	2.9457	3.0864	2.303	4.1625	5.328	4.053

Table 4.3e Trace-element concentrations in ppm for the conglomerate samples from Salgundi using ICP-MS.

Bulk rock sample	Ag	Ba	Cd	Ti (%)	Co	Ni	Cr	Cs	Ga	Mn	Pb	Rb	Sn
SAL-9	1.2000	52.7000	0.4500	0.093572	2.3667	45.428	15.733	0.0667	3.8500	12.7667	234.6500	2.7833	87.24315
SAL-9A	1.3667	55.7333	0.3833	0.096919	2.4333	42.578	18.050	0.0833	4.1667	12.5167	241.1667	2.7500	82.37113
SAL-9B	2.0667	52.8667	0.3833	0.085831	2.2833	37.550	15.600	0.0833	3.8500	12.0167	221.9167	2.7000	66.87919
SAL-9C	1.2167	54.2167	0.4333	0.08967	2.3833	42.897	15.600	0.0833	3.9000	12.7167	239.3333	2.7333	82.9862
SAL-9D	1.3657	55.7453	0.3562	0.09125	2.4522	42.673	15.453	0.0835	3.8671	12.7682	245.924	2.7143	82.9780

Bulk rock sample	Yb	Sr	Th	U	V	Cr/Th	Cr/V	Th/U	Th/Co	La/Co
SAL-9	0.7833	22.4167	3.5500	0.8000	23.9333	4.431	0.657	4.438	1.499	3.619
SAL-9A	0.8167	22.4667	4.0333	0.8667	24.1667	4.475	0.747	4.653	1.657	3.788
SAL-9B	0.6833	22.0167	3.8167	0.8167	23.2667	4.087	0.670	4.673	1.671	3.832
SAL-9C	0.8500	22.6333	3.7167	0.8000	24.4000	4.197	0.639	4.645	1.559	3.699
SAL-9D	0.85612	22.4120	3.5894	0.8000	24.200	4.305	0.638	4.487	1.463	3.626

Table 4.4a Rare Earth Elements (in ppm) data for Bilgi samples using ICP-MS

Sample #	La	Nd	Sm	Eu	Yb	Gd	ΣREE	(La/Yb)n	(La/Sm)n	(Gd/Yb)n	Eu/Eu*
BIL-13	8.07	6.42	0.75	0.16	0.38	0.91	16.80	14.35	6.77	1.216	0.591
BIL-13A	7.15	5.80	0.58	0.13	0.28	0.86	14.89	17.25	7.76	1.997	0.56
BIL-13B	4.68	3.80	0.40	0.15	0.27	0.80	9.33	11.70	7.37	2.40	0.79
BIL-15	13.91	8.13	0.87	0.20	0.32	0.75	23.43	29.37	10.06	1.89	0.74
BIL-15A	1.72	1.10	0.13	0.03	0.07	0.19	3.05	16.75	8.33	2.21	0.58
Chondrite-normalised	0.367	0.711	0.231	0.087	0.248	0.306	1.644	-	-	-	-
UCC	64	4.5	0.88	3.8	0.32	3.8	73.5				
PAAS	38.20	33.90	5.55	1.08	2.82	4.66	81.55				

Average Chondrite-normalised values (Taylor and McLennan, 1985)
$ Average Upper Continental Crust values (McLennan. 2001)
Subscript $_n$ refers to chondrite-normalized values.

Solution

La/La ÷ Yb/Yb = 8.07/0.367 ÷ 0.38/0.248 = 21.989 ÷ 1.532 = 14.35

$Eu/Eu^* = Eu_n / ½ (Sm_n + Gd_n) = 0.03/0.087 / ½ (0.13/.231) + (0.19/0.306) = 0.58$ (BIL-15A)

Table 4.4b Rare Earth Elements (in ppm) data for Jamkhandi samples using ICP-MS

Bulk rock sample	La	Nd	Sm	Eu	Dy	Yb	Gd	ΣREE	(La/Yb)n	(La/Sm)n	(Gd/Yb)n	Eu/Eu*
JAM-1	7.18	11.18	3.80	1.22	2.9	3.90	0.39	30.57	1.243	1.189	0.0306	0.79
JAM-2	17.53	24.55	5.017	0.98	1.97	1.63	0.30	51.977	7.267	0.807	0.149	0.518
JAM-3	42.77	59.75	11.37	1.92	3.01	1.82	0.28	120.92	15.88	2.367	0.125	0.883
JAM-4	5.87	7.65	1.92	0.65	2.24	1.58	0.05	19.96	2.510	1.92	0.0256	1.763
JAM-5	24.58	33.45	6.42	1.20	6.19	1.78	0.30	73.92	9.331	2.409	0.137	0.1205
Chondrite-normalised	0.367	0.711	0.231	0.087		0.248	0.306	1.644				
UCC	64	4.5	0.88	3.8		0.32	3.8	73.5				
PAAS	38.20	33.90	5.55	1.08		2.82	4.66	81.55				

Table 4.4c Rare Earth Elements (in ppm) data for Ramthal sample using ICP-MS

Bulk rock sample	La	Nd	Sm	Eu	Dy	Yb	Gd	ΣREE	(La/Yb)n	(La/Sm)n	(Gd/Yb)n	Eu/Eu*
RAM-2	1.6500	2.9500	0.4333	0.1167	0.314	0.3167	0.37	6.1507	4.344	2.396	0.947	0.87
RAM-2A	1.6833	2.7333	0.5167	0.1500	0.436	0.3667	0.38	6.266	3.828	0.752	0.839	0.99
RAM-2B	1.6500	2.5667	0.5500	0.1000	0.261	0.3167	0.32	5.7644	4.344	1.888	0.251	0.68
RAM-2C	2.8333	3.6667	0.8000	0.3000	0.617	0.5333	0.76	9.511	1.626	2.229	1.155	0.58
RAM-2D	1.6720	2.9675	0.5326	0.1500	0.424	0.3320	0.28	6.358	1.541	1.973	0.68	0.34
Chondrite-normalised	0.367	0.711	0.231	0.087		0.248	0.306	1.644				
UCC	64	4.5	0.88	3.8		0.32	3.8	73.5				
PAAS	38.20	33.90	5.55	1.08		2.82	4.66	81.55				

Table 4.4d Rare Earth Elements (in ppm) data for Salgundi samples using ICP-MS

Bulk rock sample	La	Nd	Sm	Eu	Dy	Yb	Gd	ΣREE	(La/Yb)n	(La/Sm)n	(Gd/Yb)n	Eu/Eu*
SAL-9	8.5667	11.30	2.17	0.5667	1.045	0.599	1.23	25.478	9.66	2.48	1.66	0.97
SAL-9A	9.2167	12.35	2.25	0.6000	1.340	0.687	1.27	27.71	9.07	2.59	1.50	0.99
SAL-9B	8.7500	11.45	2.17	0.5833	1.091	0.587	1.23	25.86	10.07	2.54	1.69	0.99
SAL-9C	8.8167	11.68	2.33	0.6000	1.098	0.598	1.25	26.37	10.00	2.38	1.69	0.99
SAL-9D	8.8912	11.60	2.2	0.5922	1.095	0.600	1.55	26.52	10.01	2.54	2.09	0.93
Chondrite-normalised	0.367	0.711	0.231	0.087		0.248	0.306	1.644				
UCC	64	4.5	0.88	3.8		0.32	3.8	73.5				
PAAS	38.20	33.90	5.55	1.08		2.82	4.66	81.55				

HFSE: High Field Strength Elements (Ti, U, Th)
HREE: Heavy Rare Earth Elements (Eu, Gd, Dy, Yb)
LREE: Light Rare Earth Elements (La, Nd, Sm)

CHAPTER 5

MINERALOGY AND PETROGRAPHY

5.1 Introduction

Identifying minerals and thereby the rock in which they occur are the essentials of geoscience studies. Knowledge of the minerals, their paragenesis and thermodynamics help in understanding the process of formation of the rocks in which they occur. The deformation mechanisms to which the rocks may be subjected to help in understanding the deformation history of a region. Keeping in mind the significance of the study of minerals and the rock this chapter deals with the mineralogy and the petrological characters of the lithounits taken up for study from Bilgi, Jamkhandi, Ramthal and Salgundi. This was achieved by planned field observations and preparing microsections of the samples of rocks collected from the study areas for further analysis.

5.2 Petrographic description and Classification of the lithounits studied

i. Based on field observations

On the basis of the observations made in the field and as quoted in Chapter 3, the lowermost lithounit of the Ramdurg Formation from Bilgi and Jamkhandi is found to enclose clasts of subrounded quartz and angular feldspars within siliceous to argillaceous matrix. The clasts of quartz range between 2cm – 10cm in length, while the feldspars are up to 3cms in length. The clasts enclosed in the matrix give a matrix-supported texture to the rock. The rock shows graded bedding with coarser pebbles at the base and finer ones at the top. An increase in percentage of quartz content is observed with a concomitant decline in feldspars as one move up in the studied section indicating mineralogical

maturity. The unaltered grains of feldspar which represent both the alkali and plagioclase varieties is in many ways suggestive of the detritus having been supplied by the underlying two-feldspar Granite. The composition very naturally is suggestive of the rock unit to be an arkose.

Constituting the lithounit at Ramthal are large cobbles and stretched elliptical pebbles of jasper, banded jasper and banded hematite quartzite that are subrounded to subangular constituting the framework clasts which are bounded within a ferruginous-siliceous matrix. It is found to be clast-supported showing point contacts giving the sediment a grain-support fabric. The lithounit exposed at Salgundi is compact, massive and oligomictic with rounded to sub rounded cobbles and pebbles of banded chert, jasper, banded jasper, milky quartz, banded hematite quartzite. The framework clasts are ovoid and elliptical ranging in size from 1cm to 18cms and are matrix-supported. Undoubtedly the rock is a conglomerate and is referred in Indian stratigraphy as the Salgundi Conglomerate.

ii. Based on microsection studies

- ***Bilgi and Jamkhandi***

Under the microscope the thin sections of the arkose from Bilgi shows quartz and feldspar as dominant clasts which are found to show overgrowths in crystallographic continuity with those in the matrix (Fig. 5.1a). The feldspars are represented by both, the alkali and plagioclase feldspar varieties; some grains of the latter are found to be replaced by the K-variety Microcline (Fig. 5.1b). Some of these feldspars have remained unaltered. These

replaced grains are likely to have been inherited from the basement Granite. The quartz and feldspars appears strained with some of them displaying undulose extinction.

Tourmaline, magnetite, chromite and sphene occur as important accessory minerals. The opaques magnetite and chromite display octahedral outlines (Fig. 5.2a), but have developed jagged edges on account of leaching of their constituents forming a thin rim surrounding the framework clasts (Fig. 5.2b). Sphene shows perfect wedge-shape, has a high relief and is internally cracked exhibiting high interference colour (Fig. 5.3a). The mineral tourmaline is very conspicuous by its abundant presence. Small prismatic and polygonal grains of the mineral are found within the matrix occupying spaces between the framework clasts. Its presence assumes significance as not only it is the dominant of all other accessories, but also, appears aligned.

Just as at Bilgi, at Jamkhandi also, predominant within the arkosic sandstone are clasts of feldspars and quartz. But unlike Bilgi the feldspar is mostly microcline (Fig. 5.3b) and is also present as orthoclase. The quartz grains are clear while the matrix is dominantly clayey in composition. The common subordinate minerals include sphene, micas and epidote. In contrast to Bilgi where the mineral tourmaline, is so abundant in its presence, here it is insignificant in the rock.

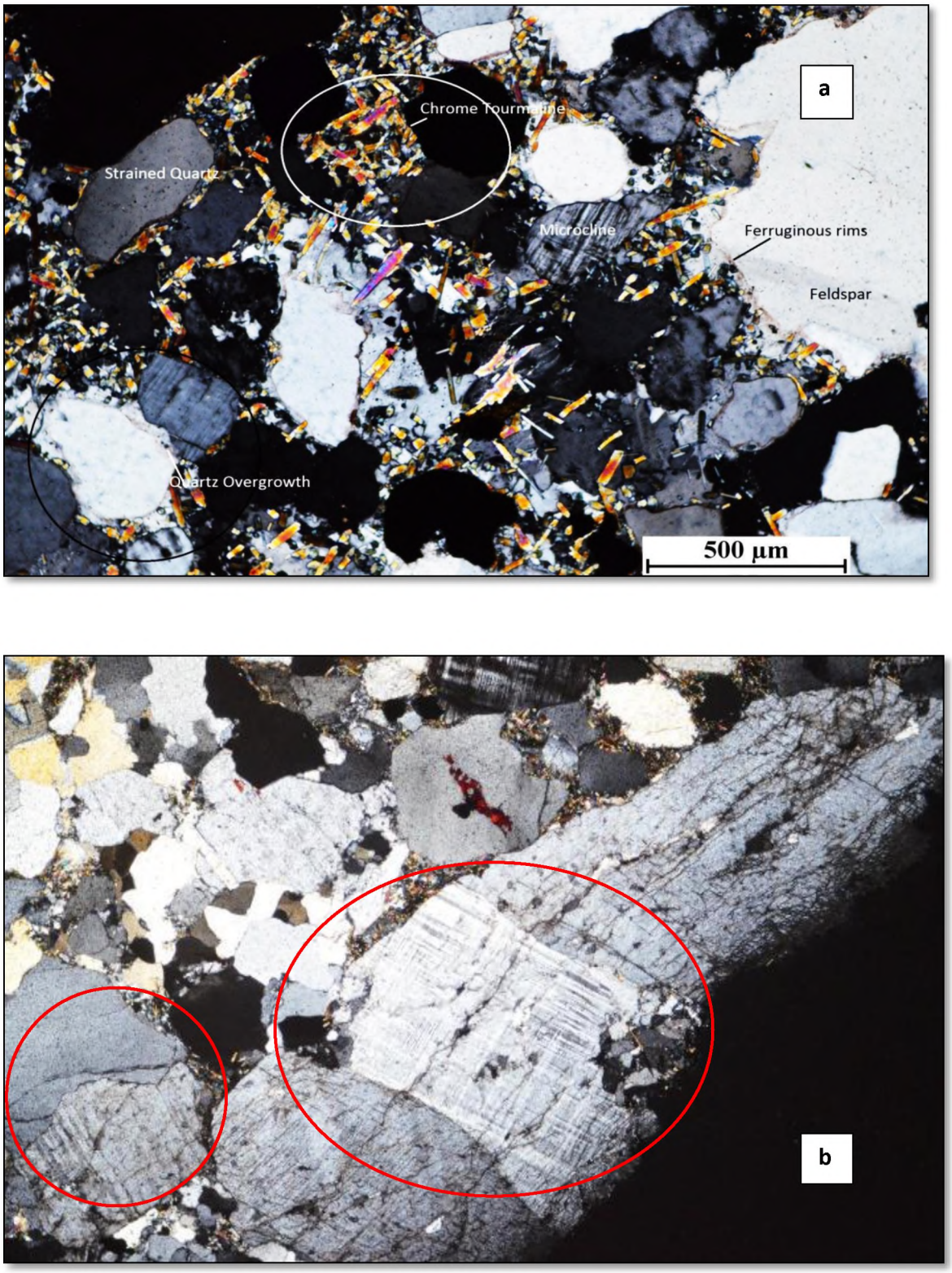

Figure 5.1 (a) Clasts of feldspars showing overgrowths in crystallographic continuity (10X, BXP), Bilgi **(b)** Plagioclase feldspar observed replacing microcline feldspar possibly inherited from basement Granite (10X, BXP), Bilgi

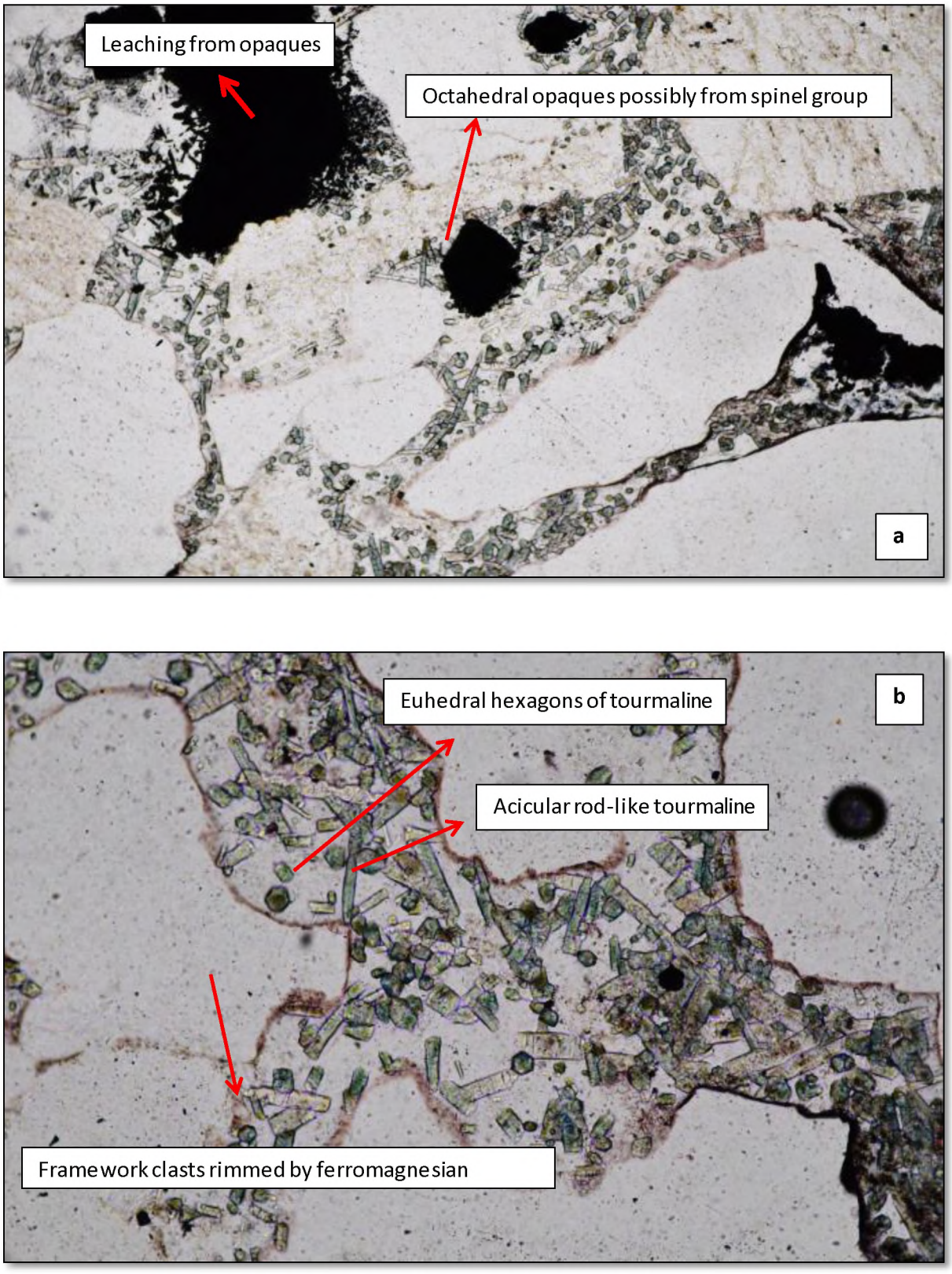

Figure 5.2 (a) Opaques of magnetite and chromite with octahedral outlines (10X, PPL), Bilgi **(b)** leaching of the constituents forming a thin rim surrounding the framework clasts (10X, PPL), Bilgi

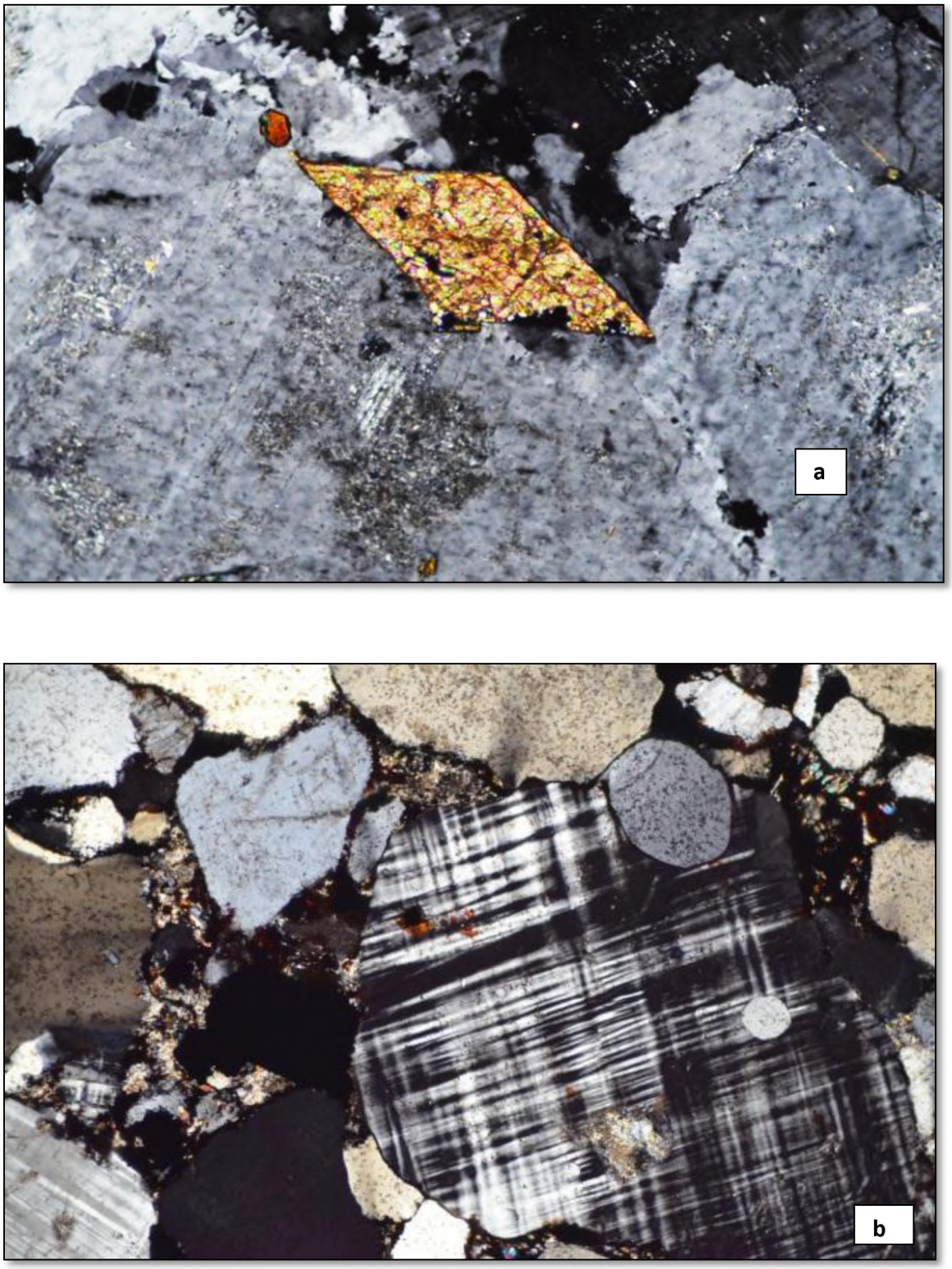

Figure 5.3 (a) Sphene as a heavy mineral in arkosic sandstone showing perfect wedge-shape, Bilgi (40X, BXP) **(b)** Microcline as the dominant feldspar, showing tartan twinning in arkosic sandstone, Jamkhandi (10X, BXP).

Of all the subordinate minerals like sphene, epidote and opaque minerals present within the host rock at Bilgi the presence of tourmaline is most conspicuous. It occurs in the matrix of the arkosic sandstone as euhedral, acicular, prismatic crystals exhibiting distinct pleochroism from dark green to yellow green. The grains have an average length of 206μm with an average width of 7.55μm. The mineral is optically negative in character with high order interference colours. The prism form is well developed with singly as well as doubly terminated crystals. The basal sections are hexagonal while, vertical sections show maximum absorption when the length is perpendicular to the vibration direction of the polarizer (Fig. 5.2a & b). These grains are confined within the matrix forming an intergranular relationship with the framework clasts of quartz and feldspars. They appear clear in nature with the absence of inclusions or striations and no visible overgrowths. Very striking is their appearance with no abraded corners or edges. Since the size of the individual tourmaline grains was not more than 206μm in length and 7.55μm across; it was impossible to separate them from the bulk rock sample for chemical analysis. As such individual grains of tourmaline were subjected to Scanning Electron Microscopy-Energy Dispersive Spectroscopy (SEM-EDS) analysis for further classification. Just as the presence of a large number of grains of tourmaline is conspicuous, their orientation also assumes significance. A detailed account of this mineral in given in chapter 10 of this thesis.

- ***Salgundi and Ramthal***

Microsections were prepared of the matrix portions of the conglomerate from both Ramthal and Salgundi avoiding the larger sized cobbles and pebbles. The matrix portions were carefully chosen in the preparation to include a few relatively larger grains.

On observing microsections of the samples of the rock from Ramthal grains of opaque minerals and cryptocrystalline varieties of silica are seen dispersed amongst subrounded clasts of quartz. All are enclosed within ferruginous matrix. There appears a coating of a thin film of iron oxide around the coarser quartz clasts. Some of the clasts are fractured and display point as well as sutured contacts.

Samples of the conglomerate from Salgundi on the other hand in thin sections show angular to rounded quartz, cryptocrystalline silica and small flakes of muscovite mica within a ferruginous to siliceous matrix, along with opaque minerals. The mica flakes showing high interference colours are clustered around the larger clasts (Fig. 5.4a) and appear oriented at high angles to an incipient cleavage (Fig. 5.4b). Overgrowth on many of the quartz grains in crystallographic continuity is very significant (Fig. 5.5a). Most of these grains exhibit sweeping undulose extinction and the mineral show signs of recrystallisation within the matrix (Fig. 5.5b).

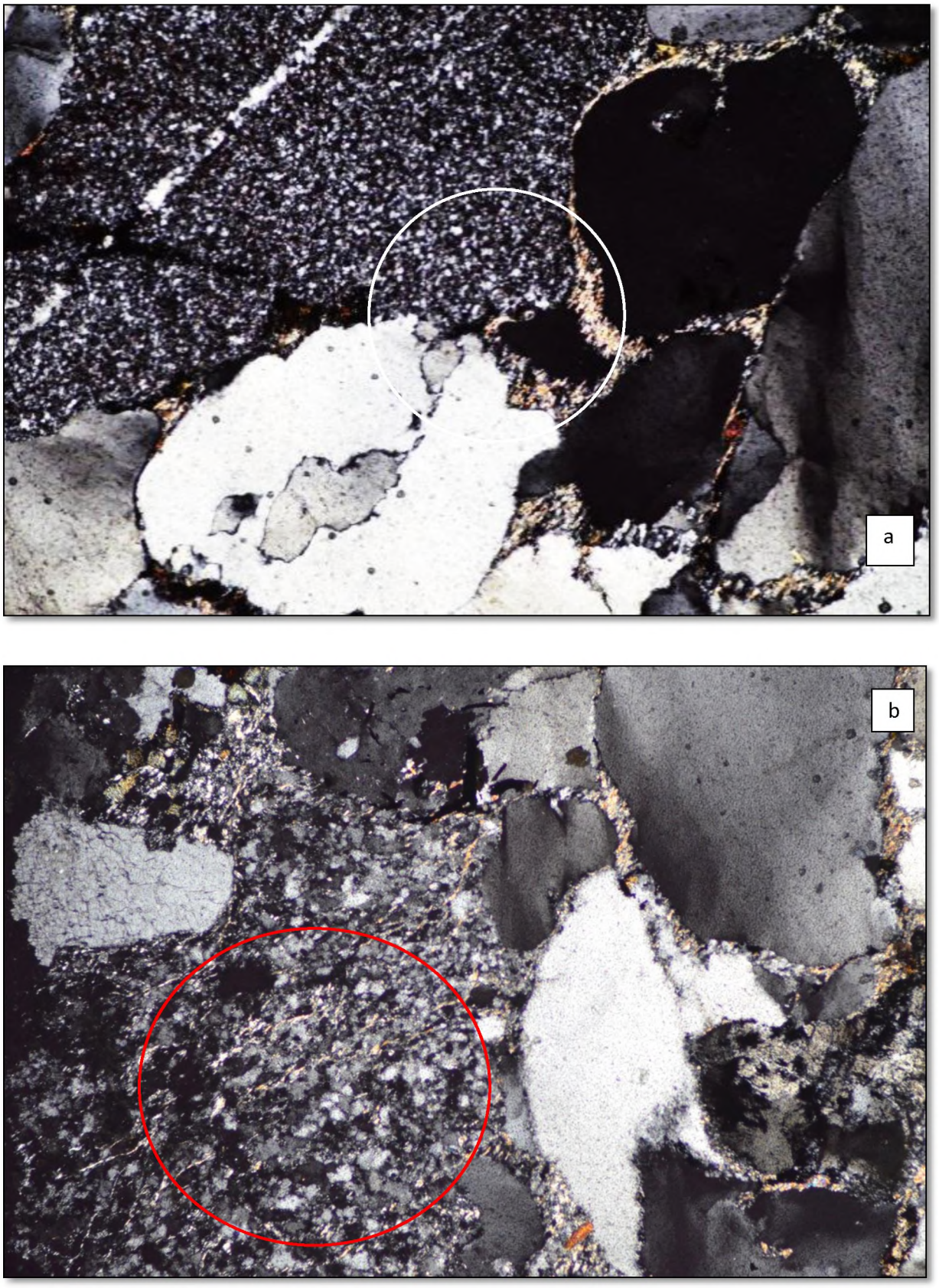

Figure 5.4 (a) Neocrystallisation of mica flakes clustering around clasts (10x, BXP) **(b)** Orientation of mica flakes at high angles to an incipient cleavage (10x, BXP), Salgundi

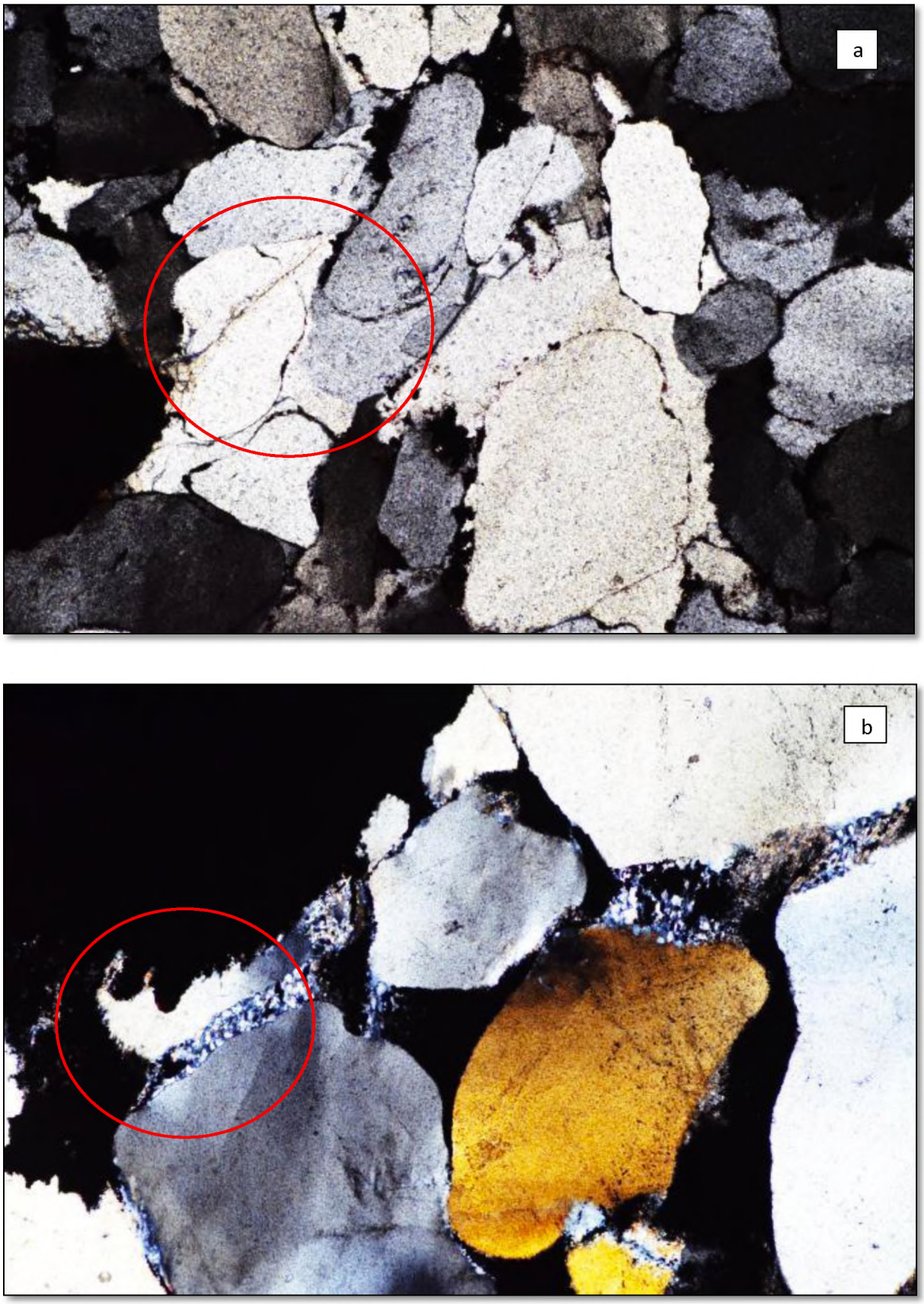

Figure 5.5 (a) Overgrowths in crystallographic continuity (10x, BXP) **(b)** Recrystallisation of matrix; sweeping undulose extinction (10X, BXP) in quartz crystals, Salgundi.

iii. Based on modal analysis

A qualitative modal mineral abundance estimated of both the lithounits from thin section from each of the areas of study are in conformity with field observations. A dominance of framework constituents of quartz (55%) is observed followed by feldspars (30%); lithic fragments, opaque and other minerals (including tourmaline) making up the remaining (15%) at Bilgi and Jamkhandi; at Salgundi and Ramthal there is a predominance of clasts of quartz 73% (both monocrystalline and polycrystalline), with opaques (09%) and lithic fragments (03%), but an absence of feldspars is noticed. Unlike other areas of study, the qualitative modal mineral abundance estimation done for samples from Bilgi show a decline in the percentage as well as grain size of feldspars from the base to top of the sequence with an increase in percentage of monocrystalline quartz. This, along with an improved sorting suggests a progressive textural and mineralogical maturity from bottom towards the top of the rock unit.

The plots based on the modal analysis on the ternary diagram Q = Quartz, F= Feldspar, RF = Rock Fragments (Pettijohn *et al.,* 1963); for the rock samples from Bilgi and Jamkhandi lie within the arkosic sandstone field (Fig. 5.6). Similarly, based on the plots drawn using the log ratio of In(Q/RF) *versus* In(Q/F) (Weltje *et al.,* 1998) for samples from Bilgi and Jamkhandi it can fairly be said that the arkosic sandstone was derived from a plutonic igneous source whereas for the samples from Salgundi and Ramthal, a metamorphic/sedimentary origin is indicated for the Mesoproterozoic cover rocks (Fig. 5.7; Table 5.1). The relief of the region must have been ranging between moderate hills to low lying plains; and as revealed from the character of the matrix, tropical humid climatic conditions must have been prevailing during the time of deposition of these rocks.

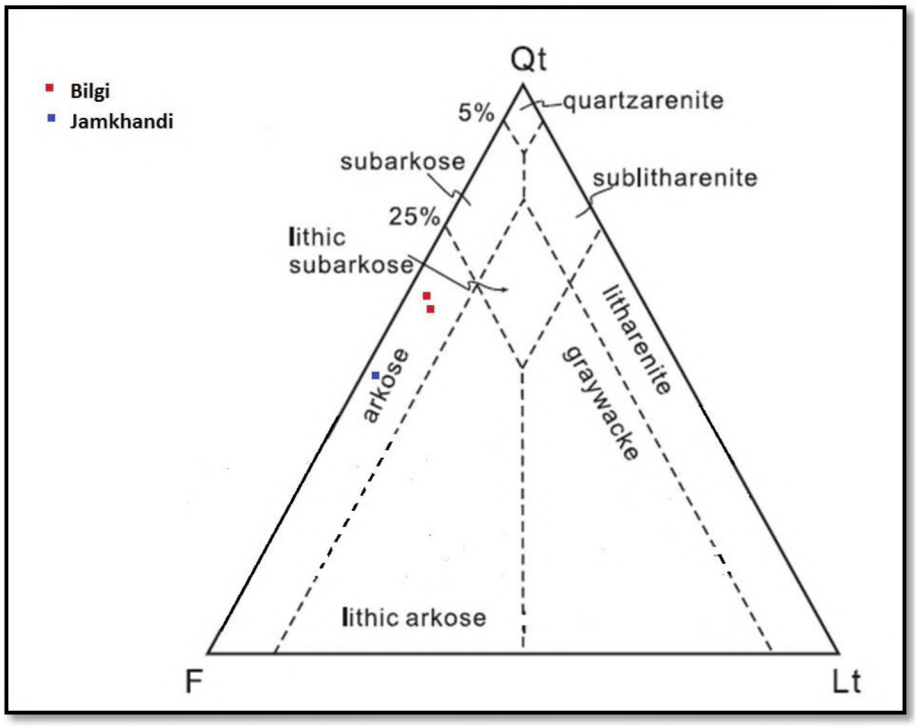

Figure 5.6 Ternary plot of Quartz-Feldspar-Lithic fragments (Q-F-Lt) based on modal analysis (*after* Pettijohn *et al.*, 1963)

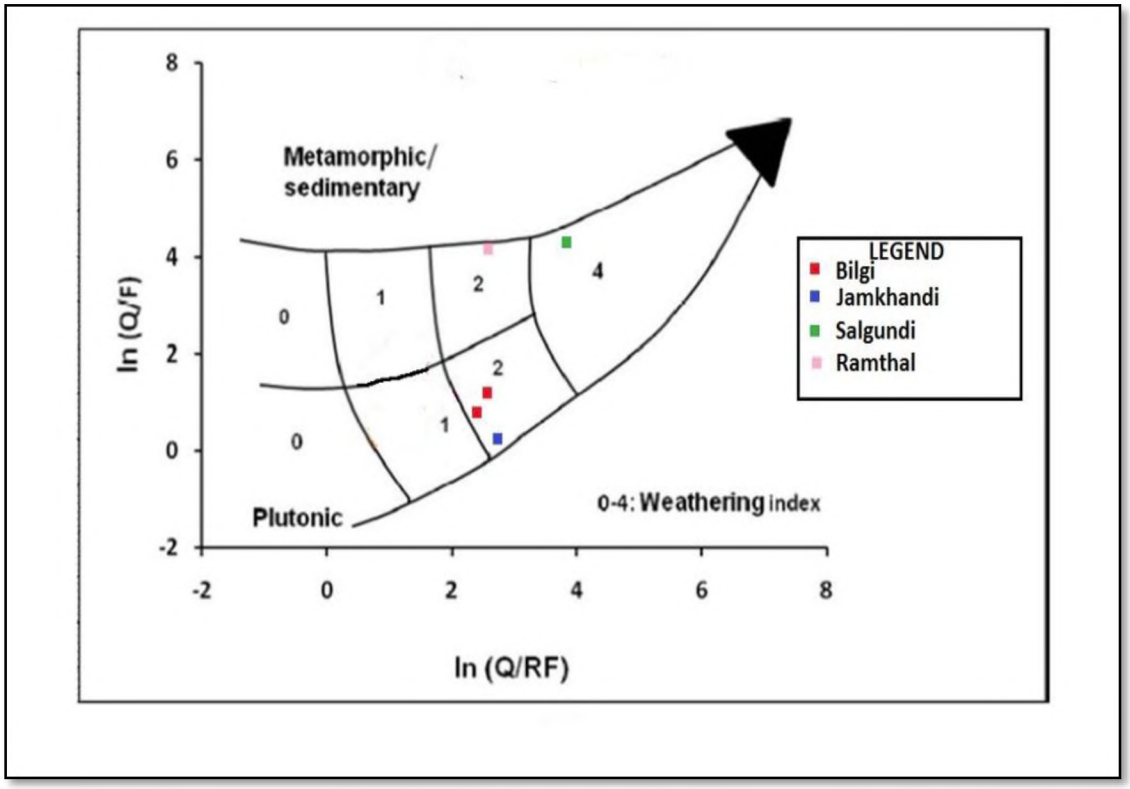

Figure 5.7 Plot of In(Q/RF) *versus* In(Q/F) *after* Weltje *et al.*, (1998) Q = Quartz, F= Feldspar, RF = Rock Fragments.

Table 5.1 Fields 1-4 refer to the semi-quantitative weathering indices derived on the basis of relief and climate as indicated in the table.

Semi-quantitative Weathering Index			Physiography (relief)		
			High (Mountain) 0	Moderate (Hills) 1	Low (Plains) 2
Climate (Precipitation)	(semi) Arid and Mediterranean	0	0	0	0
	Temperate sub humid	1	0	1	2
	Tropical humid	2	0	2	4

5.3 Interpretation

In accordance with the field observations, the mineral compositions and the plots derived based on results of modal abundance of the different minerals, the lowermost lithounit of the Ramdurg Formation exposed at Bilgi and Jamkhandi is classified to be arkosic sandstone whereas the lithounit from Salgundi and Ramthal is confirmed as a pebbly conglomerate.

The rock arkose belongs to the family of sandstones, the detritus for which is derived from the weathering and erosion of rock sources that are richer in feldspars, like granites and/or gneisses under arid to semi-arid climatic conditions (Tucker, 2011). Apart from the provenance, the relief also plays a major role in the preservation of the feldspar. This is true when the detritus is derived from a source with a high relief or if the burial was rapid after the erosion of the source rock. In such a case the arkose can still be preserved inspite

of intense chemical weathering. The arkose from Bilgi and Jamkhandi is composed of feldspars grains that have remained unaltered and fresh.

The conglomerates from Ramthal and Salgundi on the other hand were deposited within the intracratonic basin, under continental, near-shore shallow-marine environments (Dey, 2015; Jayaprakash *et al.,* 1987; Sathyanarayana, 1994; Kale *et al.,* 1996; Bose *et al.,* 2008). These conglomerates suggest terrestrial scree and fans giving a downslope to the fluvial sediments along the margins of the basin (Bose *et al.,* 2008).

Based on the above discussion it can be stated that the rock unit at Bilgi and Jamkhandi is an arkosic sandstone rich in feldspars. Many of the grains of feldspars having escaped the process of weathering are preserved as fresh and angular fragments embedded within siliceous to argillaceous matrix. Tourmaline dominates at the accessories Bilgi whereas sphene and epidote occur as subordinates. Prismatic and polygonal grains of tourmaline occupy the matrix space along with some clayey matter. The opaques belonging to spinel group of minerals are common. This arkosic rock, at Jamkhandi, shows clusters of mica around the framework clasts.

At Salgundi and Ramthal the rock identified is a pebbly conglomerate consisting of subrounded framework clasts consisting of lithic fragments of Banded Hematite Quartzite, Quartzites along with jasper banded jasper, chert, quartz as dominant pebbles and cobbles embedded within a siliceous to ferruginous matrix. The rock is mineralogically and texturally matured.

A metamorphic/sedimentary origin is indicated for rocks from Ramthal and Salgundi whereas the arkosic sandstone from Bilgi and Jamkhandi has been derived from a plutonic igneous source. During the time of deposition the topography of the region must have been ranging between moderate hills to low lying plains wherein tropical humid climatic conditions prevailed.

CHAPTER 6

GEOCHEMISTRY

6.1 Introduction

The term 'geochemistry' was coined by German-Swiss chemist Christian Friedrich Schonbein in 1838. The science of Geochemistry is an important tool dealing with principles of chemistry which helps to explain mechanisms of major geological systems of the earth. Therefore, the powdered bulk rock samples collected from the study areas of Bilgi, Jamkhandi, Salgundi and Ramthal were subjected for geochemical analysis inorder to detect the presence of major and minor oxides, besides trace and Rare Earth elements and derive the relevant data for the purpose of deriving conclusive interpretations.

6.2 Observations based on major oxide compositions

As a part of the laboratory methods employed geochemical analysis was done of a bulk composition of the rock samples from the four areas under study. An expected outcome from these analyses is that in all of the samples the percentage of SiO_2 is very high (av. 83.26%). Inorder to enable a geochemical classification of the rock unit from Bilgi and Jamkhandi based on the analysed data obtained from graphical presentations involving ratios of log (Fe_2O_3*/K_2O) *versus* log (SiO_2/K_2O) proposed by Heron (1988), Fig. 6.1a; and, log (SiO_2/Al_2O_3) *versus* log (Na_2O/K_2O) proposed by Pettijohn *et al.*, (1972), Fig.6.1b are done. The plots of the ratios in both of the graphs lie within the field marked for arkose for both Bilgi as well as Jamkhandi. This is in conformity with the field identification modal analysis and the petrologic characters of the rock unit. It thus

enhances conclusion made earlier that the lowermost rock unit of the Ramdurg Formation exposed at Bilgi and Jamkhandi is arkosic sandstone.

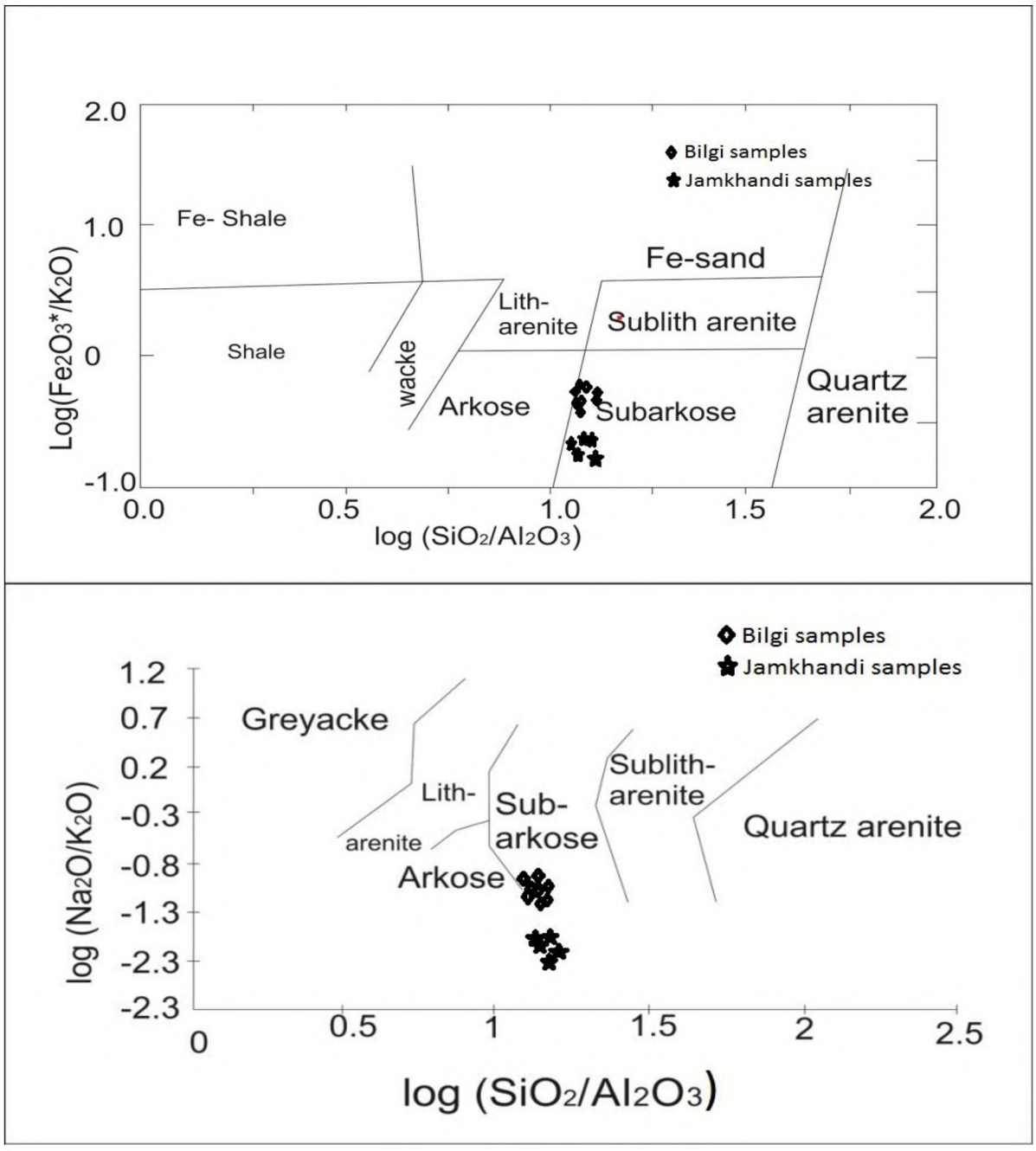

Figure 6.1 Geochemical classification **(a)** proposed by Heron (1988) involving ratios of log (Fe_2O_3*/K_2O) *versus* log (SiO_2/K_2O) **(b)** log (SiO_2/Al_2O_3) *versus* log (Na_2O/K_2O) of Pettijohn *et al.*, (1972).

Amongst the other major oxides both K_2O as well as Na_2O are very poor in the conglomerate from Ramthal and Salgundi; on the contrary the percentage of K_2O far exceeds that quoted for an average arkose (av. 3.89%; Pettijohn, 1963, Table 5.4a.) in the samples from Bilgi and Jamkhandi. From the analysis of the samples it is noted that at Bilgi, K_2O averages to 1.5% in the upper parts of the rock unit (BIL-15. BIL-15A, BIL-15B, BIL-15C, BIL-15D) and 3.78% at lower levels (BIL-13, BIL-13A, BIL-13B, BIL-13C, BIL-13D), while it amounts to an average of 4.97% at Jamkhandi. Na_2O on the other hand is only about 0.32% on an average for the rock unit at Bilgi and almost negligible for Jamkhandi (av. 0.06%). Both of the above are in line with the observations quoted earlier that the conglomerate is devoid of feldspars while, feldspars is one of the dominant clasts in the arkosic sandstone from Bilgi and Jamkhandi where Orthoclase/microcline predominates amongst the feldspars especially at the base of in this rock. Also, as the amount of plagioclase feldspar being much less in the arkosic sandstone it is reflected in a poor percentage of Na_2O (<1%). This explains excess of K_2O over Na_2O. There is a variation in the percentages of K_2O in the samples from Bilgi, it being much more in the lower parts than in the upper levels. This is in accordance with the observed decline in the feldspar content from bottom towards the top of the rock unit. In accordance, the K_2O/Na_2O ratio derived for samples from the lower part (av. 9.58%) of the arkose at Bilgi is relatively higher than that for samples from upper part (av. 4.57%). A predominance of quartz over feldspars has caused a decline in this ratio towards the upper levels of the rock unit at Bilgi. At Jamkhandi, the K_2O is quite significant; apart from the feldspars, presence of mica and illite may have also contributed to such a high ratio (for *e.g.* Pettijohn, 1963; McLennan *et al.,* 1983; Nath *et al.,* 2000; Osae *et al.,* 2006; Adeigbe and Jinoih, 2013).

The excess of SiO_2 and low amounts of Al_2O_3 are pointers to a textural and mineralogical maturity of the arkosic sandstone as well as the conglomerate from the four areas

respectively. The excessive SiO_2 detected in the analysis of the samples from Bilgi and Jamkhandi is suggestive of the detritus to have been derived from a stable cratonic area that is dominated by granitic rocks. The conglomerate from Salgundi and Ramthal has a low Al_2O_3 content which is a reflection of a negligible presence of alumina bearing minerals such as kaolinite/illite in the rock. The preponderance of a variety of silica-bearing minerals in the oligomictic conglomerate with a negligible presence of alumina bearing minerals is reflected in a higher SiO_2/Al_2O_3 ratio. These ratios determined to estimate the textural maturity of the rock reveal average values of 14.70 for Bilgi; 11.92 for Jamkhandi; 21.48 for Salgundi and 168.73 for Ramthal.

The low percentage of Al_2O_3 in the conglomerate from Salgundi (3.88%) and Ramthal (0.55%) is also, a pointer to very poor content of argillaceous matrix in the rock. This has provided a textural maturity to the rock. It is quite evident thus, that compared to the arkosic sandstone from Bilgi and Jamkhandi, the Salgundi conglomerate is better matured. Some amount of winnowing of the clay materials carrying appreciable Al_2O_3 and TiO_2 could have occurred during transportation and deposition. The arkosic sandstone from Bilgi (6.43%) and Jamkhandi (6.84%) on the other hand contain higher amount of Al_2O_3 as compared to the average arkose 3.89% of Pettijohn, 1963. This is much to be expected with the dominance of feldspars and some amount of clayey matrix in the rock. The values of $Al_2O_3/ (Fe_2O_3* + MgO)$; (Adeigbe and Jinorh, 2013) ratios point to a moderate diagenetic alteration, especially at Bilgi and Jamkhandi. The high concentrations of FeO (6.29% at Ramthal and 8.12% at Salgundi as compared to Upper Continental Crust (UCC: 4.49%; Taylor and McLennan, 1995) is a result of dominance of iron oxides in the matrix.

Thus, while the arkosic sandstone from Bilgi and Jamkhandi is rich in SiO_2, K_2O and to some extent Al_2O_3, it is poor in Na_2O; in contrast the conglomerate from Salgundi and Ramthal though having a high proportion of SiO_2, lacks both K_2O and Al_2O_3. Both the rock units are found to have negligible CaO and P_2O_5 which may be attributed to an absence of calcareous cement.

At Bilgi while the TiO_2 remains on par (av. 0.50%) with the average Upper Continental Crust (UCC; 0.50%; Taylor and McLennean, 1985) in the upper levels, it declines to av. 0.24% lower down. Also, it is found to be entirely insignificant at Ramthal (av. 0.04%), Salgundi (av. 0.18%) and Jamkhandi (av. 0.34%).

An average MgO percentage of 0.57 for the lower half of the arkose at Bilgi matches with that proposed by Pettijohn, 1963 (0.55%) for an average arkose, its value marginally increasing to 0.8% at upper levels. The average MgO content for Jamkhandi, Ramthal and Salgundi is found to be 0.14%, 0.06% and 0.50% respectively. The Fe_2O_3* content in conglomerate from both Ramthal and Salgundi is relatively higher (2.13-2.19% and 2.92-2.89% respectively) than that proposed for Proterozoic Cratonic Sandstone (PCS 0.59%, Condie 1993). In the arkosic sandstone at Bilgi on the other hand Fe_2O_3* is far poor (only 0.66%) in the lower part of the unit but increases to 2.80% in the upper level. Jamkhandi samples reveal only 1.15% of Fe_2O_3*on an average. In the same context the FeO is found to be far higher (av. 8.0%) in the upper parts of the unit at Bilgi and only 2.44% on an average lower down as compared to average Upper Continental Crust (UCC = 4.49%; Taylor and McLennan, 1985).

Heron (1988) proposed Fe_2O_3*/K_2O ratio to differentiate feldspars from lithic fragments in a sandstone. Though the arkosic sandstone at Bilgi is abundant with clasts of feldspar and quartz, it is observed that the Fe_2O_3*/K_2O ratio (av. 0.27) in the samples from lower levels is relatively less than that determined for the upper levels (av. 1.91), besides, it is only 0.224 for Jamkhandi. Expectedly, with the presence of ferruginous matrix in the conglomerate, this ratio for Salgundi (av. 9.10) and Ramthal (av.17.08) is much higher.

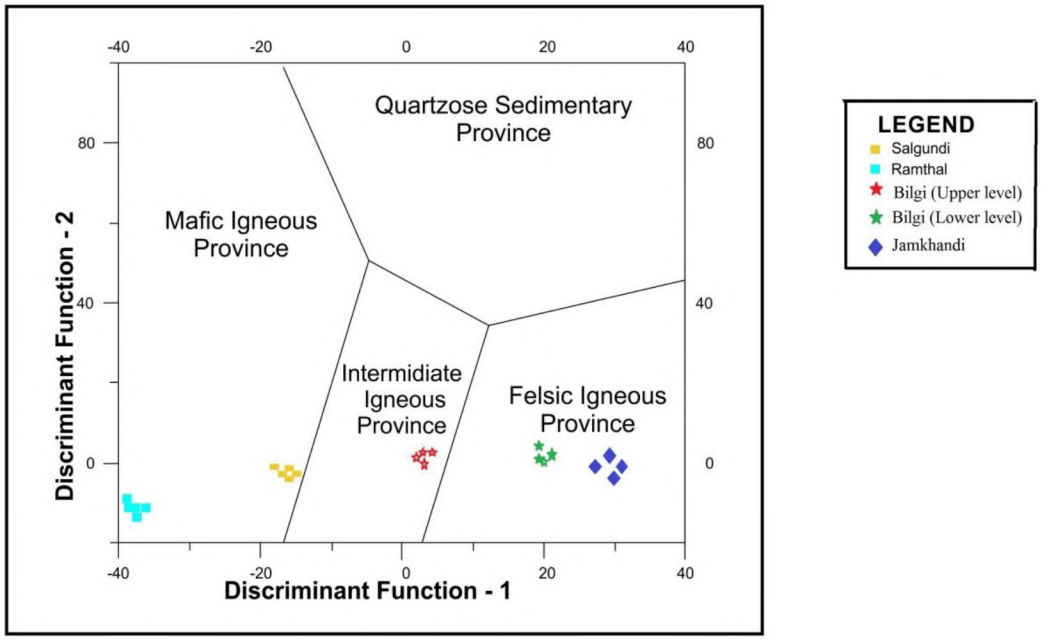

Figure 6.2 Major element provenance discriminant function diagram for Kaladgi sediments (Roser and Korsch, 1988). The discriminant functions are for the ratio plots are: Discriminant function 1 = 30.638 (TiO_2/Al_2O_3) – 12.541 (Fe_2O_3*/Al_2O_3) + 7.329 (MgO/Al_2O_3) + 12.031 (Na_2O/Al_2O_3) + 35.402 (K_2O/Al_2O_3); Discriminant function 2 = 56.5 (TiO_2/Al_2O_3) – 10.879 (Fe_2O_3*/Al_2O_3) + 30.875 (MgO/Al_2O_3) – 5.404 (Na_2O/Al_2O_3) + 11.1112 (K_2O/Al_2O_3) – 3.89

As revealed from the plots of these ratios on the major element provenance discriminant function diagrams (Roser and Korsch, 1988; Fig. 6.2) a felsic igneous source is suggested for the arkosic sandstone from Bilgi and Jamkhandi albeit with a little variance in the

lower and upper parts of the unit at Bilgi, it being more of an intermediate igneous provenance for the later. On the other hand a mafic igneous source is very imminent for the conglomerate at Ramthal and Salgundi.

Adeigbe and Jinorh, (2013); proposed Al_2O_3/ (Fe_2O_3* + MgO) ratio as a count to determine the extent of alteration. The values calculated for the samples from all of the areas under study range from 1.43 for upper levels and 4.09 for lower levels at Bilgi, 5.35 at Jamkhandi, 1.12 at Salgundi and 0.25 at Ramthal indicating low to moderate diagenetic changes.

The upper continental crust is proposed to contain by volume of approximately 21% quartz, 41% plagioclase and 21% potassium feldspar. Feldspars are the most abundant reactive (labile) minerals in the upper crust and degrade readily on chemical weathering to clay minerals. Chemically reactive solutions from soils carry away calcium, sodium and potassium from the feldspars so that the proportion of alumina to alkalis typically increases in the weathered product (Wedepohl, 1969).

A measure of the degree of weathering can be obtained by calculation of the Chemical Index of Alteration (CIA). This was calculated following the equation proposed by Nesbitt and Young (1982).

$$\text{CIA} = \frac{Al_2O_3}{Al_2O_3 + CaO^* + Na_2O + K_2O} \; x \; 100$$

where CaO^* is the amount of CaO incorporated in the silicate fraction of the rock.

In the CIA equation, CaO* is only the CaO that is present in silicates (*i.e.* plagioclase). All non-silicate CaO must be subtracted. If CaO* equals a negative number then it is set to unity in the equation. A correction is made for apatite and carbonate content. The correction to subtract the non-silicate CaO is:

$$molCaO^* = molCaO - molCO_2 - 10/3\ P_2O_5.$$

The resultant value is a measure of the proportion of Al_2O_3 *versus* the labile oxides in the analyzed sample. For unaltered albite, anorthite and K-feldspars the index value is 50; for diopside it is 0. Muscovite mica gives a value of 75 whereas for illite, montmorillonites and beidellites it ranges between 75 and 85. Kaolinite and chlorite give a value of 100. For unaltered basalts the value ranges between 30 and 45 whereas for granites and granodiorites the values are higher, ranging between 45 and 55. Average shales range from 70 to 75 owing to a large proportion of clay minerals (Wedepohl, 1969).

Solution: The working for the calculation of CIA value using sample JAM-5 as an example is presented in Table 3.5a and 3.5b.

Table 6.1a Sample example JAM-5 (Jamkhandi)

Oxide	Molecular weight
Al_2O_3	26.98 x 2 + 16 x 3 = 101.96
CaO	40.08 + 16 = 56.08
Na_2O	22.99 x 2 + 16 = 61.98
K_2O	39.1 x 2+ 16 = 94.20
P_2O_5	30.97 x2 + 16 x 5 = 141.94
CO_2	12.01 + 16 x 2 = 44.01

Table 6.1b Calculation of moles from oxides

Oxides	Moles				
	JAM-5	JAM-4	JAM-3	JAM-2	JAM-1
Al_2O_3	7.72/101.96 = 0.076	6.8/101.96 = 0.067	7.25/101.96 = 0.071	7.89/101.96 = 0.078	6.28/101.96 = 0.062
CaO	0.12/56.08 = 0.002	0.12/56.08 = 0.002	0.12/56.08 = 0.002	0.11/56.08 = 0.002	0.12/56.08 = 0.002
Na_2O	0.07/61.98 = 0.001	0.06/61.98 = 0.0009	0.06/61.98 = 0.001	0.06/61.98 = 0.001	0.06/61.98 = 0.001
K_2O	5.50/94.20 = 0.059	5.4/94.20 = 0.057	5.46/94.20 = 0.058	4.99/94.20 = 0.053	4.99/94.20 = 0.053
P_2O_5	0.05/141.94 = 0.0004	0.05/141.94 = 0.0004	0.05/141.94 = 0.0004	0.05/141.94 = 0.0004	0.05/141.94 = 0.0004
CO_2	-	-	-	-	-

$molCaO^* = molCaO - molCO_2 - 10/3\ P_2O_5$.

Sample JAM – 5: $molCaO^* = 0.002 - 0 - 3.333\ (0.0004) = 0.00067$

Sample JAM – 4: $molCaO^* = 0.002 - 0 - 3.333\ (0.0004) = 0.00067$

Sample JAM – 3: $molCaO^* = 0.002 - 0 - 3.333\ (0.0004) = 0.00067$

Sample JAM – 2: $molCaO^* = 0.002 - 0 - 3.333\ (0.0004) = 0.00067$

Sample JAM – 1: $molCaO^* = 0.002 - 0 - 3.333\ (0.0004) = 0.00067$

$$CIA = \frac{Al_2O_3}{Al_2O_3 + CaO^* + Na_2O + K_2O}\ x\ 100$$

$$CIA = \frac{0.076}{0.076 + 0.00067 + 0.001 + 0.059}\ x\ 100 = 55.61$$

The pebbly conglomerate from Salgundi (av.78) and Ramthal (av. 63) show higher values of CIA compared to Post Archean Australian Shale (PAAS, CIA: 70; Taylor and McLennan, 1985), an indication of the rocks from the source area to have undergone high degree of weathering. Having already mentioned that originally mafic igneous source provided the detritus to the conglomerate, it is quite obvious that it would reflect on the ferruginous character of the matrix at the two places (Salgundi Fe_2O_3*: av. 2.90%;

Ramthal Fe_2O_3* 2.18%). In contrast, much of the feldspars in the arkosic sandstone have been preserved unaltered. This would have a direct bearing on the CIA as is clear from the values calculated for the rock samples from Bilgi av. 59.52; Jamkhandi av. 55.30 which are much less compared to PAAS indicating less degree of weathering of the source rock.

An indication of the degree of weathering is provided further by K_2O/Al_2O_3 ratio; the greater the value, higher the degree of weathering. From the values determined for the two localities Salgundi: av. 0.066 and Ramthal: av. 0.19, it indicates higher degree of weathering for the conglomerate as compared to Salgundi. This is in line with the calculated CIA values. In case of Bilgi (lower levels: av. 0.56; upper levels: av. 0.28), the moderate values along with those determined for Jamkhandi (av. 0.73) suggests the arkosic sandstone to have received sediments from a source where the degree of weathering had been relatively low (Bauluz *et al.*, 2000).

The much higher SiO_2 percentage concomitant with a below average percentage of alumina and an average content of alkalis in both, the arkosic sandstone as well as the conglomerate reflects on the Chemical Maturity Index (CMI). In the graphical representation using $Al_2O_3+Na_2O+K_2O$ *versus* SiO_2 (Suttner and Dutta 1986) all of the values cluster in the top left hand corner within the semi-humid sub-zone (Fig. 6.3)

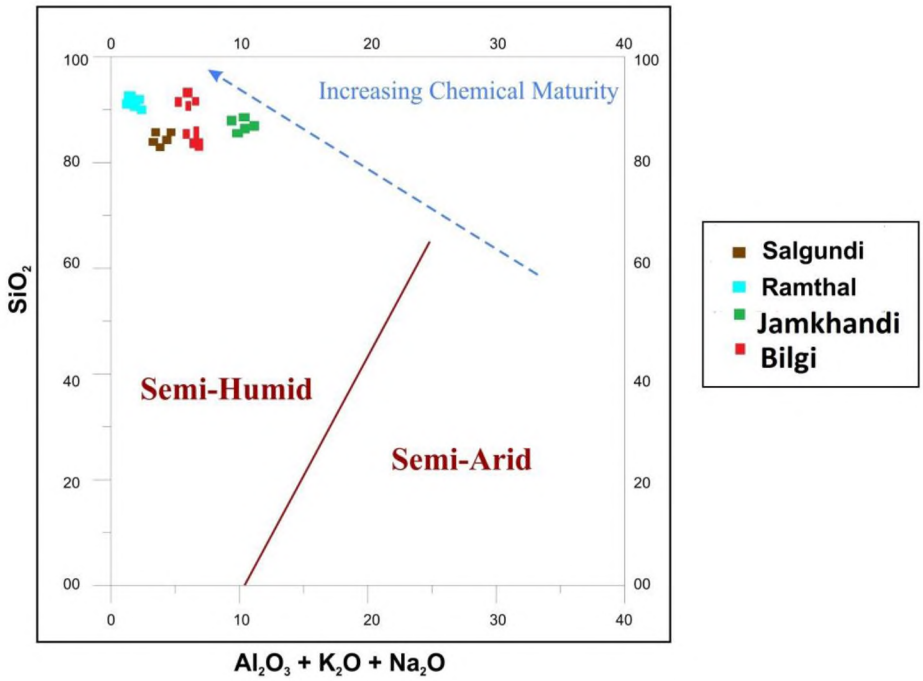

Figure 6.3 Plot of Al_2O_3+K_2O+Na_2O *versus* SiO_2 showing trend of Maturity (*after* Suttner and Dutta, 1986).

6.3 Observations based on trace and Rare Earth Element analysis from the study areas

- ***Trace Elements***

The trace elements (which are 80 in number) even though constitute a small fraction of the system they provide insights into the behaviour and origin of magmas. The heavy alkali and alkaline earth elements have a larger ionic radius; larger than the radii of even the larger octahedral sites; tend to concentrate in the melt phase when melting or crystallisation occurs; such of the elements are called incompatible. These are those elements that partition readily into a melt phase when the mantle undergoes melting.

Examples of heavy alkali and alkaline earth elements include K, Rb, Cs, Sr, Ba, Ca, Mg or Fe and more rarely Na.

- ***Rare Earth Elements***

The rare earth elements are the two rows shown at the bottom of the periodic table; the first row are the lanthanide rare earths namely; Lanthanum (La). Cerium (Ce), Praseodymium (Pr), Neodymium (Nd), Samarium (Sm), Europium (Eu) as Light Rare Earth Elements (LREE) whereas Gadolinium (Gd), Terbium (Tb), Dysprosium (Dy), Holmium (Ho), Erbium (Er), Thulium (Tm), Ytterbium (Yb), Lutetium (Lu) as Heavy Rare earth Elements (HREE) accompanied by Yttrium (Y) and Scandium (Sc). In the second row are the actinide rare earths: Actinium (Ac), Thorium (Th), Protactinium (Pa), Uranium (U). However, the term rare earth is used to refer only the lanthanides in geochemistry. Only two of the actinides Th and U have nuclei stable enough to survive over the history of the earth. Y shares the same chemical properties (like the charge and ionic radius) as the heavier rare earths and as a result behaves like rare earth element. Owing to their high charge and ionic radius, the rare earths are incompatible elements, though the degree of incompatibility varies. U and Th which are highly charged are highly incompatible, as are the lightest rare earths. However, the heavy rare earths have relatively small radii that can be accommodated to some extent in many of the common minerals, like for example plagioclase wherein Eu^{2+} readily substitutes for Ca^{2+}. Therefore, plagioclases are enriched in Eu as compared to other rare earths, and as a result the other phases associated with plagioclase become depleted in Eu. Mid Oceanic Ridge Basalt (MORB) exhibits a light rare earth- depleted pattern, which reflects the incompatible element depleted nature of the upper mantle from which these magmas are derived. The

depletion of the mantle is thought to have resulted from extraction of partial melts in which the incompatible elements are concentrated. The partial melts crystallise to form the continental crust. If this is so than the complimentary nature of the rare earth patterns of MORB and UCC is not coincidental. The Upper Continental Crust UCC is light rare earth-enriched with a negative Eu-anomaly. So if it is considered that the continental crust and the mantle are the only two reservoirs with significant concentrations of rare earth elements, and if the continental crust is light rare earth-enriched, then the mantle should be light rare earth-depleted.

A negative Eu anomaly is typical of many continental rocks, as well as sediments and seawater. This is due to the fact because many crustal rocks of granitic and granodioritic composition were produced by intracrustal partial melting. The residues of these melts were rich in plagioclase, hence retaining more of the Eu in the lower crust and creating a Eu-depleted upper crust. Sediments and seawater inherit this Eu anomaly from their source rocks in the upper continental crust.

Most of the sedimentary rocks and seawater have rare earth patterns similar to each other and to the continental crust. Inorder to make noticeable the difference in rare earth patterns between sediments, low temperature geochemists often normalise rare earth abundances to the concentrations in average shale. There are several sets of normalising values but the relative abundances are all similar. One such set is represented in table 6.2

Table 6.2 Normalizing Values used for Rare Earth Plots

	Ordinary Chondrites (Nakamura, 1974),	Orgueil (CI Chondrite) (Palme and Jones, 2005),	Ave. Shale (Piper, 1974)
La	0.329	0.245	41
Ce	0.865	0.638	83
Pr	0.130	0.0964	10.1
Nd	0.630	0.474	38
Sm	0.203	0.154	7.5
Eu	0.077	0.058	1.61
Gd	0.276	0.204	6.35
Tb	0.055	0.0375	1.23
Dy	0.343	0.254	5.5
Ho	0.077	0.0567	1.34
Er	0.225	0.166	3.75
Tm	0.035	0.0256	0.63
Yb	0.220	0.165	3.53
Lu	0.034	0.0254	0.61

Since rare earths are highly insoluble and immobile, their patterns often remain unchanged during metamorphism or deformation. Hence they can provide information of the history of the rock prior to metamorphism. Even during the production of sediment from crystalline rock, the rare earth patterns often remain unchanged and therefore have been used to identify the provenance *i.e.* the source of sedimentary rocks.

- ***High Field Strength Elements (HFSE)***

The high field strength (HFS) elements are named so owing to their high ionic charge. Examples Zr^{4+}, Hf^{4+}, Ta^{5+}, Nb^{5+} (Th^{4+} and U^{6+} or U^{4+} are also included in this group). Because of their large charge they are all small size cations with ionic radii of 64pm for Nb5+ and Ta5+, and 72 and 76 for Zr^{4+} and Hf^{4+} respectively (U^{4+} and Th^{4+} are larger). Their large charge requires one or more coupled substitutions to maintain electrical charge balance in minerals. Such substitutions are energetically unfavourable. Thus Hf and Zr are

moderately incompatible elements while Nb and Ta are highly incompatible elements. These elements are less electropositive as compared to the alkalis and alkaline and rare earths and involve greater degree of covalency in the bonds they form.

Because of their large ionic potential (i.e. ionic charge to ionic radius ratio) the HFS elements are insoluble and tend to be very immobile during the process of weathering and metamorphism. They therefore are useful to throw light in the study of ancient igneous rock suites and provide insights into the environment in which those rocks formed.

- ***Transition Metal Elements***

The chemistry of the transition elements is more complex as compared to other elements. Reasons are the transition metal elements have high electronegativity than alkali or alkaline earths, so that covalent bonding becomes significant. Bonding with oxygen in oxides and silicates is ionic but bonding with non-metals like sulphur is largely covalent. The other reason is the geometry of the *d* orbitals which are directional and thus bestow specific preferences for the geometry of coordinating anions. Their solubility is low as compared to alkalis and alkaline earths and depends upon the valence state and the availability of anions with which they can form soluble coordination complexes. Their behaviour in magmas is also variable. They range from moderately incompatible (e.g., Ti, Cu, Zn) to very compatible (e.g., Cr, Ni, Co) but their exact behaviour is generally a function of composition (both solid and melt phases) than that of the highly incompatible elements.

Trace-element concentrations in the arkose from Bilgi (BIL-13, BIL-13A, BIL-13B, BIL-15, BIL-15A, BIL-15B), conglomerate from Salgundi (SAL-9, SAL-9A, SAL-9B) and Ramthal (RAM-2, RAM-2A, RAM-2B) and arkose from Jamkhandi (JAM-1, JAM-2, JAM-3, JAM-4, JAM-5) are reported in Table 4.3a, 4.3b, 4.3c & 4.3d. In comparison with average upper continental crust (UCC) the concentrations of most trace elements are found to be generally low.

The conglomerate from Salgundi (42.22ppm) and Ramthal (28.12ppm) as well as the arkosic sandstone from Bilgi (18.25 -20.69ppm) and Jamkhandi (34.37ppm); is found to have higher Ni content compared to an average arkose, (Pettijohn, 1963) and PCS (Condie, 1993). Only at Salgundi, the conglomerate is found to give higher concentrations of Ni compared to its content in the UCC (Taylor and McLennan, 1995).

The rock units, the arkosic sandstone and the conglomerate have shown presence of opaque and heavy minerals. In accordance the analysis has revealed comparable concentrations of chromium and vanadium to those quoted for the Proterozoic Cratonic Sandstone (PCS Cr~ 24; Condie 1993). Comparatively the values of chromium are lower (Bilgi: 22.05; Salgundi: 16.09; Ramthal: 6.72ppm) compared to avg arkose and PCS except at Jamkhandi which is about 34.75ppm. The arkose from Bilgi and the conglomerate from Salgundi and Ramthal show higher values of vanadium.

As the process of diagenesis and metamorphism does not affect the distribution of REE, Th and Sc; their presence is quite useful in inferring crustal compositions. Further, unlike

elements like Zr, Hf, and Sn, the REE, Th and Sc are much less affected by heavy mineral fractionation (Cullers *et al.*, 1979; Bhatia and Crook 1986; Wronkiewicz and Condie 1987; Cox *et al.*, 1995; McLennan 2001; Mongelli and Dinelli 2001). Felsic and mafic igneous rocks along with their weathered products differ significantly in the abundances of REE and Th, the amount being much higher in felsic than in mafic rocks. Abundance of Co, Sc and Cr, on the other hand is the reverse, being more in mafic than in felsic rocks and their weathered products. As a result of a preferential partitioning into melts during crystallisation, the high-field strength elements (HFSE) like Zr, Nb, Hf, Y, Th, and U get enriched in felsic than in mafic sources (Feng and Kerrich 1990). Also, their immobile behaviour reflects on provenance compositions (Taylor and McLennan 1985). A relatively high content of Nb, Y, U, and Th in the samples of the arkosic sandstone from Bilgi and Jamkhandi along with higher ΣREE probably reflects on a control by grain size fractionation during transport, suggesting further, a contribution from a felsic source where there is high concentration of these elements (Table 4). In contrast, in the conglomerate from Salgundi and Ramthal, the concentrations of U (0.45 – 0.68ppm) and Th (1.53 – 2.2ppm) is found to be very low compared to UCC (U: 28ppm and Th: 10.7ppm; Taylor and McLennan, 1995). A mafic source is thus confirmed as these sources are known to be less concentrated in these elements. As viewed earlier, the Closepet Granite which forms the underlying basement could be one of the supplier of these elements to the arkosic sandstone at Bilgi and Jamkhandi, while, the conglomerate from Ramthal and Salgundi must have received these elements from mafic sources.

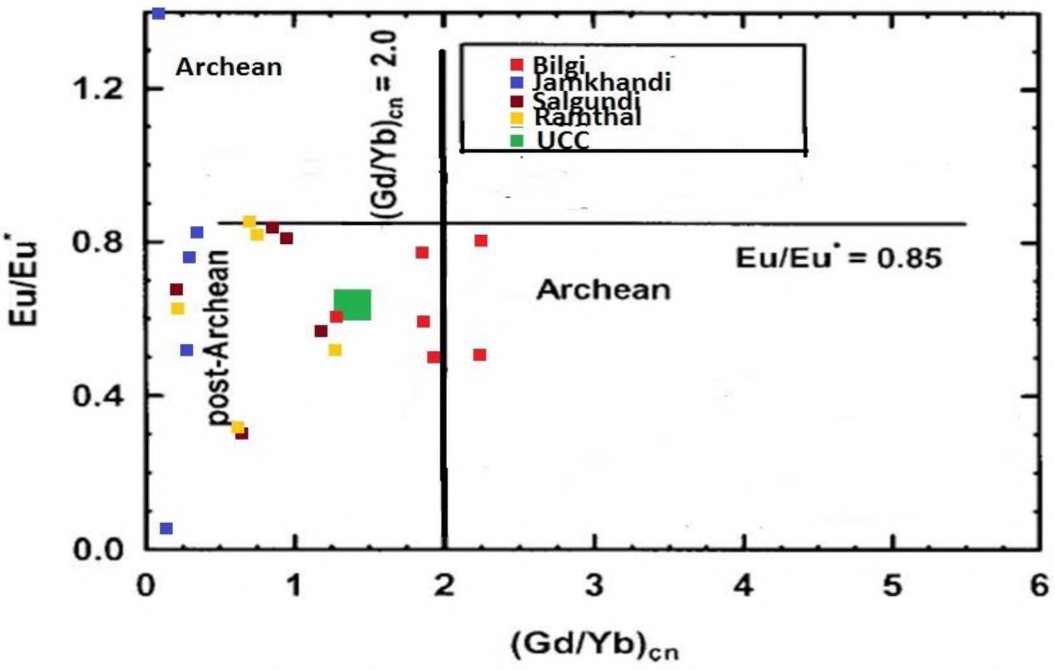

Plot of Eu/Eu* versus (Gd/Yb)cn for the Kaladgi arkose and conglomerate (after McLennan and Taylor, 1991)

Figure 6.4 Plot of Eu/Eu* *versus* (Gd/Yb)cn for the Kaladgi arkose and conglomerate (*after* McLennan and Taylor, 1991).

The plots for Eu/Eu* versus Gd/Yb for the rock unit from Bilgi, Jamkhandi, Ramthal, and Salgundi are in line with a post-Archean age and the values are in close proximity to the average UCC (*after* McLennan and Taylor, 1991, Fig. 6.4

A negative Eu anomaly is obtained for the arkosic sandstone exposed at Bilgi, Jamkhandi, and for the conglomerates exposed at Salgundi and Ramthal.

CHAPTER 7

PROVENANCE

7.1 Introduction

Under intense humid weathering conditions the unstable minerals like epidote, micas, feldspars etc. undergo partial destruction whereas the stable minerals like sphene, tourmaline, pyroxenes etc. survive and get carried to the basin of deposition. In case of cold and arid environments the unstable minerals too may get transported to the site of deposition (Irshad and Ahmed, 2013). Inorder to measure the degree of chemical weathering as an indicator to paleoclimatic conditions the Chemical Index of Alteration (CIA) is used as a measure of humidity indicator (Goldberg, K and Humayun, M, 2010).

7.2 Chemical Index of Alteration (CIA) and Chemical Maturity Index (CMI)

The Chemical Maturity Index (CMI; Suttner and Dutta 1986; Fig. 7.1) is generally inferred through the values of Chemical Index of Alteration (CIA; Nesbitt and Young 1982). Those derived for the arkosic sandstone from the graphical representation of Al_2O_3+Na_2O+K_2O *versus* SiO_2, drawn using the chemical analysis suggests a increasing Chemical Maturity by the partial removal of mobile elements such as Na and K (av. CIA: Bilgi: av. 59.52; Jamkhandi: av. 55.30). The CIA values determined for Bilgi and Jamkhandi are far below the PAAS values of 70 proposed by Taylor and McLennan 1985 as compared to the conglomerate from Salgundi (av. 78) and Ramthal (av. 63).

7.3 Provenance study

From the analysis of the samples of conglomerate from Salgundi and Ramthal, concentrations of High-Field strength elements (HFSE) such as U (0.45-0.68ppm) and Th (1.53-2.2ppm) are found to be very low compared to UCC (U: 28ppm and Th: 10.7ppm; Taylor and McLennan, 1995). Such low proportions of U and Th along with low ΣREE as compared to UCC probably reflects on a control by grain size fractionation during transport. Owing to their immobile nature they also reflect on provenance compositions (Taylor and McLennan, 1985). Also, it is an indication of a detrital contribution from a mafic source rather than felsic, as mafic sources are known to be poorer of these elements. The High-field strength elements (HFSE) tend to get concentrated more in felsic source rocks than in mafic as a result of their preferential partitioning in the melt during the process of crystallisation. (Feng and Kerrich, 1990). The arkosic sandstone from Bilgi and Jamkhandi, on the other hand has tended to be having a relatively higher content of U and Th, a clear reflection of its detritus having been derived from felsic igneous rock.

Much information on the provenance of sedimentary rocks can also be derived from the ratios of La/Co, Th/Co, Cr/Th and Eu*/Eu as they are significantly different for felsic and mafic source rocks (Cullers *et al.*, 1988; Wronkiewicz and Condie 1989; Condie and Wronkiewicz 1990; Cullers 1994). For the samples of arkosic sandstone from Bilgi and Jamkhandi, the La/Co, Th/Co, Cr/Th and Eu*/Eu values correspond closely with the values for sediments derived from felsic source rocks (Table 7.1). Thus, in confirmation of the inference drawn earlier it may well be argued that the detritus of the rock unit from these two areas has been derived from felsic source rocks. In sharp contrast, the calculated

ratios of these elements for the conglomerate from Ramthal and Salgundi point to an source ranging from felsic to mafic for the matrix.

Table 7.1 Range of elemental ratios of Bilgi arkose, Salgundi conglomerate, Ramthal conglomerate, and Jamkhandi arkose in this study compared to the ratios in similar fractions derived from felsic rocks, mafic rocks, and upper continental crust.

Elemental Ratio	Range of arkose from Bilgi[1]	Range of conglomerate from Salgundi[2]	Range of conglomerate from Ramthal[3]	Range of arkose from Jamkhandi[4]	Range of Sediment from Felsic Sources[5]	Range of Sediment from Mafic Sources[5]	Upper Continental Crust[6]
La/Co	3.82 – 6.9	3.62-3.8	3.81-5.31	3.42-11.77	1.80–13.8	0.14–0.38	1.76
Th/Co	5.5- 14.4	1.5-1.7	3.66-4.40	13.93-51.70	0.67–19.4	0.04–1.40	0.63
Cr/Th	0.67-1.2	0.22-4.43	3.18-4.29	0.33-1.26	4.00–15.0	25–500	7.76
Eu/Eu*	0.56–0.79	0.93-0.99	0.34-0.99	0.51-1.76	0.40–0.94	0.71–0.95	0.63

1, 2, 3, 4 study areas
5 Cullers (1994, 2000); Cullers and Podkovyrov (2000); Cullers *et al.* (1988).
6 McLennan (2001); Taylor and McLennan (1985).

The relative REE patterns and the size of the Eu anomaly also have been used to infer sources of sedimentary rocks (Taylor and McLennan 1985; Wronkiewicz and Condie 1989). Felsic igneous rocks usually contain negative Eu anomalies, and mafic igneous rocks contain lower little or no Eu anomalies (Cullers 1994, 2000). The Eu anomaly is the phenomenon whereby the Europium (Eu) concentration in a mineral is either enriched or depleted relative to some standard, commonly a chondrite or Mid-Oceanic Ridge Basalt (MORB). In geochemistry a Eu anomaly is said to be positive if the Eu concentration in the mineral is enriched relative to other REE and is said to be negative if Eu is depleted relative to other REE.

Trace elements like Chromium (av. 11.17 at lower levels and av. 22.05 at upper level of the sequence; Table 3.6b) and Vanadium are concentrated more at upper levels of the

sequence as compared to lower levels at Bilgi (av. 11.18 at lower levels and av. 38.53 at upper level of the sequence).

The stability of minerals has a bearing on Fe_2O_3*/K_2O ratios. Stable minerals tend to give low values while presence of unstable minerals in a rock results in higher values of this ratio. Potash feldspars are stable at low temperatures that are diagnostic of sedimentary rocks whereas the rock-forming ferromagnesian minerals are unstable. The arkosic sandstone at Bilgi in its lower part has revealed poor amount of TiO_2, Cr_2O_3 and V_2O_3 as it is only the opaque ferromagnesian minerals which are present contributing to their concentration. While Pettijohn *et al.,* 1963; subscribe TiO_2 percentage of 0.17 and MgO as 0.55% for an average arkose; at Bilgi, the relatively higher content of TiO_2 (0.50%), Fe_2O_3*(2.84%) and MgO (0.87%) in the upper part of the arkosic sandstone as compared to samples from lower levels (TiO_2=0.23%; $Fe_2O_3^*$=0.72%; MgO=0.53%) indicates an increase in the percentage of TiO_2, Fe_2O_3* and MgO from the bottom to the top.

A marked variation in the percentages of these oxides has resulted in a low Fe_2O_3*/K_2O ratio (0.27) for the lower part and a higher ratio (1.90) for the upper part of the rock unit. This clearly is indicative of a greater presence of unstable ferromagnesian minerals like tourmaline, chromium, micas etc. higher up while K-bearing feldspars have remained concentrated in the lower section of the rock.

Prismatic grains and polygonal cross sections of tourmaline are conspicuous by their presence within the matrix. The grains do not show any signs of wear and tear during

transport. Thin sections of the samples from the upper part of the arkosic rock at Bilgi reveals a greater presence of such grains than the lower part. Though the more felsic two-feldspar granite underneath the arkosic sandstone is reported to have tourmaline as an accessory, such a significant presence of the mineral in the studied thin sections of the rock unit at upper levels may well be thought of to have been due to its supply from another source lying in close proximity.

7.4 Interpretation

A low to moderate weathering of the source rocks like felsic igneous rocks as reported in pervious Chapter 6, under cool to semi-humid conditions would favour only a partial alteration of both the K and Na feldspars while much of them have survived to remain fresh also, suggesting rapid burial, and the source area to be close to the basin of deposition. Those which got altered resulted in creating the argillaceous part of the matrix. In case of the conglomerate values of CIA, Salgundi (av. 78) and Ramthal (av. 63) were found to be higher as compared to PAAS (70) again indicating semi-humid conditions with moderate degree of alteration of the source material. These values which are lower at Bilgi (av. 59.5 and Jamkhandi (av. 55.3) than the PAAS would suggest a relatively lesser degree of alteration of the source rocks.

An inference may be based on higher concentrations of TiO_2, Fe_2O_3* and MgO at upper levels of the rock sequence of an existence of FeMg- and Ti-bearing minerals like sphene, titanomagnetite etc. in the upper levels. It is also suggestive of a significant presence of mafic minerals at higher elevation which could possibly be due to a change in provenance that provided more mafic constituents during the later stages of deposition.

A positive correlation can thus be drawn between the greater existence of ferromagnesian minerals in the upper section and a new cycle of deposition that contributed these minerals from a source other than that which provided the detritus lower down the rock unit. It is thus envisaged from the significant occurrence of mafic constituents in the upper section that a different provenance contributed such minerals during the later stage of deposition.

While the Closepet Granite provided majority of the feldspars to the unit in one cycle, the larger amount of tourmaline has come at a later stage of deposition. Thus, it can be inferred that for the arkosic sandstone from Bilgi, a source other than that which provided the detritus to the lower part of the unit is very highly probable.

The la/Co, Th/Co, Cr/Th, Cr/Th and Eu*/Eu ratios derived for the arkosic sandstone and the conglomerate greatly suggest a felsic source for the detritus to the former and a felsic o mafic source to the latter. Further, the samples from Bilgi and Jamkhandi as well as for the conglomerate from Ramthal and Salgundi are found to show negative Eu anomalies suggesting the detritus was derived from the continental crust source rocks of granitic-granodioritic composition that were LREE enriched.

CHAPTER 8

DEPOSITIONAL HISTORY AND PALEOCURRENTS

8.1 Introduction

As discussed in chapter 4, the beds at Ramthal dip towards North, while at Salgundi they are inclined towards South. It is envisaged that the sedimentary succession at these two places represent parts of two limbs of a major synclinal fold, the river Malaprabha sinuating along the axis. Field observations of exposures report imbrication created by orientation of elongated pebbles both at Ramthal and Salgundi. At Ramthal the alignment suggests the upstream end to be towards east with paleocurrents flowing down west. The overlying quartzites displaying cross-bedded structures have their cross-beds inclined westwards substantiating the westward flow of currents (Fig. 4.12a & Fig. 8.1). The conglomerate at Salgundi on the other hand displays elongated pebbles whose orientation based on imbrications is suggestive of an eastward flow of paleocurrents with the upstream end towards west (Fig. 4.14b & Fig. 8.1).

As observed in the field at Ramthal and Salgundi, the vertical face of the conglomeratic bed exhibits parallelism of the long axes of the elongated (prolate) pebbles. These axes are visibly parallel to the strike of the beds. The shorter axes accordingly, as seen on the surface are oriented in the direction of dip. Such a parallelism of the long axes of the pebbles is generated in water lain deposits. Smoothly flowing streams loaded with large sized pebbles, which are normally dragged along the floor of the channel, orient them during travel and bring about a parallelism of the axes on slowing down. On offloading this will create imbrication and the orientation thus developed will be in line with the direction of flow of the current. In case of fluvial or any water-lain deposits the prolate

shaped pebbles get oriented both normal as well as parallel to the direction of current (Tucker, 2011), wherein a rolling action produces a normal-to-current orientation; whereas parallel orientation arises from a sliding motion of the pebbles (Tucker, 2011).

8.2 Interpretation

Mukerjee *et al.,* (2016) suggest decoupling effect along a detachment surface, the unconformity acting as one in this case led to separation of the Mesoproterozoic sedimentary cover from the basement rocks in the Kaladgi basin (Fig. 8.1). A part that got detached from northern block on a regional high slid down southwards under gravity gliding to get compressed against the stable southern margin of the basin producing folds. The stable northern part remained stationary and undeformed maintaining its original tilt towards south. In the folded system that got created, the study areas of Ramthal and Salgundi occupy a synclinal fold. The northern limb of the fold on which Salgundi is located has maintained the original tilt (South) while the other limb (Southern-Ramthal) got rotated to reverse the tilt of the beds towards north as a result of the folding. On unfolding to revert to original prefolding position the southern limb would be in line with the northern limb to dip southwards. In accordance now, the paleocurrent direction at Ramthal deduced from the imbrication should be pointing towards east, in line with that observed at Salgundi where the beds have maintained original tilt. It can thus be inferred that the western side marks the upstream end and the paleocurrents moved down eastwards during the initial deposition of the sediments within the basin (Fig. 8.3).

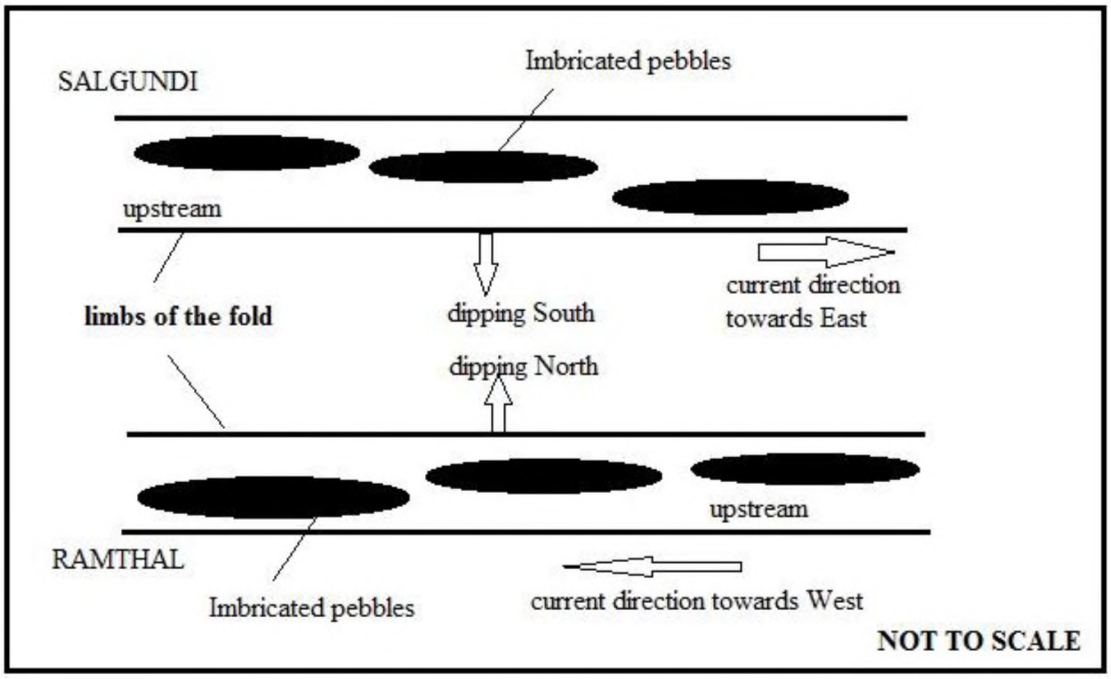

Figure 8.1 Paleocurrent directions based on imbrications

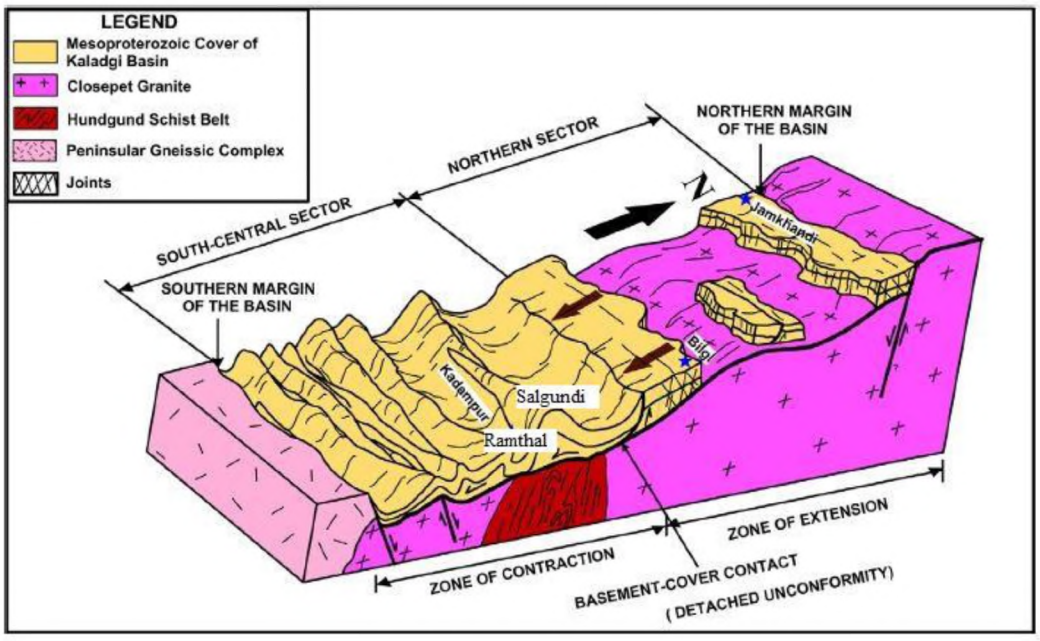

Figure 8.2 Decoupling along a detached unconformity (source: Mukerjee *et al.*, 2016)

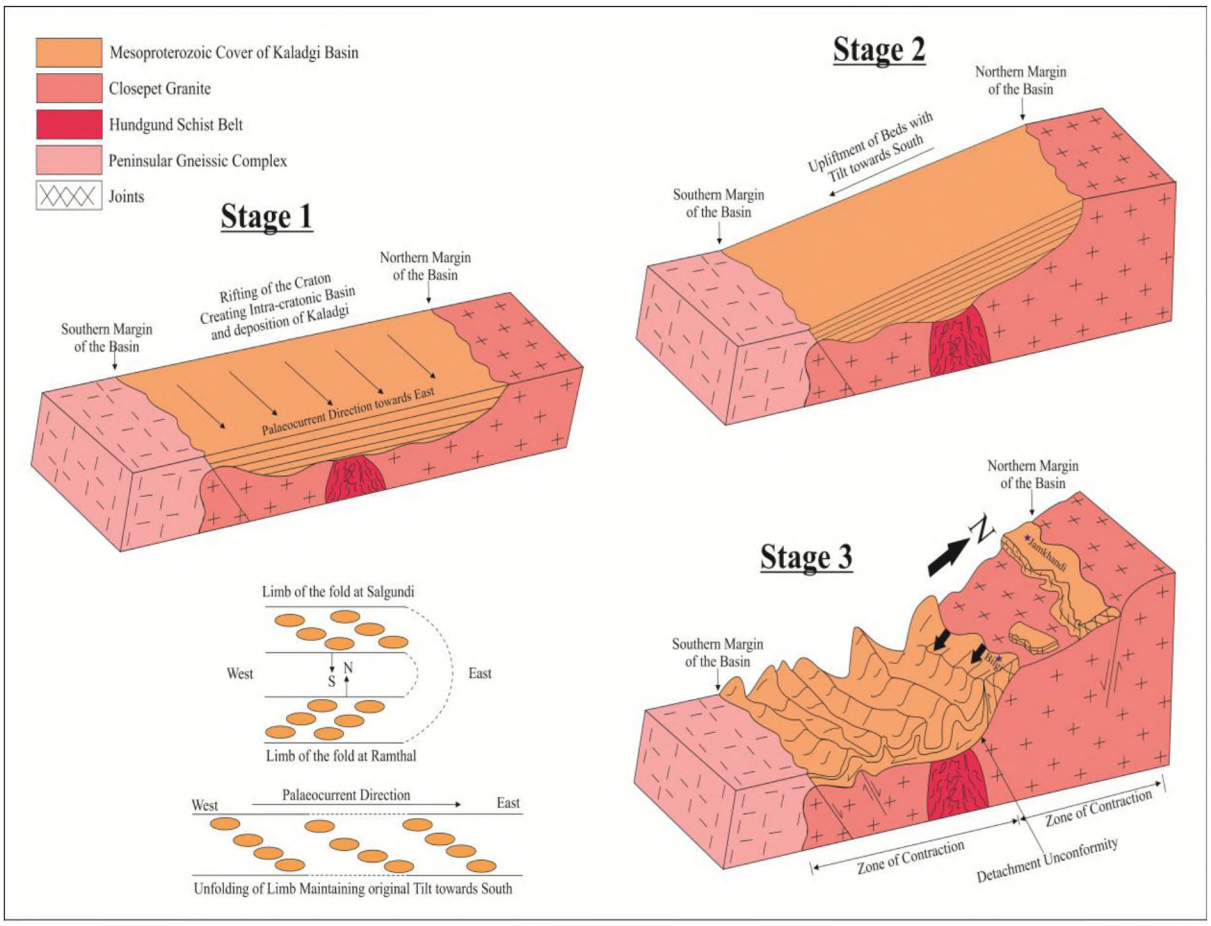
Mesoproterozoic Cover of Kaladgi Basin
Closepet Granite
Hundgund Schist Belt
Peninsular Gneissic Complex
Joints
Stage 1
Southern Margin of the Basin
Rifting of the Craton Creating Intra-cratonic Basin and deposition of Kaladgi
Northern Margin of the Basin
Palaeocurrent Direction towards East
Limb of the fold at Salgundi
West
N
S
East
Limb of the fold at Ramthal
West
Palaeocurrent Direction
East
Unfolding of Limb Maintaining original Tilt towards South
Stage 2
Northern Margin of the Basin
Upliftment of Beds with Tilt towards South
Southern Margin of the Basin
Stage 3
Northern Margin of the Basin
N
Ramkhandi
Southern Margin of the Basin
Zone of Contraction
Zone of Contraction
Detachment Unconformity

CHAPTER 9

TECTONIC AND DEFORMATIONAL HISTORY

9.1 Introduction

Deformational studies of an area help in understanding the evolutionary trend of sedimentary basins. The tectonic and geologic history of a region controls in some way the source area characteristics and the depositional environment in which sediments accumulate (Boggs, 2009). Mukherjee *et al.*, (2016), have recently described in detail the structural and tectonic features of parts of the Proterozoic Kaladgi basin in the northern part of Western Dharwar Craton. In their documentation and interpretation of structural features, they have stressed on the extensional nature of deformation in rocks exposed in the northern part of the Kaladgi Basin. The results of preliminary study carried out as a part of this thesis, an effort is made to add to the information contained in the work of Mukherjee *et al.*, through documentation of certain structural features from the areas under investigation. According to Mukerjee *et al* 2016, Bilgi area forms a part of the extensional zone towards the Northern Sector (Jamkhandi-Bilgi-Mamadapur sector). This contribution only records structural features in the arkosic rock at Bilgi; and its impact on structural and tectonic interpretation given in Mukherjee *et al.*, is not being attempted, as further studies are planned in the study area. The aim is to highlight the low to moderate temperature regime deformation in the region augmenting our existing understanding of the supposedly extensionally undeformed northern sector of the Kaladgi basin. The study presents outcrop and petrographic characters evidencing deformation features in the study area.

This research records data from the study of exposures of 25m thick arkosic sandstone lying over the Closepet Granite. The rock unit belongs to the Mesoproterozoic Saundatti Quartzite Member of Ramdurg Formation of the Bagalkot Group. Outcrops of the rock are found at Bilgi and Jamkhandi (Fig. 3.3 & 4.1). An effort is also made to analyse the genesis of fracture planes observed in the field within the Salgundi Conglomerate and overlying quartzite observed in the field at Ramthal and Salgundi which belongs to the zone of contraction towards the south-central portion of Mukerjee *et al.*, 2016 (Fig. 3.3). The arkosic rock at Bilgi strikes and Jamkhandi E-W and dips of 10° - 15°S; while the conglomerate at Ramthal and Salgundi maintain the same stike but dip about 40°N and 40°S respectively .

9.2 Closepet Granite basement at Bilgi

The field observations of the well-known Archean Closepet Granite (Friend and Nutman, 1991; Dey *et al.,* 2003; Dey *et al.,* 2009; Meert and Pandit 2015) forming the basement for the overlying Mesoproterozoic sedimentary cover at Bilgi is well described in the previous chapter (i.e. Chapter 4). It is variably porphyritic with phenocrysts of K-feldspar while, microcline, quartz and plagioclase (albitic) and perthites constitute the ground mass (Fig. 4.2). Accessory minerals include biotite, schorl, sphene and opaques. This two-feldspar Granite has been interpreted by Mukherjee *et al.,* 2016; to have remained undeformed showing no visible preferred orientation of minerals that would indicate penetrative tectonic fabric except for undulose extinction which is attributed to post-solidification microstructural adjustment during cooling.

9.3 Penetrative Deformation features in arkosic sandstone in field

Field observations of the exposures of arkosic sandstone at Bilgi shows penetrative features denoting deformation. The enclosed clasts of quartz and feldspars are differentially distributed in terms of their percentage within argillaceous-siliceous matrix.

An understanding of structural attributes of the rock becomes pertinent as certain of such features are visible within the exposures in the field. The bedding plane markedly denotes the S_0 foliation having E-W strike with dips varying from 10° to 15°S. A S1 foliation has been imparted by stretching and elongation of the clasts that are also flattened attaining an augen-shape through solid-state deformation (Fig. 9.1). This S_1 foliation has strongly developed sub parallel to S_0 as a set of closely spaced planes and is penetrative on outcrop scale. The S_0 and S_1 are transacted by a steeper set of relatively widely spaced cleavage planes representing S_2 in the rock. Reorientation of S_0 and S_1 grains and new grain development can be observed along the S_2 (Fig. 9.1).

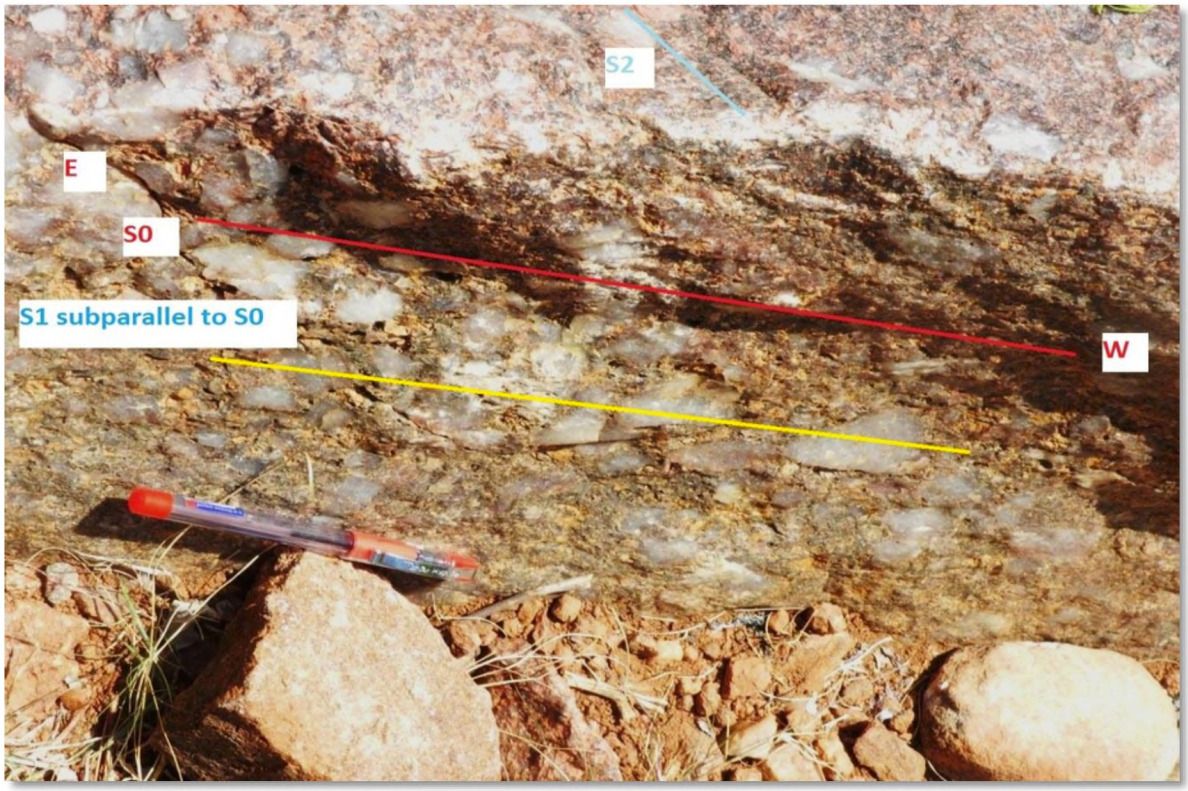

Figure 9.1 Reorientation of S_0 and S_1 grains and a new grain development along the S_2 in the arkosic rock.

9.4 Deformation related microstructures in arkosic sandstone

Deformative stresses generated during the downslide of the sedimentary sequence towards South over the basement rock facilitated the reorientation of the clasts as well as the matrix imparting in the process a S_1 foliation to the rock, which is almost sub-parallel to the S_0 bedding plane (Fig.9.1).

In conformity with the field observations made at Bilgi, in the microsections of the arkosic rock, the quartz and feldspar grains appear elongated and flattened and straightened to have developed continuous cleavage (Fig. 9.2). Further, these clasts of quartz and feldspars are aligned having their longer axis parallel within the cementing matrix in between the clasts defining the development of spaced cleavages. The cementing matrix

occupying spaces between the clasts encompasses argillaceous matter as well as prismatic needles of tourmaline. Though a few are disoriented, many of such grains are aligned having their longer edges parallel (Fig. 9.3 & 9.4).

Overgrowths on many of the detrital grains of quartz and feldspar are in crystallographic continuity (Fig. 9.5). Microstructural changes are evident in bulging and grain boundary migration amongst the framework clasts (Fig. 9.6). A number of grains of quartz and feldspars are found to be polygonised with straight grain boundaries in an aggregate depicting triple junction that intersect at 120° at such junctions (Fig. 9.2). Mutual impingement of the overgrowths, growing at equal rates on adjacent grain produces such a texture (Blenkinsop, 2000) and has led to grain boundary area reduction (GBAR). Even though GBAR occurs during deformation, its effect is more obvious after the deformation ceases (Passchier and Trouw, 2005).

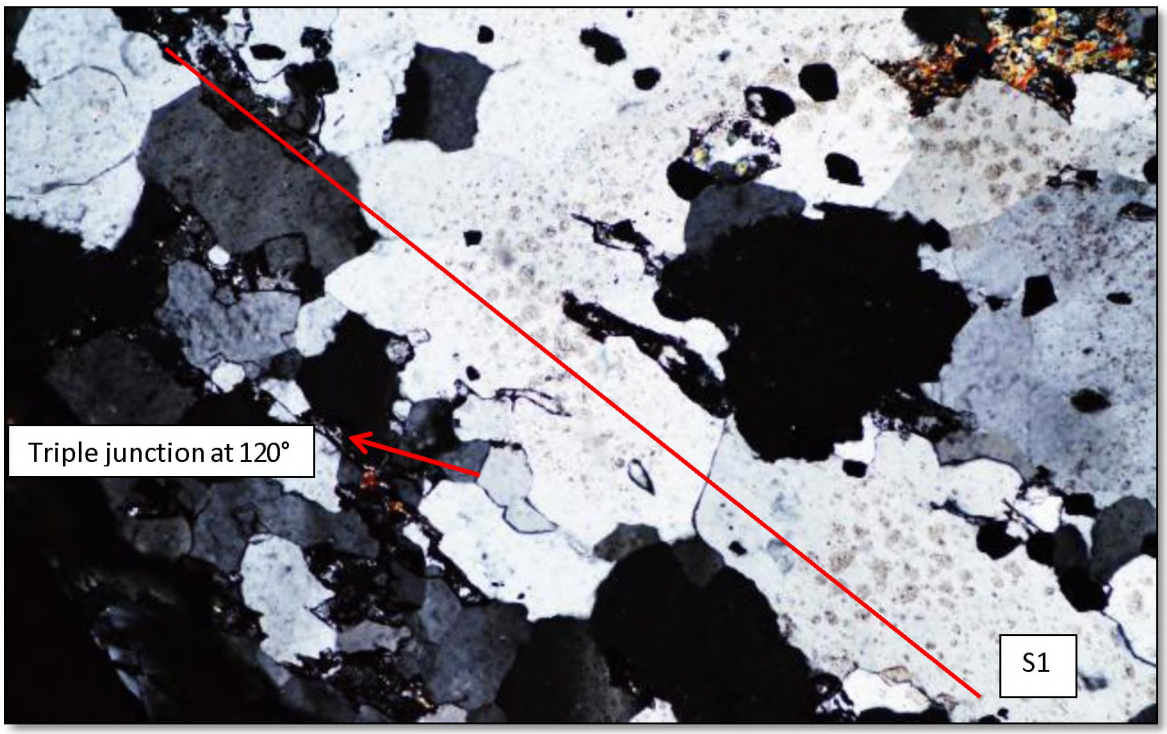

Figure 9.2 Continuous cleavages; development of 120° triple grain junctions (10X, BXP)

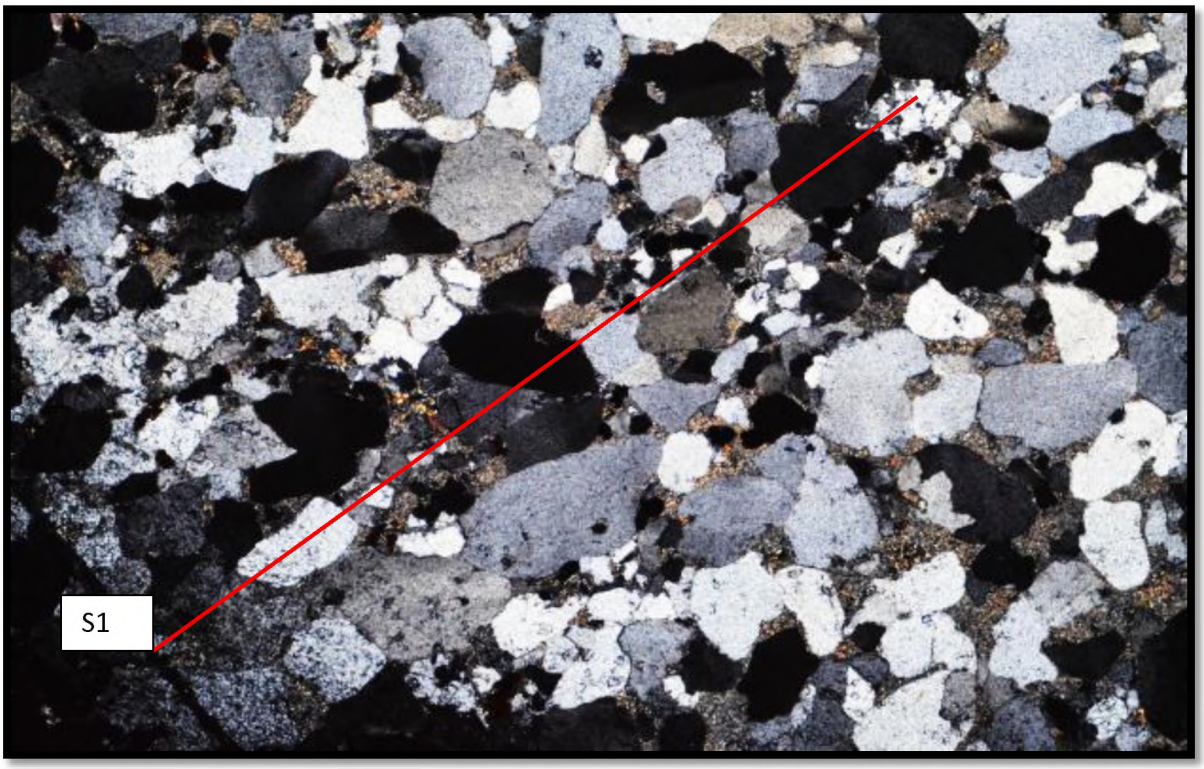

Figure 9.3 Spaced rock cleavage (S_1) (10X, BXP)

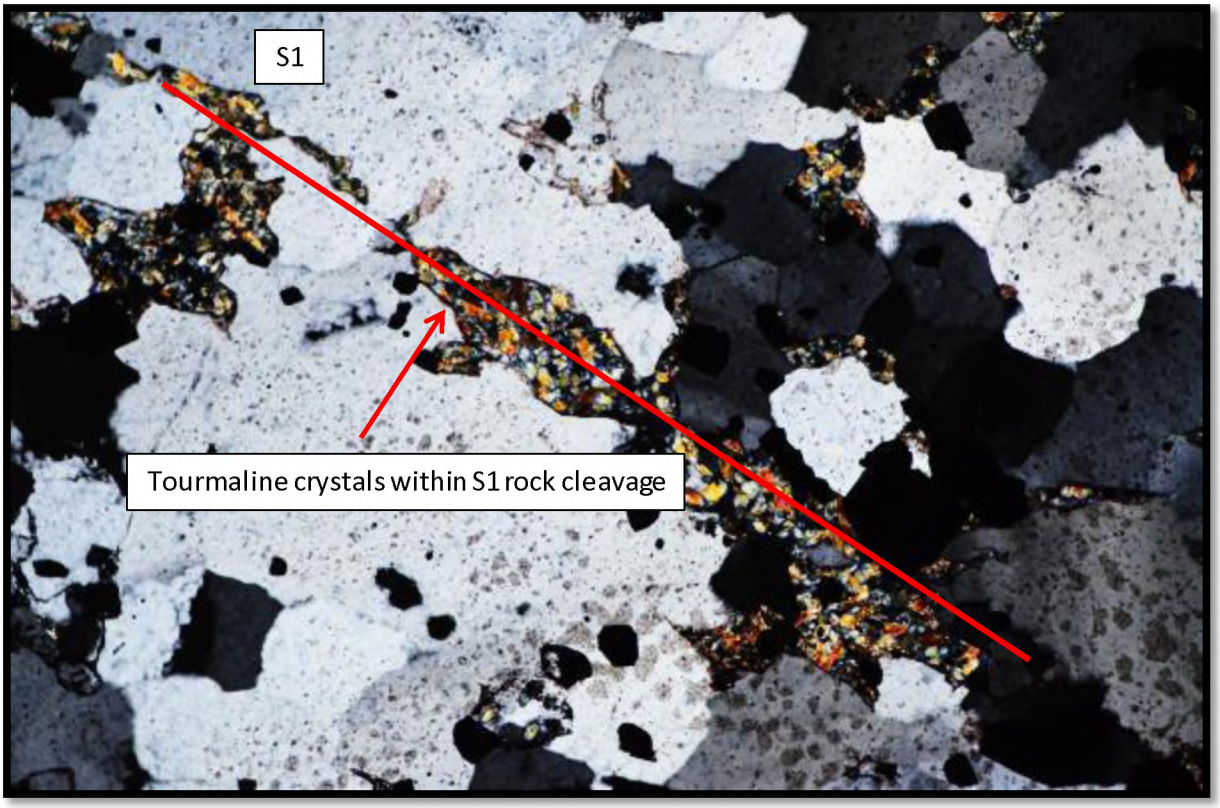

Figure 9.4 Tourmaline within the cleavage imparting S_1 foliation (10X, BXP)

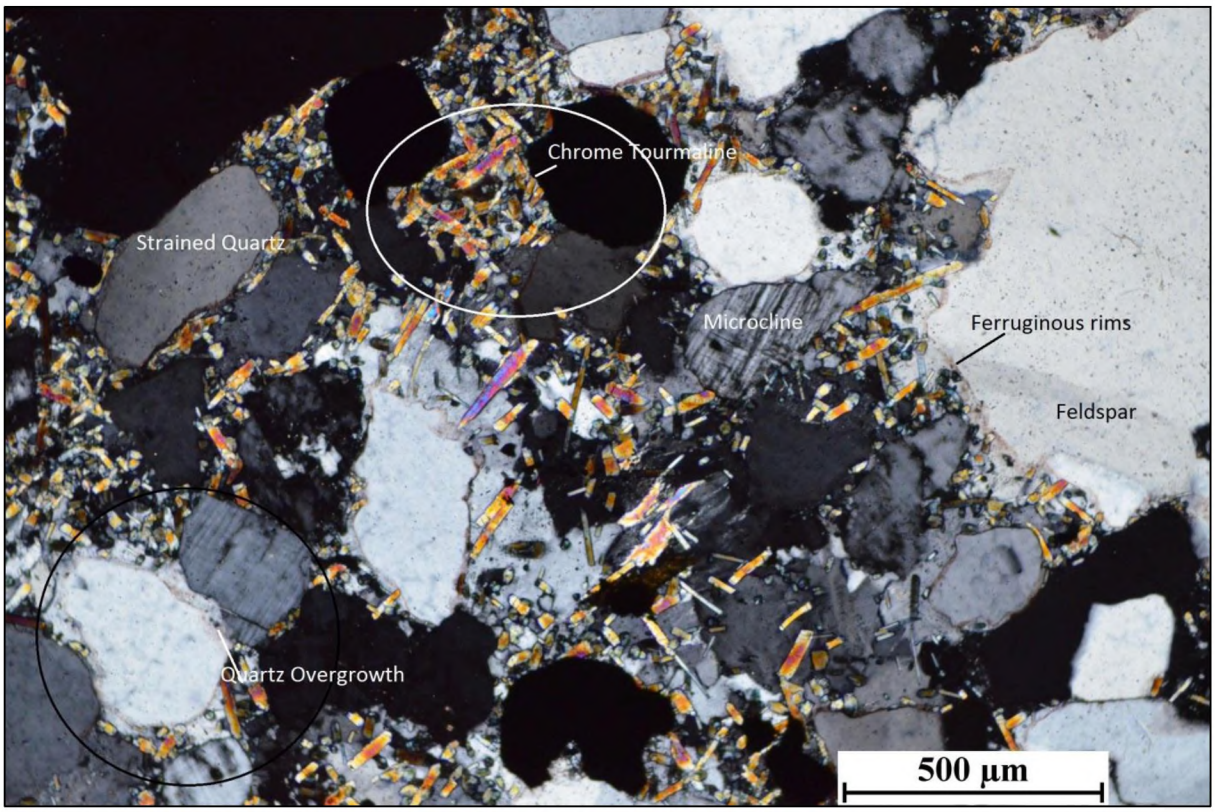

Figure 9.5 Framework clasts showing overgrowths in crystallographic continuity (20X, BXP)

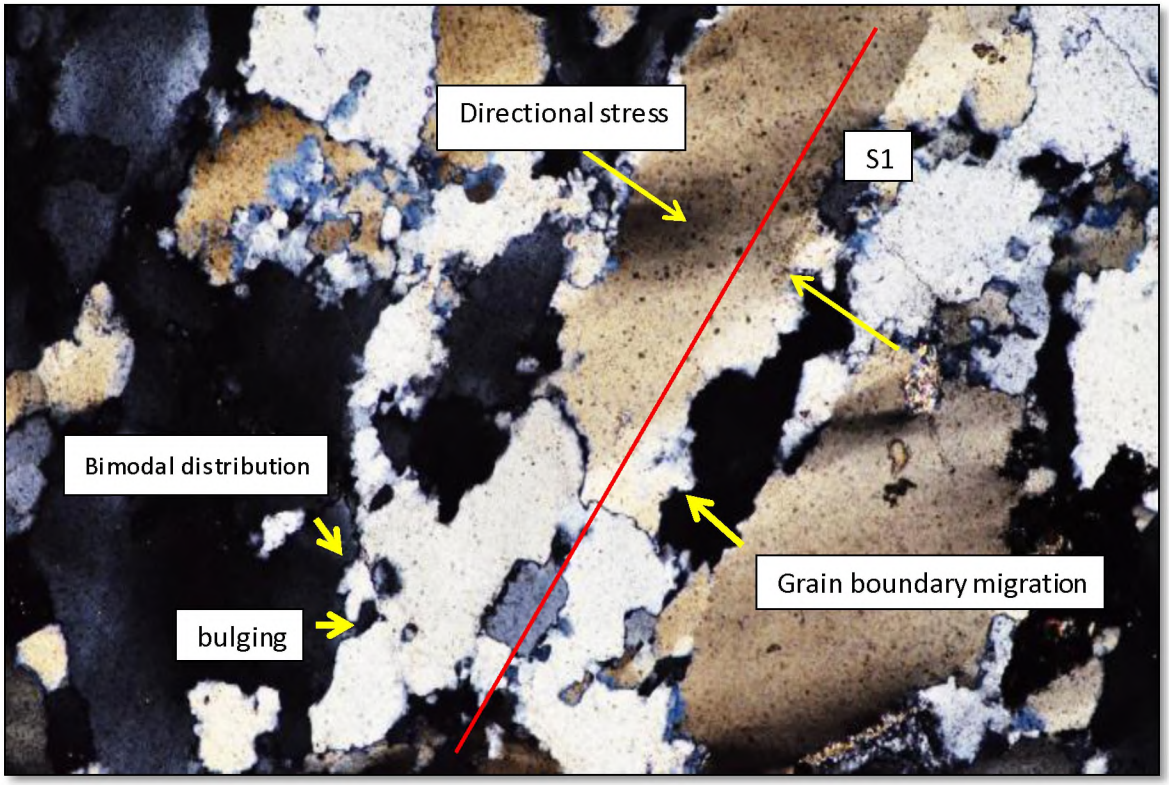

Figure 9.6 Bulging with sutured boundaries; elongation of clasts normal to the direction of stress; sweeping undulose extinction (10X, BXP)

9.5 Interpretation and Summary

Mukerjee *et al.,* 2016 have reported that the Mesoproterozoic sedimentary cover in the Northern sector of the basin at Bilgi is much less deformed whereas the south-central region of the basin is highly deformed. They have interpreted that the deformation was a result of gravity gliding of the sedimentary rocks from north towards south over the underlying basement. The nonconformable contact between the basement and the Kaladgi cover acted as a detachment surface. This unconformable contact between the Kaladgis and the older basement granites is sharp and clearly erosional all along the northern margin of the basin. They explain that in the initial stage a mild flexure of the crust was caused by the compressive stresses generated during the closing stages of the Sausar Mobile Belt (SMB) and Eastern Ghat –Rayner (EGRY) orogeny around~ 1000 – ~ 800 Ma. This resulted in an uplift of the basement of the Kaladgi basin in the northern part. The overlying sedimentary cover is considered to have slid down under gravity (gravity gliding) over the basement from north towards the south (Fig. 7.1).

In view of the above it may well be put forth that the sedimentary cover involving basal Formation of the Kaladgi to which the arkosic sandstone belongs slid downwards and got folded on encountering a stationary and stable Southern block comprising the Peninsular Gneissic Complex (Fig 8.1). The area of Bilgi situated between a contractional and extensional boundary, in accordance was subjected to mild deformative stresses accompanying the slide. The detritus of the arkosic rock composed of clasts of quartz and feldspars were thus prone to deformation and realignment facilitated by the effects of low temperature (<300°C) regime.

The original quartz and feldspar grains on being subjected to a directional stress passed through a solid state change with recrystallization occurring at points of least stress. This would obliterate the original spherical outline of a grain making them assume elliptical shapes and induce thereby a preferred directional orientation of the grains subsequently. The grain boundaries accordingly have got elongated perpendicular to the direction of acting stress developing thereby a continuous cleavage along this direction. The grain boundaries parallel to the cleavage become longer than that perpendicular to them. The elliptical grains of quartz and feldspars are thus preferentially oriented with their longer edges parallel creating straight and smooth grain boundaries. The matrix enclosing acicular to prismatic grains of tourmaline was squeezed between the clasts rearranging them in the process. Thus, a resultant of the deformation mechanisms has been the formation of planar penetratively continuous and spaced cleavage along with schistosity imparting secondary foliation (S_1) to the rock at an angle to the primary bedding foliation (S_0).

The study of microstructures in the arkosic sandstone clearly indicate involvement of deformation mechanisms leading to low temperature diagenetic overgrowths in crystallographic continuity, low temperature bulging of grain boundaries (BLG), and grain boundary migration, within the quartz and feldspar grains. Also, development of new grains within the old ones has led to bimodal distribution of the grain sizes. The process involving pressure solution transfer and recrystallisation is observed in the form of suturing of grain boundaries, development of new grains of quartz. The grains of tourmaline also show mild overprinting of S_1 by a domainally insignificant S_2 cleavage direction. The S_2 foliation is observed almost normal to S_1 foliation which probably could have been induced as a result of N-S trending tensional faults acting in the area which

needs further studies (Fig. 9.7). Such grain scale mechanisms are known to occur under low temperatures (<300°C) of deformation (Passchier and Trouw, 2005). The features of recrystallisation, overgrowths and reorientation as seen amongst the grains of quartz are deformative features that are highly suggested as having developed under such low temperature.

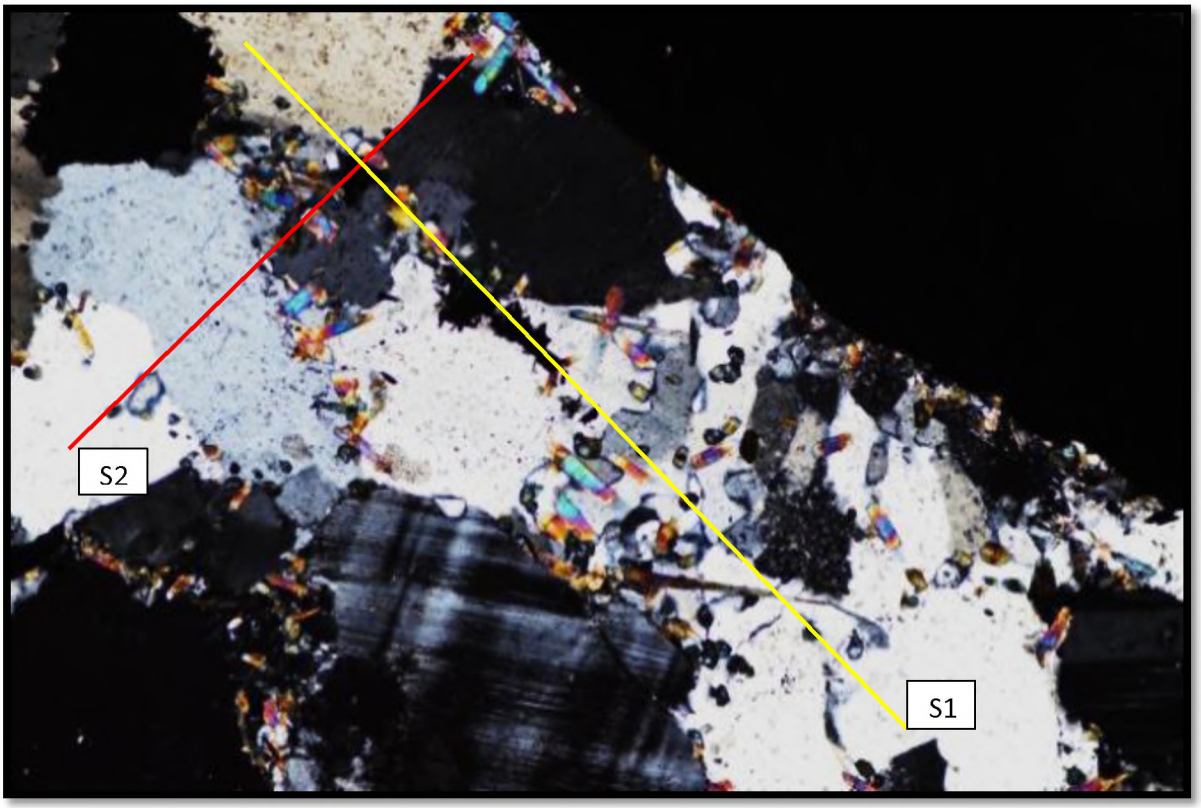

Figure 9.7 Overprinting of S_1 by domainally insignificant S_2 foliation (almost perpendicular) (10X, BXP)

The study area forms part of the Northern sector constituting the extensional domain of Mukherjee *et al.*, wherein contractional structures have not been reported. Results of our study indicate either local development of contractional structures or more likely a flattening domain in the Bilgi area which we plan to study further to understand its

implication on the structural and tectonic interpretation given by Mukherjee and others, related to evolution of the Kaladgi Basin.

The conglomerate exposed at Ramthal and Salgundi has been found to display a very prominent joint. The joint surface that cuts through the large cobbles and pebbles of silica varieties of minerals appears smooth and straight, especially at Ramthal. This joint surface can be recognised as of tensional origin and is observed conspicuously as a straight plane cutting through the pebbles and cobbles of the framework clasts. The fracture surface appears to have sliced through the large clasts creating a smooth planar surface. It is quite improbable for silica minerals to develop a straight and smooth fracture as such surfaces within them are usually conchoidal. During the process of folding of the sedimentary sequence stresses that were generated in the region, resulted in creation of tensional forces. These forces lead to stretching of beds along limbs of the fold developing smooth planar extension fractures within the rocks perpendicular to the operation of the acting force; without much shearing as no signs of any shearing is visible. As a consequence of stress release, extension fractures develop parallel to the direction of operation of the tensional force resulting from the process of stress release.

The quartzite following the conglomerate, at Salgundi, exhibits en echelon shear fractures. The operating forces in the folding of beds could cause low magnitude shearing parallel to the bedding plane. Tensional forces get generated out of shearing in shear zones. En echelon fractures formed as a result get oriented parallel to the direction of tensional forces. Secondary mineralisation of quartz has subsequently filled in the fractures.

CHAPTER 10

TOURMALINE IN ARKOSE

10.1 Introduction

In the thin section observations under the microscope the matrix of the arkosic sandstone at Bilgi is seen to enclose abundant prismatic and polygonal grains of tourmaline that are interlocked with the clasts of quartz and feldspars. The perfectly prismatic shaped crystals show angular edges there being no rounding of corners – the polygonal grains on the other hand depict their hexagonal character. They either occur in clusters squeezed within spaces between clasts or also as isolated crystals, many of which are clearly oriented parallel along their longer edges.

10.1.1 Genesis and stability of tourmaline

The mineral tourmaline occurs as an accessory in felsic igneous rocks like granitic pegmatites, low-grade metamorphic equivalents as well as a diagenetic mineral in buried sedimentary basins (Krynine, 1946; Henry and Guidotti, 1985; Henry and Dutrow 1996, Slack 1996, Henry *et al,* 1999, Marschall *et al.,* 2009; Morgan and London 1989, London *et al.,* 1996, Nakano & Nakamura 2001, Roda-Robles *et al.* 2011). Tourmalines formed at low-temperatures are stable at 150°C or less and pressure of 1000Pa (Henry *et al.,* 1999, Moore *et al.,* 2004). Those of the tourmalines which form in low-temperature metamorphic regimes (<300°C), can reveal the petrogenetic history of the host rock with its distinctive morphological and chemical characters (Dutrow and Henry, 2011; van Hinsberg *et al.,* 2011a) thereby providing insights in understanding the environments in which it grew. Even though their stability is as low as 150°C, experimental data has shown upper limits of thermal stability can be as high as 725°C to 950°C controlled by pressure

and compositions (Holtz and Johannes 1991, Morgan and London 1989, Wolf and London 1997, von Goerne *et al.*, 1999, Spicer *et al.*, 2004, Ota *et al.*, 2008, London 2011, van Hinsberg 2011).

Tourmaline has been a stable mineral in clastic sedimentary rocks and is chemically resistant during its growth in metamorphic and igneous environment. It shows neglible diffusion rates for major and trace elements, even at temperatures as high as 800°C (*e.g.*, van Hinsberg and Marschall 2007, van Hinsberg and Schumacher 2007; Henry and Dutrow, 1990, 1992, 1996). This property of tourmaline makes them an excellent source for preserving compositions (van Hinsberg *et al.*, 2011).

10.1.2 Crystallography and Chemistry of Tourmaline

The mineral tourmaline is chemically a complex borosilicate consisting of various major and trace elements. The general chemical formula of the primitive unit cell is $XY_3Z_6(T_6O_{18})(BO_3)_3V_3W$, and is considered as a Supergroup mineral having 21 species (Table 10.1; van Hinsberg *et al.*, 2011; Henry *et al.*, 2011). Based on the chemical and structural framework of the tourmaline-supergroup minerals, a new nomenclature has recently been adopted by the International Mineralogical Association's Commission on New Minerals, Nomenclature and Classification (IMA–CNMNC) (Novák *et al.*, 2009). The tourmaline species that are currently accepted by the IMA–CNMNC include those shown in Table 10.1 below.

Table 10.1 Some Tourmaline species accepted by the IMA-CNMNC (*adopted from* van Hinsberg *et al.*, 2011)

Species	***W***	***X***	***Y***	***Z***	***T***	***B***	***V***
Dravite	Na	Mg_3	Al_6	Si_6O_{18}	$(BO_3)_3$	OH_3	OH
Schorl	Na	Fe^{+2}_3	Al_6	Si_6O_{18}	$(BO_3)_3$	OH_3	OH
Chromium-dravite	Na	Mg_3	Cr_6	Si_6O_{18}	$(BO_3)_3$	OH_3	OH
Vanadium-dravite	Na	Mg_3	V_6	Si_6O_{18}	$(BO_3)_3$	OH_3	OH
Fluor-dravite	Na	Mg_3	Al_6	Si_6O_{18}	$(BO_3)_3$	OH_3	F
Elbaite	Na	$Li_{1.5}Al_{1.5}$	Al_6	Si_6O_{18}	$(BO_3)_3$	OH_3	OH
Fluor-schorl	Na	Fe_3	Al_6	Si_6O_{18}	$(BO_3)_3$	OH_3	F
Povondraite	Na	Fe^{3+}	$Fe^{3+}_4Mg_2$	Si_6O_{18}	$(BO_3)_3$	OH_3	O
Chromo-alumino-povondraite	Na	Cr^{3+}	Al_4Mg_2	Si_6O_{18}	$(BO_3)_3$	OH_3	O
Fluor-buergerite	Na	Fe^{3+}_3	Al_6	Si_6O_{18}	$(BO_3)_3$	OF_3	
Olenite	Na	Al_3	Al_6	Si_6O_{18}	$(BO_3)_3$	O_3	OH
Uvite	Ca	Mg_3	$MgAl_5$	Si_6O_{18}	$(BO_3)_3$	OH_3	OH
Fluor-uvite	Ca	Mg_3	$MgAl_5$	Si_6O_{18}	$(BO_3)_3$	OH_3	F
Feruvite	Ca	Fe^{2+}	$MgAl_5$	Si_6O_{18}	$(BO_3)_3$	OH_3	OH
Fluor-liddicoatite	Ca	Li_2Al	Al_6	Si_6O_{18}	$(BO_3)_3$	OH_3	F
Foitite		Fe^{2+}_2Al	Al_6	Si_6O_{18}	$(BO_3)_3$	OH_3	OH
Magnesio-foitite		Mg_2Al	Al_6	Si_6O_{18}	$(BO_3)_3$	OH_3	OH

A fundamental structural component of tourmaline is the six-membered ring containing corner sharing TO4 tetrahedra centres of which are mostly occupied by Si, but also have some Al^{3+} and B^{3+}.

10.2 Tourmaline in the arkosic sandstone at Bilgi

The tourmaline that is so prominent in its presence within the matrix of the arkosic sandstone assumes significance as the grains are found to occur either as prismatic or as polygonal cross-sections. Further, noteworthy is their orientation, as a large majority of the prismatic grains are seen aligned with the crystals oriented parallel defining the effects of an active unidirectional pressure the enclosing rock was subjected to. Tourmaline is one of a stable and resistant mineral. The prismatic grains and polygonal crystals of the mineral appear unabraded with their edges meeting at angles rather than getting rounded during transport. No sign of any authigenic overgrowth is noticed. Also, its distribution is inconsistent within the rock unit, being more concentrated within the matrix. There is thus, enough scope to argue its detrital character. Such a significant presence in large quantity of a subordinate mineral amongst the primary clasts of quartz and feldspars within the arkose demanded a further probe. As such, their optical characters were determined and individual grains within the bulk matrix were subjected to Scanning Electron Microscope- Energy Dispersive spectroscopy (SEM-EDS) analysis.

10.2.1 Optical characters of Tourmaline

Tourmaline is found to occur in the matrix as euhedral and acicular prismatic crystals exhibiting distinct pleochroism from dark green to yellow green with high order interference colours. The mineral is optically negative having the prism form well developed with singly as well as doubly terminated crystals (Figs. 5.2a & 5.2b), The basal sections are hexagonal and vertical sections show maximum absorption when the length is perpendicular to the vibration direction of the polarizer. The grains have remained

confined to the matrix of the rock to form an intergranular relationship with the framework clasts of quartz and feldspars. They are clear, devoid of inclusions or striations. No overgrowths are visible and the edges and corners have remained intact. Coarse grain size of the tourmalines, the perfect euhedral nature, sharp prism forms with preferred alignment with the framework clasts is highly suggestive of a short route from a source that perhaps has prevented its abrasion. Further classification is done based on Scanning Electron Microscopy-Energy Dispersive Spectroscopy (SEM-EDS) analysis using 70μm magnification.

10.2.2 Scanning Electron Microscope and chemical analysis of tourmaline crystals

The observed grains of tourmaline under SEM are seen both as acicular as well as euhedral polygonal crystals. The prism form appears well developed (Fig. 10.1a 10.1b, 10.1c, 10.1d, 10.1e, 10.1f, 10.2a, 10.2b, 10.2c & 10.2d) measuring 206μm in length and 7.55μm across. The crystals are clear and devoid of inclusions, some of them are zoned showing mild striations. A change in the composition from the core (Fig. 10.3a & 10.3b) towards the margins of individual crystals is a pointer to chemical zoning which (Fig. 10.3c & 10.3d) is discontinuous with no systematic rim-to-core patterns. Moreover, it appears quite different in all the grains. The chemical composition data for the tourmalines is presented in Table 10.2. Using this data an attempt is made to calculate the mineral formula on the basis of the general chemical formula of unit cell and a classification thereon to identify the individual species.

Table 10.2 Chemical composition data for Chromdravite obtained by SEM-EDS (*Source* Henry *et al.*, 2011)

Oxides	wt%	Molecular weights (g/mol)	Molecular Proportion (M)	Atomic Proportion A=(M* number of anions)	Number of Anions B=(A*T2)	Formula	
SiO_2	40.25	60.08	0.67	1.34	12.5	Si	6
Al_2O_3	0.67	101.96	0.007	0.021	0.20	Al	0.13
FeO	10.70	71.84	0.149	0.149	1.40	Fe	1.34
MgO	7.46	40.30	0.185	0.185	1.72	Mg	1.66
Na_2O	1.82	61.97	0.03	0.03	0.28	Na	0.54
K_2O	0.86	94.2	0.009	0.009	0.08	K	0.16
Cr_2O_3	0.46	151.99	0.003	0.009	0.90	Cr	0.6
B_2O_3	26.70	101.61	0.383	1.149	10.7	B	7
Total	88.92			2.892			
				No Oxygen (O)	27		
				T2= no of O/2.892	9.33		

Substituting the calculated data of chemical constituents in the primitive unit cell of tourmaline having the chemical formula $XY_3Z_6(T_6O_{18})(BO_3)_3V_3W$ gives

$$(Na_{0.54})_{0.54}(Mg_{1.66}\,Fe_{1.34}\,Cr_{0.6}Al_{0.13})_{3.73}(B_7O_3)_3Si_6O_{18}(OH)_4$$

The mineral formula derived thus in all probability classifies the tourmaline present within the arkosic sandstone as Chromdravite; also called Chromium-dravite, which is a rare chromium-bearing variety.

Though, for a chemical formula for a primary Chromdravite is $NaMg_3(Cr,Fe)_6(BO_3)_3Si_6O_{18}(OH)_4$, the higher content of boron, than that of the permissible limit, as derived from SEM-EDS analysis of the tourmaline grains, can be attributed to the difficulties associated with its detection in SEM-EDS.

As the content of water was unknown, the calculation to derive the mineral formula was based on 27 oxygens with the presumption of four hydroxyl molecules to have occupied the $(OH)_4$ site in the structure.

The Mg, Fe and Cr contents have been found to be lower than the prescribed limits for chromdravite.. Their uneven distribution within the grains has resulted in them to be concentrated at the borders than the core margins giving a discordant type of zoning. This happens when the diffusion rates of the cations are more towards the rims as compared to the cores, demarcating better chemical equilibrium at the borders during the process of deformation and metamorphism.

The chromdravite showing more of discordant type chemical zoning from the core towards the rims indicates an extrinsic type of system with fluctuations in the temperature, pressure and chemical rates of diffusion. This can owed to the accommodative nature of the tourmaline structure that can adapt to any chemical environment. Chemical zoning from the core to the rims suggests the diffusion rates of the cations to have occurred at a slower pace (Palmer *et al.*, 1992).

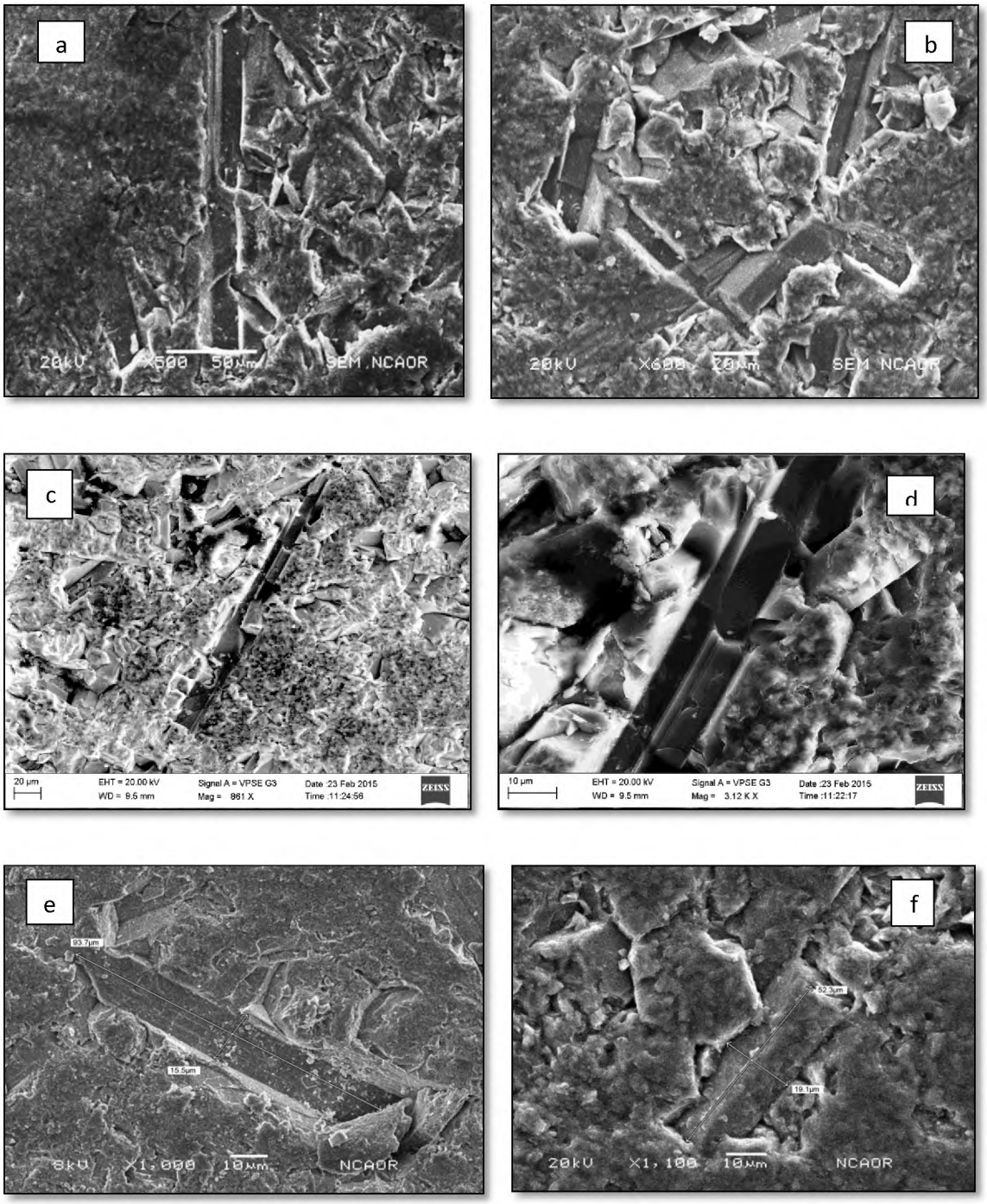

Figure 10.1 (a), (b), (c), (d), (e) & (f) Scanning Electron Microscope - Back Scattered Electron (SEM-BSE) images of chromdravite showing the perfect euhedral shape with prism forms and striations

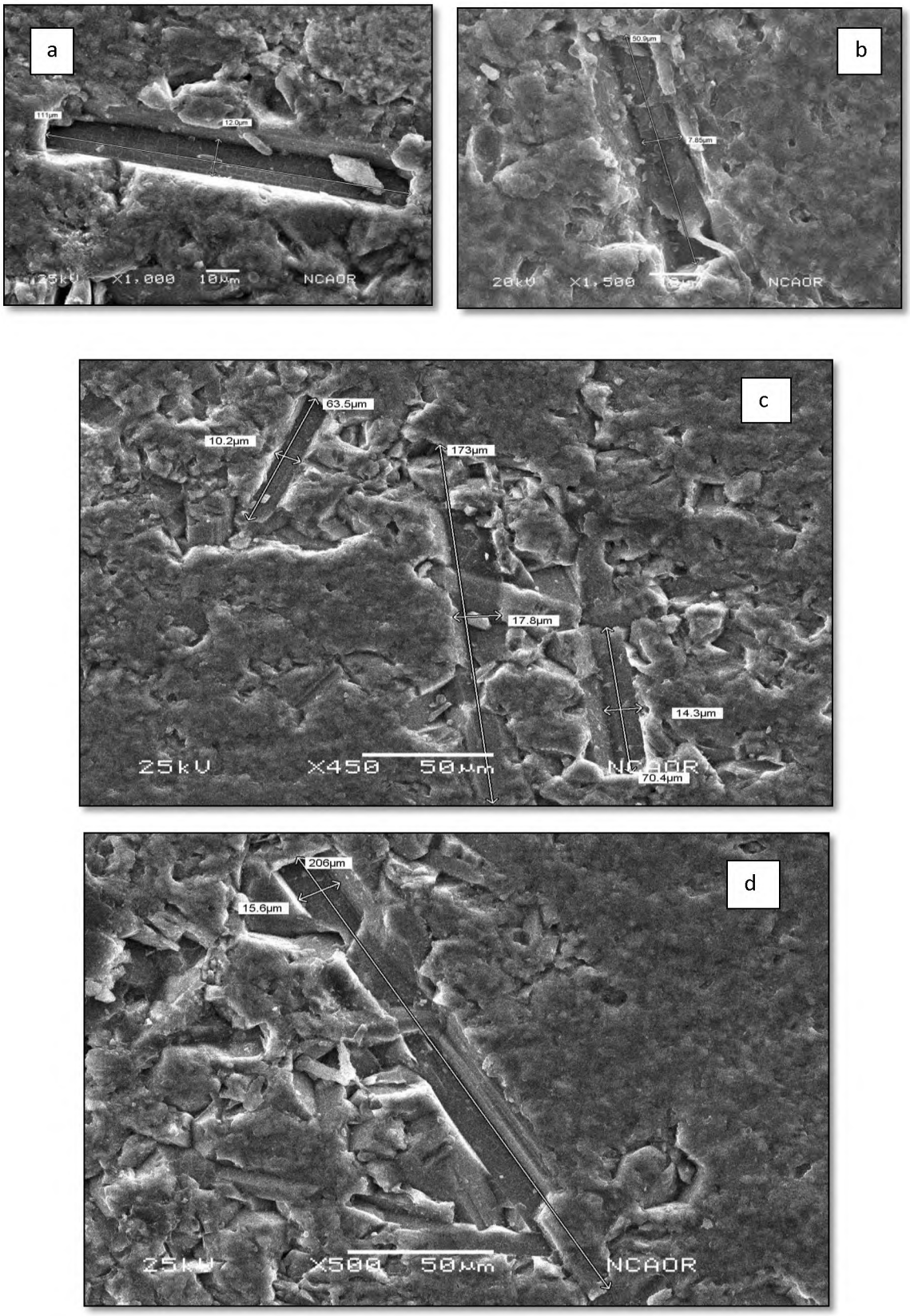

Figure 10.2 (a), (b), (c) & (d) Scanning Electron Microscope - Back Scattered Electron (SEM-BSE) images of chromdravite showing the perfect euhedral shape with prism forms and striations

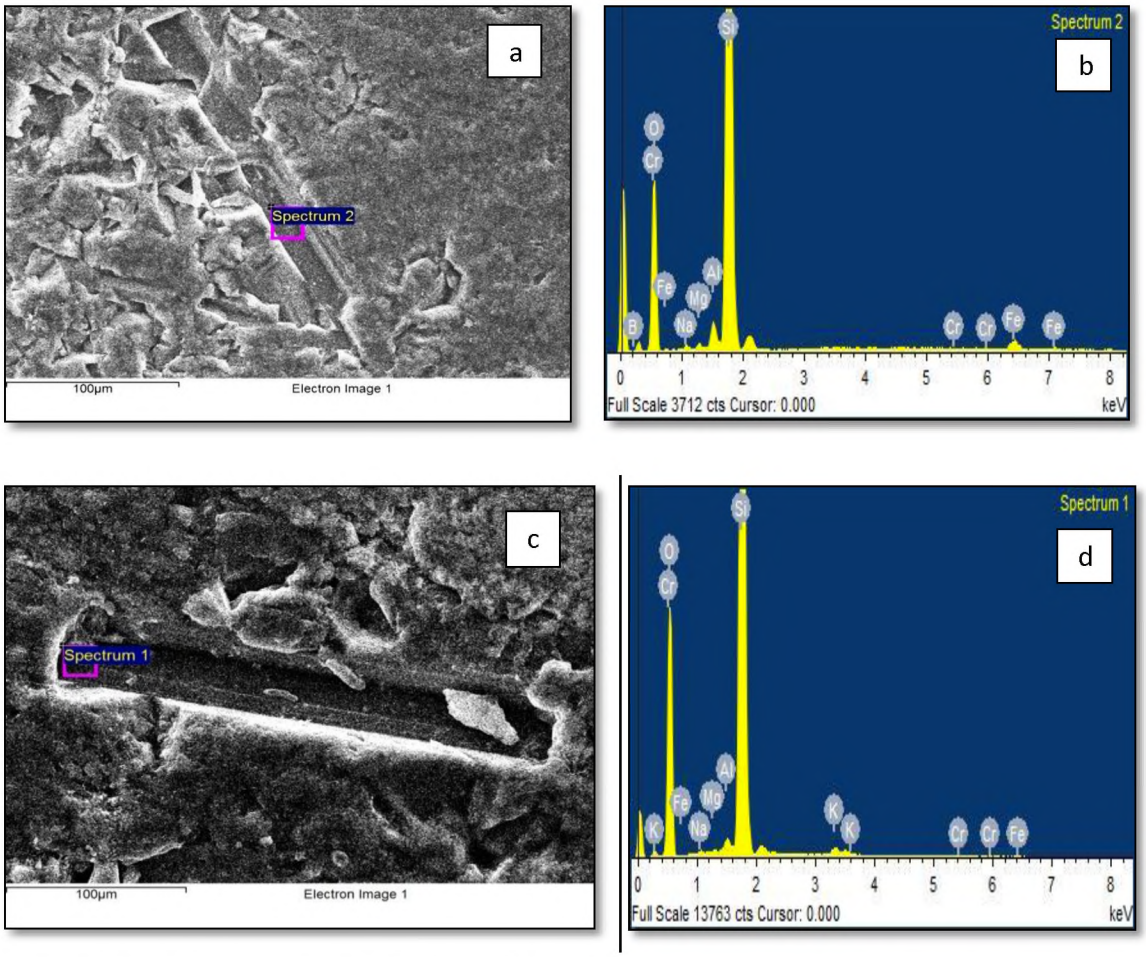

Figure 10.3 (a) Chromdravite analysis from the core portion under SEM **(b)** Spectrum of chromdravite from the core under SEM-EDS **(c)** Chromdravite analysis from the margin portion under SEM **(d)** Spectrum of chromdravite from the margin under SEM-EDS.

10.3 Interpretation

A few observations can be made from the analytical studies and the microstructures observed in the arkosic sandstone at Bilgi. Microstructures in the host rock show features including bulging, grain boundary migration (GBM) development, formation of granoblastic triple junctions between quartz and feldspars that are indicative of cohesive deformation associated with low grade metamorphism spaced as well as continuous cleavages have developed during the process of deformation. Many of the prismatic crystals of tourmaline appear oriented within the matrix occupying spaces between clasts

defining spaced cleavages in the host rock imparting a foliation at low to moderate temperature deformation regime.

It is interpreted by Mukherjee *et.al.*, (2016) that at about 1.0 – 0.8 Ga there was crustal flexure and uplift of the older rocks and Closepet Granite towards the northern part of the Kaladgi basin leading to tectonic steepening of the basement and subsequently gravity sliding of the younger cover rocks towards south from the northern end. The requisite low to moderate *P-T* conditions of (<300°C?) and the southerly directed stresses operating during the gravity gliding of the cover rocks must have enabled development of domainally significant cleavage in this part of the Kaladgi Basin. It is interpreted that Chromdravite that defines the schistosity (S_1) sub-parallel to the bedding plane of the host rock (S_0) got oriented as a result of the tectonic and chemical phenomena discussed earlier. Further, as other minerals in the host rock, the chromdravite also shows overprinting of S_1 by domainally significant S_2 foliation. The discussion supports the contention that the tourmalines in the study area were aligned syntectonically during the first deformation in this part of the Kaladgi Basin, synchronous with development of first schistosity, S_1, and was further deformed during the subsequent second deformation resulting in formation of the second schistosity, S_2. However, there was no significant grain growth during the S_2 development which possibly only involved passive rotation and subgrain formation in tourmaline along with other minerals in the host rock. The orientation of tourmaline can thus categorically be stated as deformation assisted.

CHAPTER 11

SUMMARY AND CONCLUSIONS

11.1 Summary

The Kaladgi basin, hitherto referred to as an intracratonic basin has drawn attention of many workers. This basin hosts a huge thickness of Proterozoic sediments that rest over an Archean basement. Kale and Phansalkar, (1991); Bose *et al.,* (2008); Dey *et al.,* (2009) and Mukerjee *et al.,* (2016) have carried out a substantial work related to sedimentation history, facies, paleoweathering and geochemistry, and deformational history in the Kaladgi basin respectively. Studies related to provenance and paleocurrents help in not only understanding the relief and the then existing climatic conditions of a region, but also, the geological history of the deposited sediments. Composition of a sedimentary rock can be related to the source area conditions. Tectonics and geological history control the characteristics of the provenance as well as the depositional environment (Boggs, 2009). Inferences towards deformation history of a region can be based on observations done in the field for penetrative features and supported by microstructures. The evolution of a sedimentary basin can be delineated by understanding the deformational history of the area.

The older rocks which serve as a basement for the Kaladgi sequence of rocks are the Granites towards the north, central and south eastern part; Hungund Schist Belt towards the east and the Peninsular Gneissic Complex towards the south of the basin. In this research work, the lowermost sedimentary rock unit belonging to the Mesoproterozoic Salgundi Conglomerate Member of Ramdurg Formation of the Bagalkot Group, well

exposed at Bilgi, Jamkhandi, Ramthal and Salgundi in the Kaladgi basin has been taken up for study. As a part of the research, data was recorded from study of this sedimentary unit which is well exposed along hill slopes at Bilgi with a thickness of about 25m and at Jamkhandi about 5m thick, in Karnataka, South India. Here, this lithounit rests unconformably over the pink Closepet Granite with non-conformity. Large exposures of the same Member are also seen at Ramthal, over a hillock which are about 6m thick and at Salgundi, covering a ridge and are nearly 30m thick.

An attempt is made in this study to put forth a detailed account of the observations made in field and, in the microsections supplemented also, with geochemical analysis. From the study of the lithounit at Ramthal and Salgundi, attempts are made to relate how the provenance of the host rock at both these places and paleoclimatic environments had an effect on the composition of this unit. It reports the use of imbrications observed at these two places in deducing the paleocurrents that must have prevailed at the time of deposition and thereby make a statement on the then existing physiography in the region. Sincere efforts have been made in studying the arkosic sandstone from Bilgi and Jamkhandi; wherein the mineral assemblage in the rock and microstructures observed, supported by geochemical analysis are used to conclude on the deformational mechanisms to which the rock unit was subjected to and, thereby the depositional history and the effects of the deformation. A geochemical analysis of the samples from the two rock units for major oxides, trace elements and Rare Earth Element concentrations assisted in deducing the source rock history as well as their chemical maturity.

Mukerjee *et al.,* 2016 have recently described the structural and deformational characters of the northern part of the sedimentary cover rocks from the Kaladgi basin. In their study and findings on the structural and tectonic features, they have stressed on the extensional nature of deformation in the northern part of the basin. The research area, *i.e.* Bilgi chosen for study forms a part of the extensional structure belonging to the Northern part of the basin (*i.e.* the Jamkhandi-Bilgi-Mamadapur). The findings from this research with respect to this part of the basin at Bilgi stress only on the structural features observed in the outcrops and petrographic characters noted under the microscope evidencing deformation, and its impact on structural and tectonic interpretation given in Mukherjee *et al.,* 2016 is not being attempted, as further studies are planned in the area. The presence of a rare variety of tourmaline in the arkosic sandstone at Bilgi is also reported in this study for the first time. The existence of this mineral though, is attributed to a detrital genesis, its predominance over other subordinate minerals as also, the orientation of many of the grains attracts attention. The presence of this tourmaline is authenticated based on its optical characters and SEM-EDS studies carried on individual grains substantiated by geochemical analysis.

11.2 Conclusions

Even though the Kaladgi basin is studied extensively by many workers on a larger scale, minute intricacies have remained untouched. These include studies on individual lithounits with respect to their lithological characters, textural features, provenance, deformation history, paleocurrent directions and mapping on a larger scale of the area. Therefore, the lowermost rock unit constituting of conglomerate and arkosic sandstone belonging to the

Salgundi Conglomerate Member of the Ramdurg Formation in the Bagalkot Group of the Kaladgi-Badami sequence of rocks was taken up for study. The lithounit well exposed at Bilgi, Jamkhandi, Salgundi and Ramthal provided an opportunity to understand the paleocurrents, provenance, development of mineral and deformation history of the Mesoproterozoic Bagalkot Group. To understand this, field studies were combined with analytical studies to come to a conclusive result. Inorder to understand the deformation history of the area, field studies were combined with micro section observations.

At Bilgi, the study is also based on the structural and petrographic aspects of the Mesoproterozoic sedimentary cover rocks and the underlying Archean Granites inorder to understand the deformational history in the extensional region of Northern sector in the Kaladgi basin.

The study area at Bilgi forms part of the Northern sector constituting the extensional domain wherein contractional structures have not been reported. A preliminary study of basement Archaean Closepet Granite and non-conformably overlain Mesoproterozoic arkose of Kaladgi Supergroup has shown evidences on outcrop and thin section scale of penetrative solid state deformation in the area. These evidences include formation of augen feldspars, stretching and flattening of quartz and feldspars and strong lineation in the Closepet Granite, and, penetrative cleavage development defined by flattened and elongate quartz and feldspars and alignment of tourmaline grains in the arkosic rock. Microstructures in the arkose show features including bulging, subgrain development, formation of granoblastic triple junctions between quartz and feldspars indicative of

cohesive deformation possibly associated with low grade metamorphism (?). Results of this study indicate either local development of contractional structures or more likely a flattening domain in the Bilgi area which is planned to study further inorder to understand its implication on the structural and tectonic interpretation given in Mukherjee et al., related to evolution of the Kaladgi Basin.

The arkosic sandstone exposed at Bilgi and Jamkhandi represents the lowermost Member of the Ramdurg Formation in the Bagalkot Group of Kaladgi Supergroup. The clasts of quartz and feldspar are variably distributed within the unit. A decline in feldspars is matched with a concomitant increase in monocrystalline quartz from bottom upwards. The clasts are cemented by and large by a siliceous-argillaceous matrix. Many of the feldspars have remained unaltered and are angular –sub angular signifying their close proximity to the source rock, and a rapid burial.

The basin of deposition must have been shallow as the overlying quartzitic sandstones display cross-bedded structures and ripple marked surfaces. Periods of regression marked by warm humid climates has resulted in leaching of iron oxide forming rims around clasts and incrustations along joint planes as observed in its microsections and, in the field respectively at Bilgi.

Tourmaline constitutes a prominent proportion of the cementing matrix along with opaque minerals, sphene and mica. Majority of the detritus for the sequence has been derived from

the immediately underlying Closepet Granite. But the sequence is also, thought to have derived the detritus from a different source other than Closepet Granite, A confirmation in this regard needs further investigation. The statement made above is based on the presence of the chromdravite variety of tourmaline within the sequence. This variety of tourmaline is absent in the underlying Closepet Granite. Also, since it is found that in the upper levels of the sequence the proportion of chromdravite increases, it is more due to a different cycle of deposition.

Microscopic observation reveals development of spaced and continuous cleavages, a feature signifying effects of deformative forces. The clasts of quartz and feldspar appear stretched and elongated; formation of overgrowths, bulging and triple boundary junctions are the microstructures that have developed from the operative deformative mechanisms..

The modal abundances and the geochemical analysis formed the basis for plotting graphs using the ratios of various oxides. The plots made for the Bilgi – Jamkhandi rock unit are found to occupy the field marked for arkosic sandstone, confirming its genesis from an erosive cycle of underlying felsic rocks. Such graphs for Ramthal-Salgundi confirm the rock as a conglomerate.

The tourmaline that is so prominent in its presence within the detrital matrix of the rock at Bilgi has prismatic polygonal crystals. A subparallel orientation of the prismatic grains

and the development of spaced cleavage along with the stretched and elongated quartz and feldspar clasts provide clues to a low-temperature assisted deformation.

The SEM-EDS analysis significantly helps in classifying the tourmaline as a rare variety 'chromdravite'. Though the proportions of MgO, FeO, Cr_2O_3 are lower than the accepted values for primary tourmaline, it more likely has been provided by the basement of Archean constituents which leaves a scope for further studies in this regard.

The study documents the petrographic characteristics of the tourmaline and the bearing of mild cleavage forming deformation on the orientation of tourmaline. The contention that the tourmalines in the study area could have oriented syntectonically during the first deformation in this part of the Kaladgi Basin in the Northern part, synchronous with development of first schistosity S_1, and was further deformed during the subsequent second deformation resulting in formation of the second schistosity, S_2. However, there was no significant grain growth during the S_2 development which possibly only involved passive rotation and subgrain formation in the existing clasts and other minerals in the host rock. The alignment of tourmaline is therefore, deformation assisted.

At Jamkhandi a down current migration of ripples and sand waves results in the build-up of cross-stratification. These structures develop when sediment is carried over the stoss-side by currents and is dropped down the lee-side of the structure. The presence of lenticular bedding, ripple type cross-lamination reactivation surface could have formed by

rapid sedimentation. The turbulent environments prevailing at the time of deposition indicates periodic flooding.

Rapid sedimentation leads to the formation of ripple type cross-lamination which occurs in a variety of depositional environments such as fluvial floodplains and river deltas, due to periodic flooding inclusive of turbulent sedimentation. This could possibly have formed during the periodic flooding (flash floods) experienced by the area at the time of deposition.

At Ramthal and Salgundi, the lithounit conglomerate seen exposed has a thickness of about 6m - 30m but displays converging dips, towards North at Ramthal and towards South at Salgundi. These two occupy a synclinal zone.. The conglomerate is oligomictic becoming monocrystalline in the direction of dip. The framework clasts of the size of cobbles and pebbles are rounded to sub angular in nature and of a varied composition with constituents ranging from varieties of silica to rock fragments of BHQ. The size of the framework clasts suggests deposition of having occurred along marginal parts of the basin with a proximity to the source area. The source from which the constituents were drawn must have been originally a mafic igneous rock (*i.e.* the Hungund Schist Belt) which was later metamorphosed. Hot, humid and oxidizing conditions must have prevailed during the depositional history of the rock that subsequently underwent deformation.

The conglomerate is mineralogically matured with abundance of silica varieties and lacking in feldspars. While percentage of Fe_2O_3* increases along with SiO_2 at both places

that of Al_2O_3, K_2O, CaO and Na_2O are much less. The Al_2O_3+Na_2O+K_2O *versus* SiO_2 plot indicating Compositional Maturity Index is relatively higher at both, Salgundi and Ramthal suggesting removal or lack of mobile elements like Na_2O and MgO. The lower concentrations of U and Th in the samples with lower ΣREE probably reflect a control by grain size fractionation during transport providing to a contribution from a mafic source with lesser concentration of such elements. Bivariant log/log plot of the ratio of Qp/F + R values represent the region to have been a moderate to low lying plain experiencing hot, tropical, oxidizing, humid climatic conditions. Further, the Eu/Eu* *versus* Gd/Yb determined for the conglomerate at Ramthal and Salgundi denote a post-Archean age which is in accordance with the Mesoproterozoic age determined by earlier workers.

The transporting agency, which must have been a swiftly flowing stream having sufficient velocity, would generally carry pebbles and boulders and align them with their longer axis in the direction of flow. The imbrications preserved within the conglomerates provide information on paleocurrents to have flown from east towards west at Ramthal (South of the basin) indicating the upstream side towards east whereas at Salgundi (North of the basin) the paleocurrent directions deduced point towards their movement from west to east. Based on these observations in the field and reconstruction to a prefolding position of the limbs of the fold based on the dip directions, a conclusion drawn points the upstream side of the basin (basin high) to be towards the west. This is concluded based on the fact that the original tilt of the beds on both, the northern as well as the southern part of the basin was towards south. Presence of cross-bedded feature in the immediately succeeding quartzitic sandstones is a clear indication of the basin having been shallower at times.

The jointing surface developed in the conglomerate parallel to the strike must have originated as a result of the tensional stresses leading to stretching of beds along limbs of the fold. The joint is extensional and oriented perpendicular to the direction of operating force.

11.3 Scope for further work

1. Investigations need to be carried out with structural and tectonic evolution of the basin based on deformation.

2. A confirmation regarding two different provences at Bilgi needs to be studied. This is also with respect to the large amount of chrome tourmaline within its sequence.

BIBLIOGRAPHY

Adeigbe, O.C., Jinoih, Y.A., 2013. Geochemical Fingerprints; Implication for Provenance, Tectonic and Depositional Settings of Lower Benue Trough Sequence, Southeastern Nigeria. *Journal of Environment and Earth Science*, 3, 10.

Balesh, K.B., Das, S.S., Dayal, A.M., Kale, V.S., 1999. Occurrence of tiny digitate stromatolite [Yelma digitate grey, 1984], Yargatti Formation, Bagalkot Group, Kaladgi basin, Karnataka, India. *Current Science*, 75, 360-365.

Baulaz, B., Mayayo, M.J., Fernandez-Nieto, C., Lopez, J.M.G., 2000. Geochemistry of Precambrian and Paleozoic siliciclastic rocks from the Iberian Range (NE Spain): implications for source-area weathering, sorting, provenance and tectonic setting. *Chemical Geology*, 168, 135-150.

Beckinsale, R.D., Drury, S.A., Holt, R.W., 1980. 3360m.yr. Gneisses from the south Indian craton. *Nature (London)*, 283, 469-170.

Beckinsale, R.D., Reeves-Smith, G., Gale, N.H., Holt, R.W., Thompson, B., 1982. Rb–Sr and Pb–Pb whole rock isochron ages and REE data for the Archaean gneisses and granites, Karnataka state, South India. *In: Indo-US Workshop on the Precambrian of South India, National Geophysical Research Institute, Hyderabad, India*, Volume of Abstracts, 35–36.

Bhaskar Rao, Y.J., Naha, K., Srinivasan, R., Gopalan, K., 1991. Geology, Geochemistry and Geochronology of the Archaean Peninsular Gneiss around Gorur, Hassan District, Karnataka, India. *Proceedings of the Indian Academy of Sciences,* 100, 399–412.

Bhatia, M.R., Crook, A.W., 1986. Trace element characteristics of graywackes and tectonic setting discrimination of sedimentary basins. *Contributions to Mineralogy and Petrology*, 92, 181–193.

Blenkinsop, T., 2002. *Deformation microstructures and mechanisms in minerals and rocks.* Kluwer Academic Publishers.

Boggs, S., 2009. *Petrology of Sedimentary rocks,* second ed. Cambridge University Press.

Bose, P. K., Sarkar, S., Mukhopadhyay, S., Saha, B., Eriksson, P.G., 2008. Precambrian basin-margin fan deposits: Mesoproterozoic Bagalkot Group, India. *Precambrian Research,* 159, 260–274.

Condie, K.C., 1993. Chemical composition and evolution of the upper continental crust: contrasting results from surface samples and shales. *Chemical Geology*, 104, 1–37.

Condie, K.C., Wronkiewicz, D.J., 1990. The Cr/Th ratio in Precambrian pelites from the Kaapvaal craton as an index of craton evolution. *Earth and Planetary Science Letters,* 97, 256–267.

Cox, R., Lowe, D.R., 1995. A conceptual review of regional-scale controls on the composition of clastic sediment and the co-evolution of continental blocks and their sedimentary cover. *Journal of Sedimentary Research*, 65, 1–21.

Cullers, R.L., 1994. The controls on the major and trace element variation of shales, siltstones, and sandstones of Pennsylvanian–Permian age from uplifted continental blocks in Colorado to platform sediment in Kansas, USA. *Geochimica et Cosmochimica Acta*, 58, 4955–4972.

Cullers, R. L., 2000. The geochemistry of shales, siltstones and sandstones of Pennsylvanian–Permian age, Colorado, USA: Implications for provenance and metamorphic studies. *Lithos*, 51, 181–203.

Cullers, R.L., Basu, A., Suttner, L.J., 1988. Geochemical signature of provenance in sand-size material in soils and stream sediments near the Tobacco Root batholith, Montana, USA. *Chemical Geology*, 70, 335–348.

Cullers, R.L. Chaudhuri, S. Kilbane, N. Koch, R. 1979. Rare earths in size fractions and sedimentary rocks of Pennsylvanian–Permian age from the mid-continent of the USA. *Geochimica et Cosmochimica Acta*, 43, 1285–1302.

Cullers, R.L., Podkoyrov, V.N., 2000. Geochemistry of the Mesoproterozoic Lakhanda shales in southeastern Yakutia, Russia: Implications for mineralogical and provenance control, and recycling. *Precambrian Research*, 104, 77–93.

Dey, S., 2006. Petrology and geochemistry of selected clastic rocks of the Kaladgi Supergroup and basement Closepet Granites from Bagalkot District, Karnataka, India. *Unpublished Ph.D. thesis, Jadavpur University, Kolkata*.

Dey, S., 2015. Geological history of the Kaladgi-Badami and Bhima basins, South India: Sedimentation in a Proterozoic intracratonic setup. *Geological Society, London, Memoirs,* 43, 283-296.

Dey, S., Rai, A.K., Chaki, A., 2009. Geochemistry of Granitoids of Bilgi Area, northern part of Eastern Dharwar Craton, Southern India – example of transitional TTGs derived from depleted source. *Journal of Geological Society of India*, 73, 854–870.

Dey, S. Gajapathi Rao, R. Gorikhan, R.A., Veerabhaskar, D., Sunil, K., Kumar, M.K., 2003. Geochemistry and origin of northern Closepet granite from Gudur-Guledagudda area, Bagalkot district, Karnataka. *Journal of Geological Society of India*, 62, 152–168.

Dutrow, B.L., Henry, D.J., 2000. Complexly zoned fibrous tourmaline, Cruzeiro mine, Minas Gerais, Brazil: A record of evolving magmatic and hydrothermal fluids. *Canadian Mineralogist*, 38, 131–143.

Dutrow, B.L., Henry, D.J., 2011. Tourmaline: A Geologic DVD. *Elements*, 7, 301–306.

Feng, R., Kerrich, R., 1990. Geochemistry of fine-grained clastic sediments in the Archean Abitibi Greenstone belt, Canada: Implications for provenance and tectonic setting. *Geochimica Cosmochimica Acta*, 54, 1061–1081.

Folk, R.L., 1974. *Petrology of Sedimentary Rocks. Hemphill Publishing Company, Texas.* 182.

Foote, R.B., l876. Geological features of the Southern Mahratta Country and adjoining districts. *Geological Society of India Memoires*, 12(I), 86.

Friend, C.R., Nutman, A.F., 1991. SHRIMP U–Pb geochronology of the Closepet granite and Peninsular Gneiss, Karnataka, south India. *Journal of Geological Society of India*, 38, 357–368.

Goldberg, K., Humayun, M., 2010. The applicability of the Chemical Index of Alteration as a paleoclimatic indicator: An example from the Permian of the Parana Basin, Brazil. *Palaeogeography, Paleoclimatology, Paleoecology*, 293, 1-2, 175-183.

Govinda Rajulu, B.V, Satish, P.N., 1968. Occurrence of authigenic tourmalines in the lower Kaladgi quartzitic sandstones of Saundatti, Mysore state. *35, A, 5, 675-683.*

Henry, D. J., Dutrow, B.L., 1990. Ca substitution in Li-poor aluminous tourmaline. *The Canadian Mineralogist*, 28, 111–124.

Henry, D.J., Dutrow, B.L., 1992. Tourmaline in a low-grade clastic metasedimentary rock — an example of the petrogenetic potential of tourmaline. *Contributions to Mineralogy and Petrology*, 112, 203–218.

Henry, D.J., Dutrow, B.L., 1996. Metamorphic tourmaline and its petrologic applications. In: Grew, E.S., Anovitz, L.M. (Eds.), Boron: Mineralogy, Petrology and Geochemistry. *Reviews in Mineralogy*, 33, 503–557.

Henry, D.J., Kirkland, B.L., Kirkland, D.W., 1999. Sector-zoned tourmaline from the cap rock of a salt dome. *European Journal of Mineralogy*, 11, 263-280.

Henry, D.J., Novák, M., Hawthorne, F.C., Ertl, A., Dutrow, B.L., Uher, P., Pezzotta, F., 2011. Nomenclature of the tourmaline-supergroup minerals. *American Mineralogist*, 96, 895–913.

Herron, M.M., 1988. Geochemical classification of terrigenous sands and shales from core or log data. *Journal of Sedimentary Petrology*, 58, 820-829.

Holtz, F., Johannes, W., 1991. Effect of tourmaline on melt fraction and composition of first melts in quartzofeldspathic gneiss. *European Journal of Mineralogy*, 3, 527-536.

Irshad, R., Ahmad, A.H.M., 2013. Petrography and Major element geochemistry of Habo Formation sediments, Kachchh, Western India: Clues for Provenance. *Asian Journal of Science and Technology*, 4, 010-022.

Jarvis, K.E., 1988. Inductively coupled plasma mass spectrometry: A new technique for the rapid or ultra-level determination of the rare-earth elements in geological materials. *Chemical Geology,* 68, 31–39.

Jayananda, M., Moyen, F.F., Martin, H., Peucat, J.J., Auvray, B., Mahabaleswar, B., 2000. Late Archaean (2550–2520 Ma) juvenile magmatism in the Eastern Dharwar Craton, Southern India: constraints from Geochronology, Nd–Sr isotopes and whole rock geochemistry. *Precambrian Research*, 99, 225–254.

Jayananda, M., Peucat, J.J., Chardon, D., Krishna Rao, B., Fanning, C.M., Corfu, F., 2013. Neoarchean greenstone volcanism and continental growth, Dharwar craton, southern India: constraints from SIMS U–Pb zircon geochronology and Nd isotopes. *Precambrian Research*, 227, 55–76.

Jayaprakash, A.V., 2007. Purana Basins of Karntaka. *Memoir Geological Survey of India*, 129, 1–137.

Jayaprakash, A.V., Sundaram, V., Hans, K., Mishra, R.N., 1987. Geology of the Kaladgi-Badami Basin, Karnataka.: Purana Basins of Peninsular India (middle to late Proterozoic), *Geological Society of India, Memoir 6,* 201–225.

Kale, V.S., Ghunkikar, V., Paul, T.P., Peshwa, V.V., 1996. Macrofacies architecture of the first transgressive suite along the southern margin of the Kaladgi Basin. *Journal of Geological Society of India,* 48, 75–92.

Kale, V.S., Phansalkar, V.G., 1991. Purana basins of Peninsular India: a review. *Basin Research*, 3, 1–36.

Kale, V.S., Pillai, S.P., 2011. A reinterpretation of two chertbreccias from the Proterozoic basins of India. *Journal of Geological Society of India*, 78, 429-445.

Krynine, P.D., 1935. Arkose deposits in the humid tropics: A case study of sedimentation in southern Mexico. *American Journal of Science*, 29, 353-363.

Krynine, P.D., 1946. The tourmaline group in sediments. *Journal of Geology*, 54, 65–87.

London, D., 2011. Experimental synthesis and stability of tourmaline: a historical perspective. *Canadian Mineralogist*, 49, 117-136.

London, D., Morgan, G.B.I., Wolf, M.B., 1996. Boron in granitic rocks and their contact aureoles. In: Grew, E.S., Anovitz, L.M. (Eds.), Boron: Mineralogy, Petrology and Geochemistry: *Reviews in Mineralogy*, 33, 299–330.

Maibam, B., Goswami, J.N., Srinivasan, R., 2011. Pb–Pb zircon ages of Archean metasediments and gneisses from the Dharwar craton, southern India: Implications for the antiquity of the Eastern Dharwar craton. *Journal of Earth System Science,* 120, 643–661.

Marschall, H.R., Korsakov, A.V., Luvizotto, G.L., Nasdala, L., Ludwig, T., 2009. On the occurrence and boron isotopic composition of tourmaline in (ultra)high-pressure metamorphic rocks. *Journal of the Geological Society,* 166, 811–823.

McLennan, M.S., 2001. Relationships between the trace element composition of sedimentary rocks and upper continental crust. *Geochemistry Geophysics Geosystems, American Geophysical Association.* 2.

McLennan, S.M., Taylor, S.R., 1991. Sedimentary rocks and crust evolution: Tectonic setting and secular trends. *Journal of Geology*, 99, 1–21.

McLennan, S.M., Taylor, S.R., Eriksson, K.A., 1983. Geochemistry of Archean Shales from the Pilbara Super group, Western Australia. *Geochimica et Cosmochimica Acta*, 47, 1211 – 1222.

Meert, J.G., Pandit, M.K., 2015. The Archaean and Proterozoic history of Peninsular India: tectonic framework for Precambrian sedimentary basins in India. In: Mazumder, R., Eriksson, P.G. (Eds.), Precambrian Basins of India: Stratigraphic and Tectonic Context. *Geological Society, London, Memoirs*, 43, 29–54.

Meert, J.G., Pandit, M.K., Pradhan, V.R., Banks, J., Sirianni, R., Stroud, M., Newstead, B., Gifford, J., 2010. Precambrian crustal evolution of Peninsular India: A 3.0 billion year odyssey. *Journal of Asian Earth Sciences*, 39, 483–515.

Miall, A.D., Catuneanu, O., Eriksson, P.G., Mazumdar, R., 2015. A brief synthesis of Indian Precambrian basins: classification and genesis of basin-fills, *Geological Society, London, Memoirs,* 23.

Middlemost, E.A.K., 1989. Iron oxidation ratios, norms and the classification of volcanic rocks. *Chemical Geology*, 77, 19-26.

Mojzsis, S.J., Devaraju, T.C., Newton, R.C., 2003. Ion microprobe U-Pb determinations on zircon from the late Archaean granulite facies transition zone of southern India. *Journal of Geology*, 111, 407–425.

Mongelli, G., Dinelli, E., 2001. The geochemistry of shales from the ''Frido Unit,'' Liguride Complex, Lucanian Apennines, Italy: Implications for provenance and tectonic setting. *Ofioliti*, 26, 457–466.

Moore, J.N., Christenson, B.W., Allis, R.G., Browne, P.R.L., Lutz, S.J., 2004. The mineralogical consequences and behavior of descending acid-sulfate waters: an example from the Karaha–Telaga Bodas geothermal system, Indonesia. *The Canadian Mineralogist,* 42, 1483–1499.

Morgan, G.B., London, D., 1989. Experimental reactions of amphibolite with boron bearing aqueous fluids at 200 MPa — implications for tourmaline stability and partial melting in mafic rocks. *Contributions to Mineralogy and Petrology*, 102, 281–297.

Mukherjee, M.K., Das, S., Modak, K., 2016. Basement–cover structural relationships in the Kaladgi Basin, southwestern India: Indications towards a Mesoproterozoic gravity gliding of the cover along a detached unconformity. *Precambrian Research*, 281, 495-520.

Naha, K., Srinivasan, R., Gopalan, K., Pantulu, G.V., Subba Rao, M.V., Vrevsky, A.B., Bogomolov, S.Ye., 1993. The nature of the basement in the Archaean Dharwar craton of southern India and the age of the Peninsular Gneiss. *Proceedings Indian Academy of Sciences,* 102, 547–565.

Nakamura, N., 1974. Determination of REE, Ba, Fe, Mg, Ba, and K in carbonaceous and ordinary chondrites, *Geochimica et Cosmochimica Acta,* 38, 7577-775.

Nakano, T., Nakamura, E., 2001. Boron isotope geochemistry of metasedimentary rocks and tourmalines in a subduction zone metamorphic suite. *Physics of the Earth and Planetary Interiors*, 127, 233-252.

Naqvi, S.M., Khan, R.M.K., Manikyamba, C., Rammohan, M., Khanna, T.C., 2006. Geochemistry of the NeoArchaean high-Mg basalts, boninites and adakites from the Kushtagi–Hungund greenstone belt of the Eastern Dharwar Craton

(EDC); implications for the tectonic setting. *Journal of Asian Earth Sciences*, 27, 25–44.

Nath, B.N., Kunzendorf, H., Pluger, W.L., 2000. Influence of Provenance, weathering and sedimentary processes on the elemental ratio of the fine grained fraction of the bed load sediments from the Veinbanad lake and the adjoining Continental shelf, southwest coast of in clim. *Journal of Sedimentary Research*, 70, 1081 – 1094.

Nesbitt, H.W., Young, G.M., 1982. Early Proterozoic climates and plate motions inferred from major element chemistry of lutites. *Nature,* 299, 715–717.

Novák, M., Henry, D.J., Hawthorne, F.C., Ertl, A., Uher, P., Dutrow, B., Pezzotta, F., 2009. Nomenclature of the tourmaline-group minerals. *Report of the Subcommittee on Tourmaline Nomenclature to the International Mineralogical Association's Commission on New Minerals, Nomenclature and Classification.*

Osae, S., Asiedu, D.K., Banoeng-Yakubo, B., Koeberl, C., Dampare, S.B., 2006. Provenance and tectonic setting of late Proterozoic Buem sandstones of southeastern Ghana: Evidence from geochemistry and detrital modes. *Journal of African Earth Sciences,* 44, 85–96.

Ota, T., Kobayashi, K., Katsura, T., Nakamura, E., 2008. Tourmaline breakdown in a pelitic system: implications for boron cycling through subduction zones. *Contributions to Mineralogy and Petrology,* 155, 19-32.

Padmakumari, V.M., Sambasiva Rao, V.V., Srinivasan, R., 1998. Model Nd and Rb-Sr ages of shales of the Bagalkot Group, Kaladgi Supergroup, Karnataka. *In: National Symposium on Late Quaternary Geology and Sea level Changes. Cochin University, Kochi,* 70.

Palme, H., and Jones, A., 2005. Solar System Abundances of the Elements, in: Davis, A.M. (Ed.), *Meteorites, Comets, and Planets, Treatise on Geochemistry, v1*. Elsevier, Amsterdam, 41-62.

Palmer, M.R., London, D., Morgan, G.B., Babb, H.A., 1992. Experimental determination of fractionation of 11B/10B between tourmaline and aqueous vapor: A temperature- and pressure-dependent isotopic system. *Chemical Geology*, 101, 123-129.

Passchier, C.W., Trouw, R.A.J., 2005. *Microtectonics (second edition*). Springer-Verlag, Berlin, Germany.

Peshwa, V.V., Phadke, A.V., Phansalkar, V.G., Soman, G.R., Deolankar, S.B., 1989. Geology of the Kaladgi Basin and associated rocks in parts of northern Karnataka and Western Maharashtra: A study based on Remote Sensing

Techniques. *Unpublished ISRO-RESPOND Project Report; Geology Department, Poona University.* 118+18pl.

Pettijohn, F.J., 1963. Chemical composition of sandstones, excluding carbonate and volcanic sands. *In: Fleischer M, editor. Data of Geochemistry, US Geological Survey Professional Paper*, 440-S, 19.

Pettijohn, F.J., Potter, P.E., Siever, R., 1972. *Sands and sandstones. Springer-Verlag, New York*.

Pillai, P.S., Kale, V.S., 2011. Seismites in the Lokapur Subgroup of the Proterozoic Kaladgi basin, south India: a testimony to synsedimentary tectonism. *Sedimentary Geology,* 240, 1–13.

Pillai Patil, S., Peshwa, V.V., Nair, S., Sharma, M., Shukla, M., Kale, V.S., 1997. Occurrence of a Manganese bearing horizon in the Kaladgi Basin. Journal of Geological Society of India, 53, 201-204.

Piper, D. Z. 1994. Rare earth elements in the sedimentary cycle: a summary. *Chemical Geology,* 14, 285-304.

Radhakrishna, B.P., Vaidyanathan, R., 1994. Geology of Karnataka. *Geological Society of India,* Bangalore, 298.

Ramakrishnan, M., Vaidyanadhan, R., 2008. Geology of India, *Geological Society of India, Bangalore,* 1

Roda-Robles, E., Pesquera, A., Gil-Crespo, P.P., Torres-Ruiz, J., 2011. Occurrence, paragenesis and compositional evolution of tourmaline from the Tormes Dome area, Central Iberian Zone, Spain. *Canadian Mineralogist*, 49, 207-224.

Roser, B.P., Korsch, R.J., 1988. Provenance signature of sandstone–mudstone suites determined using discriminant function analysis of major element data. *Chemical Geology,* 67, 119–139.

Roy, A., 1983. Structure and tectonics in the cratonic areas of North Karnataka. *In: Sinha Roy, S. (Ed.), Structure and Tectonics of the Precambrian Rocks, Hindusthan Publishing Company, New Delhi,* 10, 81–96.

Sathyanarayan, S., 1994. *The younger Proterozoic Badami Group, Northern Karnataka*. In: Ravindra, B. M and Raganathan N. Geo-Karnataka. Mysore Geological Department, Bangalore. Centenary, 227-233.

Sharma, M., Pandey, S.K., 2012. Stromatolites of the Kaladgi Basin, Karnataka, India: Systematics, biostratigraphy and age implications. *The Palaeobotanist*, 61, 103-121.

Slack, J.F., 1996. Tourmaline associations with hydrothermal ore deposits. In Boron: Mineralogy, Petrology and Geochemistry (E.S. Grew & L.M. Anovitz, eds.). *Reviews in. Mineralogy,* 33, 559-644.

Spicer, E.M., Stevens, G., Buick, I.S., 2004. The low-pressure partial-melting behaviour of natural boron-bearing metapelites from the Mt. Stafford area, central Australia. *Contributions to Mineralogy and Petrology*, 148, 160-179.

Suttner, L.J., Dutta, P.K., 1986. Alluvial sandstone composition and paleoclimate, I. Framework mineralogy. *Journal of Sedimentary Petrology,* 56(3), 329-345.

Taylor, S., McLennan, S., 1985. *The Continental Crust, Its Composition and Evolution*. Oxford, Blackwell, 311.

Taylor, S. R., McLennan, S.M., 1995. The geochemical evolution of the continental crust. *Reviews of Geophysics,* 33, 241-265.

Tucker, E.M., 2011. *Sedimentary rocks in the field: A practical guide.* 4th edition, Wiley-Blackwell Publishing Company.

van Hinsberg, V.J., Henry, D.J., Dutrow, B.L., 2011. Tourmaline as a petrologic forensic mineral: a unique recorder of its geologic past. *Elements,* 7, 327–332.

van Hinsberg, V.J., Marschall, H.R., 2007. Boron isotope and light element sector zoning in tourmaline: implications for the formation of B-isotopic signatures. *Chemical Geology,* 238, 141-148.

van Hinsberg, V.J., Schumacher, J.C., 2007. Intersector element partitioning in tourmaline: a potentially powerful single crystal thermometer. *Contributions to Mineralogy and Petrology*, 153, 289-301.

van Hinsberg, V.J., Schumacher, J.C., 2011. Tourmaline as a petrogenetic indicator mineral in the Haut-Allier metamorphic suite, Massif Central, France. *Canadian Mineralogist*, 49, 177-194.

von Goerne, G., Franz, G., Wirth, R., 1999. Hydrothermal synthesis of large dravite crystals by the chamber method. *European Journal of Mineralogy*, 11, 1061-1078.

Viswanathiah, H.M.N., 1969. Badami series: A new post Kaladgi formation of Mysore State. *Geological Society of India Bulletin,* 5, 94-97.

Viswanathiah, M.N., Murthy, T.R.S., 1977. Potash feldspathisation of conglomerate and subfeldsarenites of Kaladgi Group, Bilgi, Bijapur district, Karnataka, India. *Indian Mineralogist*, 18, 85·93.

Wedepohl, K.H., 1969. The composition of the continental crust. *Geochimica et Cosmochimica Acta*, 59, 1217-1232.

Weltje, G.J., Meijer, X.D., Deboer, P.L., 1998. Stratigraphic inversion of siliciclastic basin fills: a note on the distinction between supply signals resulting from tectonic and climate foreing. *Basin Research*, 10, 129-153.

Williams, H., Turner, F.J., Gilbbert, C.M., 1954. *Petrography. Freeman, San Francisco*, 406

Wolf, M.B., London, D., 1997. Boron in granitic magmas: stability of tourmaline in equilibrium with biotite and cordierite. *Contributions to Mineralogy and Petrology*, 130, 12-30.

Wronkiewicz, D. J., Condie, K.C., 1987. Geochemistry of Archean shales from the Witwatersrand Supergroup, South Africa: Source-area weathering and provenance: *Geochimica et Cosmochimica Acta*, 51, 2401–2416.

Wronkiewicz, D.J., Condie, K.C., 1989. Geochemistry and provenance of sediments from the Pongola Supergroup, South Africa: Evidence for a 3.0-Ga-old continental craton. *Geochimica et Cosmochimica Acta*, 53, 1537–1549.

Yamada, Y., 2010. X-ray fluorescence analysis by fusion bead method for ores and rocks. *The Rigaku Journal*, 26(2), 15-21.